



# **An Algorithm for Femtocell Positioning based on Signal Strength Measurements**

**João Martins Minas da Piedade**

Thesis to obtain the Master of Science Degree in

**Electrical and Computer Engineering**

## **Examination Committee**

President: Prof. Fernando Duarte Nunes

Supervisor: Prof. António José Castelo Branco Rodrigues

Co-Supervisor: Prof. José Eduardo Charters Ribeiro da Cunha Sanguino

Members of the Committee: Prof. Francisco António Bucho Cercas

Eng. Artur Paulo Goulart Vargas

**April 2013**



To my Parents and all my loved ones...



# Acknowledgements

First of all, I would like to thank my supervisor Professor António Rodrigues for the opportunity to work on this thesis and for sharing his knowledge and experience. I also thank Professor José Sanguino (co-supervisor) for helpful discussions and for making available key documentation on the subject of positioning.

The support of Engs. Artur Vargas (co-supervisor), Pedro Pimentel and João Mestre at Alcatel-Lucent Portugal, was especially important to achieve an inside view on the femtocell technology. They also provided data from a walk-test and the means to complement those data with the results of new experimental measurements. This information was essential for the development of the algorithm described in this thesis. The opportunity to perform actual measurements further contributed to improve my technical knowledge on the subject of femtocell positioning, Their suggestions, advice, documentation, and time spent answering all my questions are also gratefully acknowledged.

I thank Nuno Rodrigues for his friendship and help in reviewing this thesis and Nuno Fontes for his patience and encouragement. With Miguel Alexandre I had many helpful discussions through our common journey at Instituto Superior Técnico in which an enduring friendship was built. João Oliveira, João Guerreiro, Miguel Correia, Marcos Ramalho, José Lima Raposo, Bernardo Figueiredo, Filipe Camelo and João Clemente were important for their friendship and support.

Maria was always present in good and bad times, and for this I thank her deeply.

Last but not least, I thank my parents and grandmothers, for their love, patience and help.



# Abstract

Femtocells deployment has various technical challenges. A major one is the interference between a given femtocell and surrounding cells of different types. To minimize this effect in network planning, so that an efficient coverage may be achieved, it is important to know the location of femtocells as accurately as possible. Because femtocells are essentially indoor devices their positioning is also relevant for many location-based services, particularly those related to emergencies. In the present thesis an algorithm for femtocell positioning was developed. The construction and validation of the algorithm relied on data from mobile terminal positions and signal power measurements. This information was used in conjunction with propagation models and lateration methods to yield the latitude and longitude coordinates of a given femtocell. The algorithm includes a module for estimating the position of mobile terminals which do not have GPS capabilities. The performance of two lateration methods (Hyperbolic and Circular) was tested using in both cases Received Signal Code Power (RSCP) and Received Signal Strength Indication (RSSI) parameters. The influence of using mobile coordinates from GPS positioning or estimated by the above mentioned module was also evaluated. The best results were obtained for the algorithm combining Circular Lateration with RSCP. This procedure was always able to locate femtocells within the FCC 911 requirements when the coordinates of the mobile terminals were based on GPS positioning. Although significantly larger errors were observed when this capability was not available in the mobile terminals, the estimates were still considered useful. Finally, the algorithm here developed constitutes a very inexpensive solution to femtocell positioning because it does not require major changes in network architecture (e.g. new location servers).

## Keywords

Femtocells, Positioning, Lateration, Propagation Models, RSCP, Distance



# Resumo

A implementação de femtocélulas tem vários desafios técnicos. Um dos mais importantes está relacionado com a interferência entre uma dada femtocélula e as células de diferentes tipos existentes na sua vizinhança. Para minimizar este efeito durante o planeamento de uma rede e alcançar, assim, uma cobertura eficiente, é importante conhecer a localização das femtocélulas com a maior exactidão possível. Uma vez que as femtocélulas são essencialmente dispositivos de interior, o seu posicionamento é também relevante para muitos serviços baseados em localização, particularmente os relacionados com emergências. A presente tese teve por tema o desenvolvimento de um algoritmo para posicionamento femtocélulas. A construção e validação do algoritmo foi baseada em dados de posicionamento de terminais móveis e medições de potência de sinal. Esta informação foi utilizada juntamente com modelos de propagação e métodos de lateração para obter a latitude e longitude de uma determinada femtocélula. O algoritmo inclui um módulo para estimar a posição de terminais móveis sem capacidades GPS. Testou-se o desempenho de dois métodos de lateração (Hiperbólica e Circular), usando em ambos os casos parâmetros “Received Signal Code Power” (RSCP) e “Received Signal Strength Indication” (RSSI). Foi também avaliado o efeito do uso de coordenadas de terminais móveis provenientes de posicionamento GPS ou estimadas pelo módulo acima mencionado. O melhor desempenho correspondeu ao algoritmo combinando Lateração Circular e RSCP. Este método foi sempre capaz de localizar as femtocélulas dentro dos requisitos impostos pela norma FCC 911, quando as coordenadas dos terminais móveis eram baseadas em dados de posicionamento GPS. Apesar dos erros serem significativamente maiores quando esta capacidade não existia nos terminais móveis, as estimativas obtidas podem ainda ser consideradas úteis. Convém, finalmente, referir que o algoritmo desenvolvido na presente tese constitui uma solução muito barata para obter o posicionamento de femtocélulas, uma vez que não exige grandes alterações na arquitectura da rede (por exemplo, novos servidores de localização).

## Palavras-chave

Femtocélulas, Posicionamento, Lateração, Modelos de Propagação, RSCP, Distância



# Table of Contents

Acknowledgements .....	v
Abstract .....	vii
Resumo .....	ix
Table of Contents .....	xi
List of Figures .....	xiv
List of Tables .....	xvi
List of Acronyms .....	xvii
List of Symbols .....	xxi
List of xxiii	
1 Introduction .....	1
1.1 Overview .....	2
1.2 Motivation and Contents .....	6
2 Femtocells Aspects .....	9
2.1 Basic Concepts .....	10
2.1.1 Network Architecture .....	10
2.1.2 Air Interface .....	13
2.1.3 Coverage and Capacity .....	17
2.2 Mobility Management .....	19
2.2.1 Introduction .....	19
2.2.2 Femtocell Characterization .....	20
2.2.3 Access Control .....	23
2.2.4 Cell Selection and Reselection .....	24
2.2.5 Cell Handover .....	25
2.3 Propagation Models .....	26
2.3.1 Introduction .....	26
2.3.2 Outdoor and Indoor Models .....	28

3	Fundamentals of Positioning .....	31
3.1	Basic concepts .....	32
3.2	Positioning Infrastructures .....	35
3.3	Basic Positioning Methods .....	36
3.3.1	Proximity Sensing .....	36
3.3.2	Lateration .....	37
3.3.3	Other Methods .....	43
3.4	Accuracy and Error Sources .....	45
3.5	State of the Art .....	47
4	Models and Algorithm Development .....	49
4.1	Models .....	50
4.1.1	Propagation Models .....	50
4.1.2	Positioning Models .....	53
4.2	Algorithm Development .....	55
4.2.1	Algorithm Overview .....	56
4.2.2	UE Positioning Algorithm .....	57
4.2.3	Femtocell Positioning Algorithm .....	59
4.3	Algorithm Assessment .....	61
5	Results Analysis .....	65
5.1	Scenario Description .....	66
5.2	Measurements .....	67
5.2.1	Overview .....	67
5.2.2	Measurement Results .....	70
5.3	Result Analysis .....	75
5.3.1	Positioning Methods .....	75
5.3.2	GPS Dependency .....	78
5.3.3	RSS Parameters .....	81
6	Conclusions and Future Work .....	85
	Annex A. Link Budget .....	91
	Annex B. Propagation Models .....	95
	Annex C. Interference Management .....	101
	Annex D. Positioning Procedures .....	105
	Annex E. Additional Results .....	107

References ..... 113

# List of Figures

Figure 1.1. Annual worldwide wireless data traffic estimated up to 2016 (adapted from [1]) .....	2
Figure 1.2. Macro cell data rate versus range for indoor and outdoor environments (adapted from [4]) .....	3
Figure 1.3. Scheme of a typical connection between a home femtocell and a mobile operator network (adapted from [5]) .....	4
Figure 2.1. Reference architecture of HNB access network (extracted from [16]) .....	10
Figure 2.2. Analogy between WCDMA and a Restaurant Room (extracted from [19]) .....	14
Figure 2.3. Mapping Upper-Layers into Lower-Layers. (a) Downlink. (b) Uplink. (extracted from [3]) .....	15
Figure 2.4. Theoretical Peak User Data Rates (extracted from [21]) .....	16
Figure 2.5. Indoor users served by outdoor macro cells (extracted from [23]) .....	17
Figure 2.6. Serving indoor users with dedicated femtocells, and outdoor users with serving macrocell sites (extracted from [23]) .....	18
Figure 2.7. Comparison of cell sizes for different technologies (extracted from [3]) .....	18
Figure 2.8. Two-layer network (extracted from [3]) .....	20
Figure 2.9. HCS priority levels for different kinds of cells (extracted from [25]) .....	21
Figure 2.10. Separate femtocell PLMN ID (extracted from [3]) .....	22
Figure 2.11. Separate femtocells from macrocells by means of dedicated frequencies or reserved PSCs. (a) Dedicated carrier. (b) Shared carrier. (extracted from [3]) .....	23
Figure 2.12. Illustration of indoor and outdoor losses (extracted from [20]) .....	27
Figure 2.13. Urban Structure (extracted from [20]) .....	28
Figure 3.1. Positioning infrastructures (extracted from [14]) .....	34
Figure 3.2. Proximity Sensing (extracted from [14]) .....	36
Figure 3.3. Circular Lateration in 2D (extracted from [14]) .....	38
Figure 3.4. Potential error of Circular Lateration (extracted from [14]) .....	41
Figure 3.5. Hyperbolic Lateration in 2D (extracted from [14]) .....	41
Figure 3.6. Potential error of Hyperbolic Lateration (extracted from [14]) .....	43
Figure 3.7. Angulation in 2D (extracted from [14]) .....	43
Figure 3.8. Potential error of Angulation (extracted from [14]) .....	44
Figure 4.1. Path Loss Decision .....	52
Figure 4.2. Area and distance limitations (a) UE (b) Femtocell .....	55
Figure 4.3. Algorithm architecture .....	56
Figure 4.4. UE Positioning Module .....	58
Figure 4.5. Pythagoras theorem applied to the distance between an UE and a BS .....	59
Figure 4.6. Femtocell Positioning Module .....	60
Figure 4.7. Positioning Algorithm. (a) Femtocell. (b) UE. ....	62
Figure 5.1. Side view of Portobello Road .....	67
Figure 5.2. Measurement Set .....	68
Figure 5.3. Map with some measurement points .....	69
Figure 5.4. Detected BS's covering Portobello Road .....	72
Figure 5.5. Location errors. Circular Lateration vs. Hyperbolic Lateration vs. RSS-based Circular Lateration .....	73

Figure 5.6. Location error regarding weak signals.....	73
Figure 5.7. Circular Lateration Vs. Hyperbolic Lateration (Femtocell as non-serving cell).....	76
Figure 5.8. Circular Lateration Vs. Hyperbolic Lateration (Femtocell as Serving Cell).....	77
Figure 5.9. Mean error for UE's positioning. Circular Lateration Vs. Hyperbolic Lateration .....	79
Figure 5.10. Femtocell location error as the percentage of UE's increases .....	80
Figure 5.11. Proposed Algorithm. RSCP Vs. RSSI (Femtocell as Serving Cell) .....	81
Figure 5.12. Proposed Algorithm. RSCP Vs. RSSI (Femtocell as Non-Serving Cell) .....	82
Figure 5.13. Proposed Algorithm. RSCP Vs. RSSI (GPS Dependency) .....	83
Figure B.1. Definition of the parameters used in the COST 231 – WI model (extracted from [30]).....	95
Figure B.2. Definition of the street orientation angle $\varphi$ (extracted from [30]) .....	96
Figure C.1. Interference scenarios in a two-layer network (extracted from [54]).....	102
Figure D.1. Message flow between the UE and the network. (a) UE based. (b) UE assisted. (extracted from [58]).....	105
Figure D.2. Messages procedures between the RNC and SAS (extracted from [58]).....	106
Figure E.1. Comparison between all the methods developed for when the femtocell is the Serving Cell (Femtocell 1).....	107
Figure E.2. Comparison between all the methods developed for when the femtocell is the Serving Cell (Femtocell 2).....	108
Figure E.3. Comparison between all the methods developed for when the femtocell is a Neighbor Cell (Femtocell 1).....	109
Figure E.4. Comparison between all the methods developed for when the femtocell is a Neighbor Cell (Femtocell 2).....	110
Figure E.5. Comparison between all the methods developed for GPS Dependency (Femtocell 1) ...	111
Figure E.6. Comparison between all the methods developed for GPS Dependency (Femtocell 2) ...	112

# List of Tables

Table 2.1. Functional split for UTRAN function in the HNB access (extracted from [7]).....	12
Table 2.2. Functional split for HNB function in the HNB access (extracted from [7]) .....	13
Table 2.3. Comparison between HSUP A and HSDPA (extracted from [22]).....	17
Table 2.4. Comparison between Closed and Open Access femtocells (extracted from [26]).....	24
Table 2.5. Wall and floor types for MWM and weighted average loss (extracted from [35]) .....	29
Table 3.1. Overview of positioning methods (adapted from [14]) .....	33
Table 5.1. Reference Scenario Characteristics .....	66
Table 5.2. UE's set up .....	68
Table 5.3. Example of a measurement set extracted from TEMS investigation .....	70
Table 5.4. Information of each site .....	71
Table 5.5. RSCP values used for Femtocell Location Error .....	74
Table 5.6. Distance of all UE's in respect to the femtocell.....	74
Table 5.7. Mean Error and Standard Deviation .....	76
Table 5.8. Mean Error and Standard Deviation .....	77
Table 5.9. Mean Error and Standard Deviation .....	78
Table 5.10. Mean Error and Standard Deviation for UE Positioning .....	79
Table 5.11. Mean Error and Standard Deviation (% of UE without GPS capabilities increases) .....	80
Table 5.12. Mean Error and Standard Deviation .....	82
Table 5.13. Mean Error and Standard Deviation .....	83
Table 5.14. Mean Error and Standard Deviation .....	84
Table 6.1. Correspondence between the propagation models and the scenarios for femtocell positioning .....	87
Table 6.2. Correspondence between the propagation models and the scenarios for UE Positioning.....	87
Table A.1. HSDPA and HSUPA processing gain and SNR definition (adapted from [53]).....	92
Table E.1. Mean Error and Standard Deviation for Serving Cell (Femtocell 1) .....	108
Table E.2. Mean Error and Standard Deviation for Serving Cell (Femtocell 2) .....	108
Table E.3. Mean Error and Standard Deviation for Neighbor Cell (Femtocell 1).....	109
Table E.4. Mean Error and Standard Deviation for Neighbor Cell (Femtocell 2).....	110
Table E.5. Mean Error and Standard Deviation for GPS Dependency (Femtocell 1).....	111
Table E.6. Mean Error and Standard Deviation for GPS Dependency (Femtocell 2).....	112

# List of Acronyms

16-QAM	16-Quadrature Amplitude Modulation
3GPP	Third Generation Partnership Project
ACL	Allowed CSG List
AGNSS	Assisted Global Navigation Satellite System
A-GPS	Assisted GPS
AMC	Adaptive Modulation and Coding
AoA	Angle of Arrival
BS	Base Station
BoD	Bandwidth on Demand
CAPEX	Capital Expenditure
CDMA	Code Division Multiple Access
CGI	Cell Global Identity
CN	Core Network
CoO	Cell of Origin
CPE	Customer Premises Equipment
CPICH	Common Pilot Channel
CSG	Closed Subscriber Group
CSV	Comma-Separated Values
DAS	Distributed Antennas System
DCH	Dedicated Channel
DL	Downlink
DoA	Direction of Arrival
E-AGCH	Enhanced Absolute Grant Channel
E-DCH	Enhanced Dedicated Channel
E-DPCCH	Enhanced Dedicated Physical Control Channel
E-DPDCH	Enhanced Dedicated Physical Data Channel
E-HICH	Enhanced HARQ Indicator Channel
E-RGCH	Enhanced Relative Grant Channel
eHNB	Evolved Home Node B

EIRP	Equivalent Isotropic Radiated Power
EU	European Union
FCC	Federal Communications Commission
FDD	Frequency Division Duplexing
FLP	Forward Linear Prediction
FPSL	Free Space Path Loss
FRESH	Frequency Shift
GPS	Global Positioning System
GSM	Global System for Mobile Communication
HARQ	Hybrid Automatic Repeat Request
HCS	Hierarchy Cell Structure
HMS	Home Node B Management System
HNB	Home Node B
HNBAP	Home Node B Application Protocol
HNB-GW	Home Node B Gateway
HSDPA	High Speed Downlink Packet Access
HS-DPCCH	High Speed Dedicated Physical Control Channel
HS-DSCH	High Speed Downlink Shared Channel
HS-PDSCH	High Speed Physical Downlink Shared Channel
HS-SCCH	High Speed Shared Control Channel
HSUPA	High Speed Uplink Packet Access
IP	Internet Protocol
LA	Location Area
L-GW	Local Gateway
LIPA	Local IP Access
LoS	Line of Sight
LTE	Long Term Evolution
MAC	Medium Access Control
MCC	Mobile Country Code
MM	Mobility Management
MNC	Mobile Network Code
MRM	Measurement Report Message
MWM	Multi-Wall Model
NaN	Not a Number

NCL	Neighbor Cell List
NLoS	Non-Line of Sight
OPEX	Operational Expenditure
PCAP	Positioning Calculation Application Protocol
PLMN	Public Land Mobile Network
PSC	Primary Scrambling Code
QPSK	Quadrature Phase Shift Keying
RAN	Radio Access Network
RANAP	Radio Access Network Application Protocol
RF	Radio Frequency
RLC	Radio Link Control
RMS	Root Mean Square
RMSE	Root Mean Square Error
RNC	Radio Network Controller
RRC	Radio Resource Control
RSCP	Received Signal Code Power
RSS	Received Signal Strength
RSSI	Received Signal Strength Indication
RTT	Round-Trip Time
SAS	Stand Alone SMLC
SC	Scrambling Code
SeGW	Security Gateway
SGSN	Serving GPRS Support Node
SIB	System Information Block
SIC	Successive Interference Cancellation
SIR	Signal-to-Interference Ratio
SMLC	Serving Mobile Location Centre
SOHO	Small Offices and Home Offices
SRNC	Serving Radio Network Controller
TDD	Time Division Duplexing
TDoA	Time Difference of Arrival
ToA	Time of Arrival
TTI	Time Transmission Interval
UARFCN	UTRA Absolute Radio Frequency Channel Number

UE	User Equipment
UL	Uplink
UMTS	Universal Mobile Telecommunications System
UTM	Universal Transverse Mercator
UTRA	UMTS Terrestrial Radio Access
UTRAN	UMTS Terrestrial Radio Access Network
WCDMA	Wideband Code Division Multiple Access
WGS-84	World Geodetic System 84
WI	Walfisch-Ikegami
WiFi	Wireless Fidelity
WLAN	Wireless Local Area Network
WLS	Weighted Least Square

# List of Symbols

$\alpha$	Angle of arriving pilot signal
$\Delta f$	Signal bandwidth
$\mu$	Mean
$\sigma$	Standard Deviation
$d_n$	Distance of the n sample
$F$	Receiver noise figure
$G_{div}$	Diversity gain
$G_{SH}$	Soft Handover gain
$G_p$	Process gain
$G_{TX}$	Gain of the transmitting antenna
$G_{RX}$	Gain of the receiving antenna
$I$	Number of walls types
$k_f$	Number of penetrated floors
$k_{wi}$	Number of penetrated walls of type i
$L_c$	Cable loss attenuation
$L_{glass}$	Glass loss Attenuation
$L_f$	Loss between adjacent floors
$L_{FS}$	Free Space path loss
$L_P$	Total path loss
$L_{P_{ind}}$	Indoor path loss attenuation
$L_{P_{out}}$	Outdoor path loss attenuation
$L_u$	User body attenuation
$L_{wi}$	Loss of wall type i
$M_{FF}$	Fast fading margin
$M_I$	Margin of Interference
$M_{SFF}$	Slow fading margin
$N$	Total noise power
$N_{hop}$	Number of hopping slots
$N_{sec}$	Number of sectors
$\rho_i$	Measured pseudorange
$P_{Tx}$	Transmitter output power
$P_{Rx}$	Receiver power
$r_i$	Circumference radius (distance)
$t_n$	Time for the n sample
$v_{max}$	Maximum admissible velocity
$x_i$	Target's estimated position
$x_t$	Target's true position
$(x, y)$	Cartesian coordinates of the target

$(X_i, Y_i)$

Cartesian coordinates of a BSi

# List of Software

MapInfo Professional

Matlab R2012a

Microsoft Excel

Microsoft Word

Microsoft PowerPoint

OmniGraffle Professional

TEMS Investigation



# Chapter 1

## Introduction

This chapter presents a brief overview of the work. Before establishing work goals, the scope and motivations are presented. At the end of this chapter, the structure of this thesis is provided.

## 1.1 Overview

The mobile data usage has been growing at a very high rate in recent years, driven, mainly by an increased use of data-intensive devices (e.g. 3G USB dongles, smart phones) and an increased usage per device. This necessarily raised the interest of operators in providing users with higher data rates, to improve their experiences, e.g. Internet applications. Figure 1.1 shows the annual worldwide wireless data traffic growth per month projected up to 2016 [1], which approximately corresponds to an yearly increase by a factor of two.

In cellular networks, 70% of the calls and more than 90% of the data services are made from indoor environments (home, office and public places) [2],[3]. Network operators, therefore, felt a strong need to provide good indoor coverage, not only for voice traffic but also for high speed data services [4]. This cannot be efficiently achieved only through macro cell systems installed outdoors because, (i) as illustrated in Figure 1.2, their data rate is significantly dampened indoors; (ii) costly periodical network updates would probably be necessary to keep up with the predicted indoor data traffic growth (Figure 1.1) without occurrence of overloads; and (iii) the evolution of indoor traffic needs for each specifically located macro cell would be very difficult to predict, leading to problems in adequate managing of coverage.

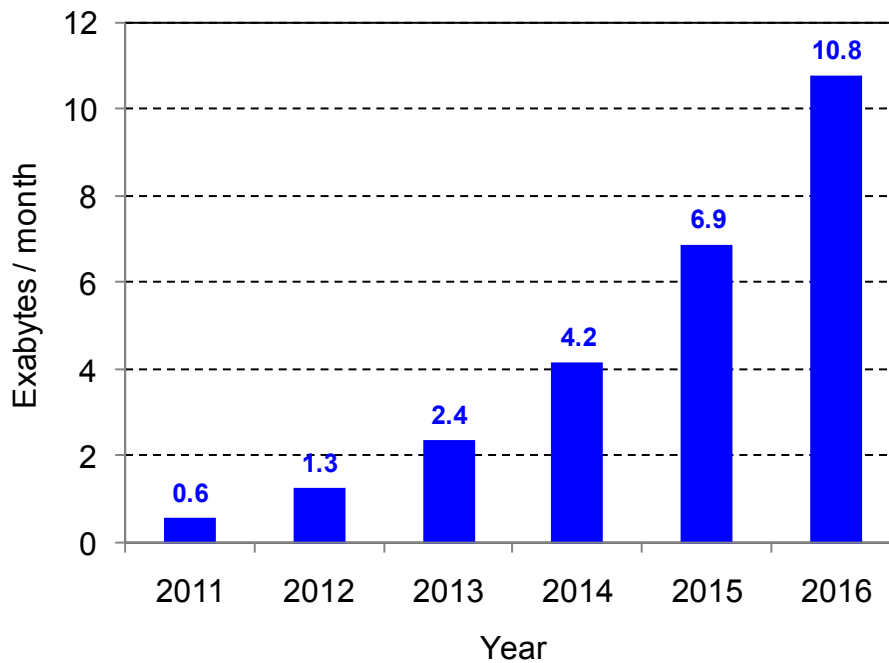


Figure 1.1. Annual worldwide wireless data traffic estimated up to 2016 (adapted from [1])

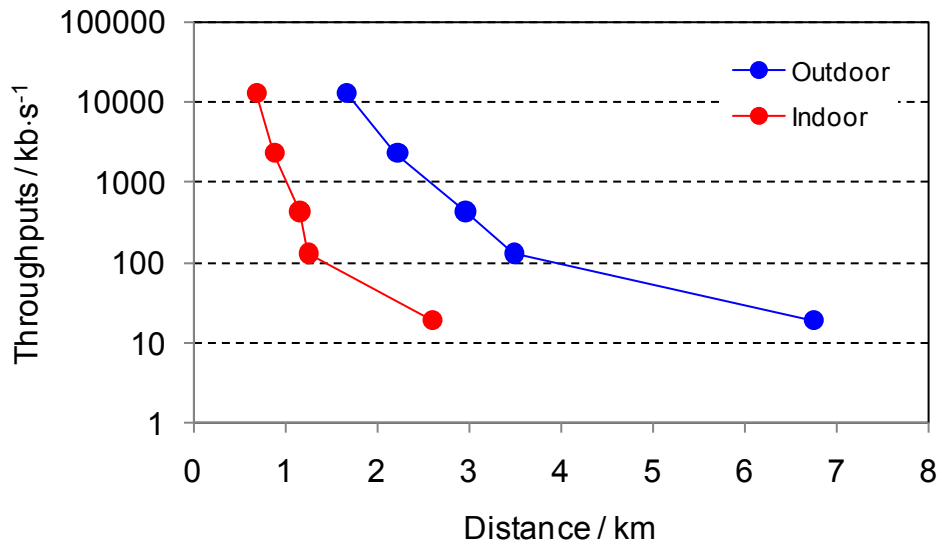


Figure 1.2. Macro cell data rate versus range for indoor and outdoor environments (adapted from [4])

Operators thus began to invest in indoor solutions, such as distributed antennas systems (DAS) and picocells, in view of their dissemination as hotspots for large business centers, shopping malls and office centers [3]. The rationale behind DAS implementation is to extend the coverage of the Base Stations (BS) by splitting the transmitted power between separated antennas. Picocells are cells that have a wider coverage range compared to the femtocells. Both these systems improve the indoor coverage and offload traffic from outdoor macrocells, increasing the service quality and giving higher data rates to users, because the radio links become significantly better [3]. They are also more cost effective than outdoor macrocells, but they are still very expensive for some indoor applications, such as small offices and home offices (SOHO) or home users, due to their small-scale operation. One of the problems is the fact that DAS and picocells require installation and maintenance by the network service providers, and the corresponding costs are necessarily reflected in the tariffs paid by end users.

Femtocells, also called “home base stations”, are access points with cellular network capabilities that connect to an operator mobile network, using Internet connections (such as DSL, cable, optical fiber, etc.). A typical connection between a femtocell and a mobile operator network is represented in Figure 1.3. Unlike DAS and picocells, they may be installed by users and, as such, operators started to regard them as a convenient low cost solution for indoor applications.

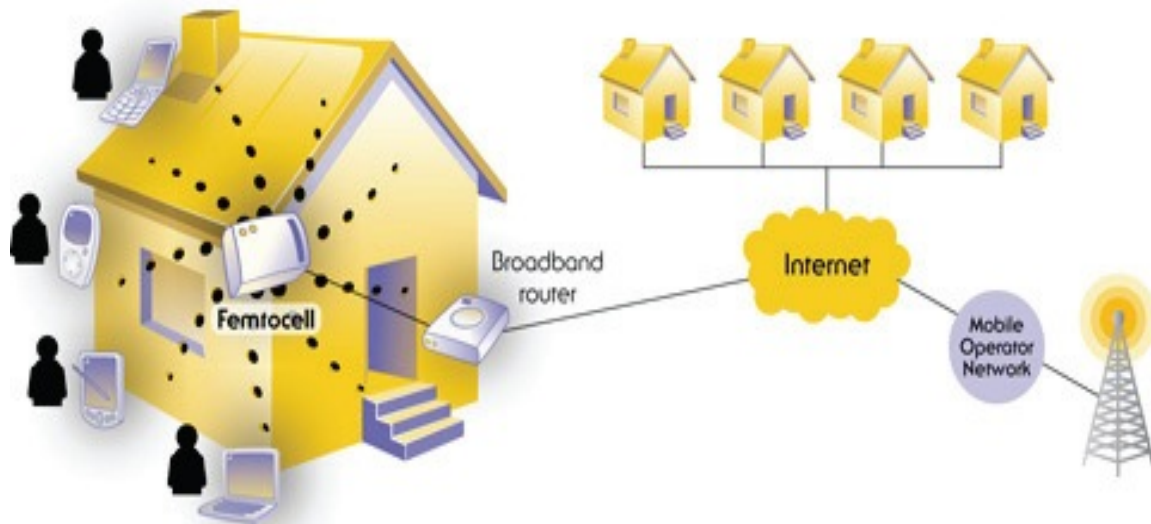


Figure 1.3. Scheme of a typical connection between a home femtocell and a mobile operator network (adapted from [5])

Bell Labs of Alcatel-Lucent studied the concept of femtocell for the first time, in 1999 [3]. By 2002 [3], Motorola announced the first 3G-based home station, but it was not until 2005 that the concept of “home base station” started having worldwide acceptance. In 2007, at the 3GSM conference several vendors showed their femtocell products and in the same year the Small Cell Forum (formerly Femto Forum) [6] was created to promote femtocells standardization and their deployment all over the world. The first sign that femtocells had become a mainstream wireless access technology was in 2008, when they were introduced in the Third Generation Partnership Project (3GPP) Release 8 [7]. In this 3GPP Release, femtocells are referred as Home Node B (HNB) and Evolved Home Node B (eHNB), Universal Mobile Telecommunications System (UMTS) and Long Term Evolution (LTE) femtocells, respectively.

Traditional wireless networks have a large number of network elements with mobility-specific functions that increase the service provider capital expenditure (CAPEX). Moreover the dependencies between networks elements increase the operational complexity resulting in higher operational expenditure (OPEX). The wireless coverage of indoor environments through femtocell systems mitigates these problems, thus offering benefits both for operators and users. From the operators point of view femtocells are considered an extension of the macrocells coverage, but with the advantage that users can install them. This reduces the CAPEX/OPEX for the operators, because (i) they no longer need to extend their network for better indoor coverage and capacity, and (ii) as traffic is offloaded from the macro network the corresponding data throughput per user as well as the quality of service improves. Moreover the extension of macro wireless networks through home (or small office) based femtocell systems can provide better coverage and higher data rates for subscribers with less expensive tariffs because of CAPEX/OPEX reduction for operators. Further benefits of better coverage may be, for example, longer handset use without need of battery recharging. This battery life extension is given due to the fact that less transmitted power, between the User Equipment (UE) and the BS, is used.

This reduction in the transmitted power is related to the distance, because the closer the UE and BS are the less the transmitted power is.

Femtocells deployment has technical challenges. Major problems are the macrocell to femtocell, femtocell to macrocell and femtocell to femtocell radio frequency (RF) interferences. The first two are mainly caused by the utilization of femtocells in the same frequency band or in frequency bands adjacent to those of the macrocells. The third arises from dense femtocells distribution in the same environment [8][9][10]. A further issue is the cell association and biasing, as users are associated to a given BS [9].

For more efficient network planning, for transmitting location information during emergency calls (e.g, Federal Communications Commission E911 requirements in the United States [11] and European Union (EU) E112 requirements in Europe [12]), and for radio access control, operators need to know the location of femtocells. Different solutions have been proposed to achieve this goal, namely [13], [14]:

- **Global Positioning System (GPS).** Some femtocells are equipped with a GPS receiver, but this technology has poor reception in indoor environments. Nevertheless, femtocells are not expected to be move often, so the last stored coordinates may provide a good estimate of their position.
- **Cell Sensing.** Femtocells can estimate their position by sensing the neighboring macrocells, using triangulation methods based on received signal power, time of arrival and angle of arrival. This type of solution is, however, only possible if there are at least three macrocells in the vicinity of the femtocell.
- **TV Signal.** This strategy may be a cheaper alternative to the GPS method. The advantages are that these TV signals have high power levels and use a wide range of frequencies, which makes it more efficient against fading.
- **Internet Protocol (IP) Address.** It is possible to identify the location of the femtocell by the IP address of the Internet connection. However this information may not be reliable, unless the Internet and mobile operators work together, due to the constraints on sharing client information between the two. This method could be a reliable option when a single operator offers a combined gateway for both the broadband router and the femtocell.
- **Customer Address.** In this case the femtocell is associated with the home address of the subscriber. This method has the advantage that the exact address of the femtocell is known. A major inconvenient is, however, the requirement that the subscriber informs the operator every time he wants to move the equipment to another location.

A more general solution would in principle be provided if the femtocell position could be defined based received power signals of the UE's. Indeed this is an advantageous solution because it does not need any changes in the network and therefore, it is cheaper solution for network operators.

## 1.2 Motivation and Contents

As mentioned in the previous section one of the most important challenges concerning the use of femtocells is the ability to determine their location. Accurate femtocell positioning is crucial in the context of, for example, emergency calls, network planning or radio access control, This requires the availability of reliable femtocell-positioning algorithms and the development of such an algorithm was the main goal of this thesis. The work was based on power measurements at the UE, mainly the Received Signal Code Power (RSCP) from a walk-test carried out in the UK by Alcatel-Lucent Portugal. A suitable propagation model was then applied to calculate the distance from the UE to the femtocell. After calculating the distances for all the UE's surrounding the femtocell, a positioning method is applied in order to calculate the location of the femtocell. This positioning method depends on the environment of each UE. This algorithm was also applied for calculating the location of the UE's in order to see the behavior of the error in the location of a femtocell.

A partnership with Alcatel-Lucent Portugal, a supplier of solutions for advanced communications, was established. This collaboration had a very important role on providing assistance on several technical details, insights on the technology, as well as providing data for a better development of the algorithm.

This thesis is composed of 6 chapters, including the present one, followed by a set of annexes. In chapter 2 it will be presented an introduction to femtocells technology, Mobility Management (MM) and propagation models. Femtocells basic concepts are explained and network architecture and radio interface are shown. Also, the MM is illustrated due to the constraints that femtocell have in the handover and the impact that it will have in the model development. Afterwards, a brief overview of propagation models, for both indoor and outdoor environments, is given.

Chapter 3 will present the theory for positioning systems. In this chapter, an introduction to the basic concepts is presented. Also, a brief overview on the positioning infrastructures is given. The positioning methods used in the developed algorithm are also described. Finally, the methods for evaluating the positioning algorithm are given along with the error sources.

Chapter 4 presents the models and the algorithm developed. First, the propagation and the positioning models are described. Also, the reasons for the models that have been chosen over others are explained. After the models description, the algorithm developed is illustrated. In this section an overview of the algorithm structure is given first, to better understand all the components of the algorithm. To finalize this chapter the propagation and positioning algorithms are described in detail.

In chapter 5 a result analysis of the proposed algorithm is made. A description of the scenario is done to enhance the selection of the propagation and positioning models. Also, a description of the measurements is made, mainly in terms of the tools that were used and the results that were obtained with them. The result analysis is presented in three parts: (i) a comparison between the positioning algorithms is given; (ii) a comparison between the received power parameters is done; (iii) GPS dependency is discussed. In this last part, the errors between the UE's that use GPS capabilities and the UE's that do not use are compared. Also an evolution of the error for when the UE's that do not

have GPS capabilities are added and the others are removed is given.

The final chapter of the thesis summarizes every conclusion drawn from the work done. Some final recommendations, regarding future work, are also given in order to continue developing femtocell-positioning algorithms.



# Chapter 2

## Femtocells Aspects

This chapter provides an overview of UMTS Femtocells, mainly focussing on the capacity aspects of the radio interfaces. MM in femtocells is explained, mainly in terms of handover, access control, cell selection and reselection. Lastly, the propagation models for indoor and outdoor coverage are analyzed.

## 2.1 Basic Concepts

This section provides an overview of the fundamental concepts concerning femtocells. The first part presents the network architecture, along with its main elements. A brief description of the air interface follows. Finally, capacity and coverage are overviewed.

### 2.1.1 Network Architecture

3GPP Release 8, defined for the first time femtocells in 2008, as HNB [15]. The problem with this new technology is the fact that unlike the UMTS Terrestrial Radio Access Network (UTRAN), the HNB access network has to integrate hundreds of thousands of low-capacity home base stations that can be moved, added and changed by the end users at any time. Figure 2.1 shows the reference architecture of a HNB access network.

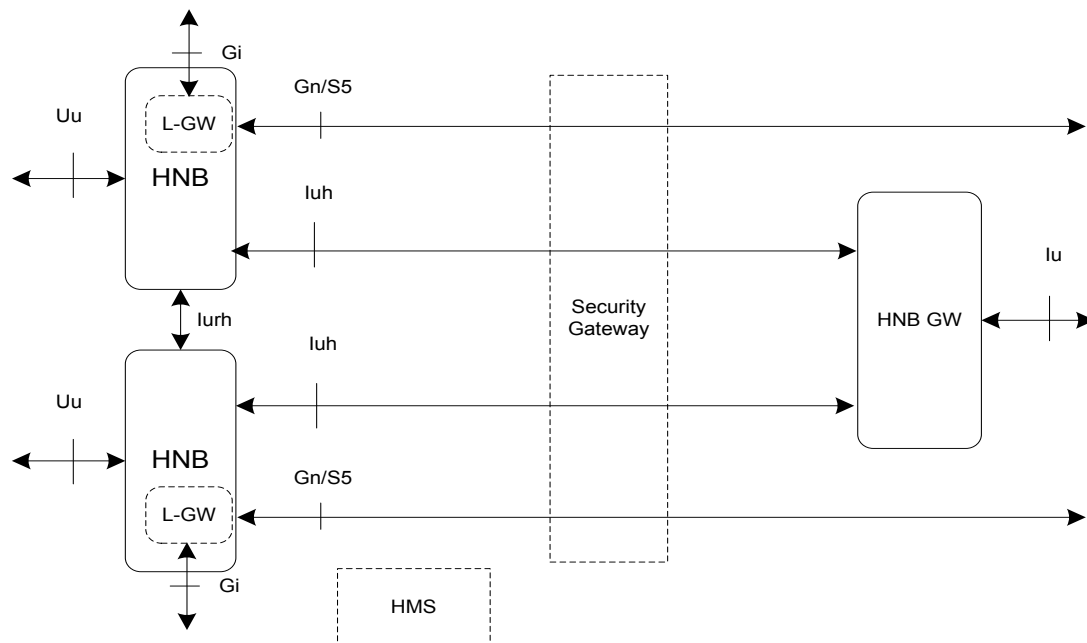


Figure 2.1. Reference architecture of HNB access network (extracted from [16])

One of the key considerations for this architecture is the functional splitting of the traditional Radio Network Controller (RNC) role between HNB and Home Node B Gateway (HNB-GW), where the HNB is responsible for the radio aspects and the HNB-GW is responsible for the connectivity to the Core Network (CN). The Iu interface between the HNB-GW and the CN has the same purpose as the interface between the RNC and CN. The Local Gateway (L-GW) is only present when the HNB is operating in Local IP Access (LIPA) mode. The HNB access network consists of five functional

entities:

- HNB – Customer Premises Equipment (CPE) that connects a UE over the UTRAN wireless air interface to a mobile operator’s network using a broadband IP backhaul. Provides Radio Access Network (RAN) connectivity using the Iuh interface, supports the NodeB and most of the RNC functions and also HNB authentication, HNB-GW discovery, HNB registration and UE registration over Iuh.
- HNB-GW – Mobile network operator’s equipment, through which the HNB gets access to the mobile operator’s CN. It serves the purpose of a RNC presenting itself to the CN as a concentrator of HNB connections. It provides the concentration function for the user plane and for the control plane.
- Security Gateway (SeGW) – Mandatory logical function. It may be implemented in the HNB-GW or as a physical entity. Establishes and manages IPsec tunnels, to each HNB for integrity and encryption purposes, providing secure access over the HNB-GW to the CN.
- HNB Management System (HMS) – Is based on the TR-069 family of standards [17]. Performs location verification of the HNB and assigns the appropriate serving elements. It facilitates the HNB-GW discovery.
- L-GW – This function is only present in the HNB when it is operating in LIPA mode. It is responsible for the deactivation of the Gn/S5 interface connection. Supports the internal direct user plane path towards the corresponding HNB user plane functions. Helps sending the first packet to the Serving GPRS Support Node (SGSN)/SGW and buffering the subsequent downlink packets, in idle mode.

Certain functions require coordination between the HNB and HNB-GW due to the functional split described before. The Radio Access Network Application Protocol (RANAP) supports the UTRAN functions in the HNB, and the Home Node B Application Protocol (HNBAP) supports the HNB functions between the HNB and the HNB-GW. The HNB-GW, as mentioned before, provides concentration functions for both the user plane and the control plane. Table 2.1 and Table 2.2 describe the functional split, for both UTRAN function in HNB access and HNB function in HNB access.

Table 2.1. Functional split for UTRAN function in the HNB access (extracted from [7])

Function	HNB	HNB-GW	CN
RAB management functions:			
RAB establishment, modification and release	X	X <sup>Note1</sup>	X
RAB characteristics mapping I <sub>u</sub> transmission bearers	X	X	
RAB characteristics mapping U <sub>u</sub> bearers	X		
RAB queuing, pre-emption and priority	X		X
Radio Resource Management functions:			
Radio Resource admission control	X		
Broadcast Information	X	X <sup>Note 2</sup>	X
Iu link Management functions:			
Iu signalling link management	X	X	X
ATM VC management		X	X
AAL2 establish and release		X	X
AAL5 management		X	X
GTP-U Tunnels management	X	X	X
TCP Management		X	X
Buffer Management	X	X	
Iu U-plane (RNL) Management:			
Iu U-plane frame protocol management			X
Iu U-plane frame protocol initialization	X		
Mobility management functions:			
Location information reporting	X		X
Handover and Relocation			
Inter RNC hard HO, Iur not used or not available	X	X	X
Serving RNS Relocation (intra/inter MSC)	X	X	X
Inter system hard HO (UMTS-GSM)	X	X	X
Inter system Change (UMTS-GSM)	X		X
Paging Triggering	X		X
Paging Optimization		X	
GERAN System Information Retrieval	X		X
Security Functions:			
Data confidentiality			
Radio interface ciphering	X		
Ciphering key management			X
User identity confidentiality	X		X
Data integrity			
Integrity checking	X		
Integrity key management			X
Service and Network Access functions:			
CN Signalling data	X		X
Data Volume Reporting	X		
UE Tracing	X		X
Location reporting	X		X
Iu Co-ordination functions:			
Paging co-ordination	X		X
NAS Node Selection Function		X	
MOCN Rerouting Function		X	X
Note 1: This function could be needed for TNL address translation in the HNB-GW when there is no user plane direct transport connection between HNB and CN			
Note 2: HNB-GW is able to perform the filtering of SABP messages i.e. determines from the SAI list to which HNB the SABP message needs to be sent and then distributes the SABP messages to the appropriate HNBs. This is an optional function in HNB-GW.			

Table 2.2. Functional split for HNB function in the HNB access (extracted from [7])

Function	HNB	HNB-GW	CN
HNB Registration <sup>Note 1</sup>			
HNB Registration Function	X	X	
HNB-GW Discovery Function	X		
HNB de-registration Function	X	X	
UE Registration for HNB <sup>Note 1</sup>			
UE Registration Function for HNB	X	X	
UE de-registration Function for HNB	X	X	
lurh user-plane Management functions			
lurh User plane transport bearer handling	X	X	
Functions for multiplexing CS user plane on the Uplink	X	X	
<b>Traffic Offload Functions</b>			
LIPA	X		X
<b>Enhanced Interference Management</b>			
Mitigation of Interference from HNB to Macro	X		
<b>UE Access Control / Membership Verification</b>			
IDLE mode	X <sup>Note2</sup>	X	X
Connected mode (inbound relocation to HNB cells)		X	X
CSG ID validation	X	X	
CSG Subscription Expiry	X	X	X
<b>lurh Connectivity Functions</b>			
lurh Establishment	X	X <sup>Note 3</sup>	
Exchange of lurh Connectivity data for neighbor HNBs	X	X	
Note 1: Protocol support for this group of functions is provided by the HNB Application Protocol.			
Note 2: Access control or membership verification at the HNB are optional.			
Note 3: If the HNB-GW is involved in lurh Establishment, it acts only as pure relay for this signalling.			

## 2.1.2 Air Interface

This section presents the air interface of UMTS femtocells. Most vendors have focused the development of UMTS based HNBs since UMTS delivers higher data rates and deals better with high interference levels than Global System for Mobile communication (GSM) [18]. In UMTS Terrestrial Radio Access (UTRA), Code Division Multiple Access (CDMA) is the medium access technology used. However, for UMTS, the 3GPP Release 99 specifies the use of Wideband Code Division Multiple Access (WCDMA) (identified in Figure 2.1 as Uu). WCDMA is analogous to the situation where people in the same room and speaking the same language can understand each other, but people speaking another language are perceived as noise, Figure 2.2 shows this analogy. This technology uses the spread spectrum that allows users to transmit all over the available bandwidth, being the different transmissions separated by an orthogonal code, called spreading code. The data

signal is multiplied by a spreading code that increases the bandwidth of the signal, and the data is only extracted when the spreading code within the receiver is matched. The WCDMA chip rate of 3.84 Mcps, leads to a carrier bandwidth of approximately 5 MHz.

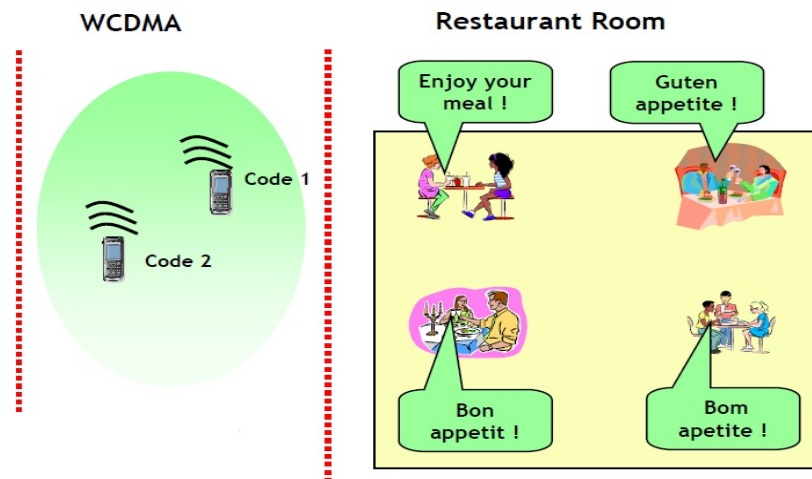


Figure 2.2. Analogy between WCDMA and a Restaurant Room (extracted from [19])

Each HNB uses a code of its own called a scrambling code, allowing the UE to differentiate the downlink signals coming from different femtocells. Also femtocells can distinguish different UEs by their scrambling code. An intelligent management of the scrambling codes can reduce the interference arising from surrounding femtocells in the UE. When entering the femtocell for the first time the UE needs to check all the available spreading codes, so to maintain the registration time as low as possible, the number of available spreading codes must be kept low.

WCDMA supports highly variable user data rates, where Bandwidth on Demand (BoD) is well supported. The user data is kept constant during each 10 ms frame, although data capacity among users can be changed from frame to frame. With this fast radio capacity allocation, the network can achieve an optimum throughput for packet data services.

WCDMA supports two basic operation modes: Frequency Division Duplex (FDD) and Time Division Duplex (TDD), but currently UMTS only considers FDD operation mode. In Europe, UMTS bands are [1920, 1980] MHz for Uplink (UL) and [2110, 2170] MHz for Downlink (DL) [20].

In UMTS, channels are often transmitted by mapping several upper layers channels into one lower-layer sub-channel. In a similar way, one upper-layer channel can be split across several lower-layer channels. There are three kinds of channels: logical, transport and physical channel. There are two types of channels: dedicated and common ones. The mapping of logical channels happens in the Medium Access Control (MAC) layer, being the transport channels mapped on the physical layer [3][19]. Figure 2.3 (a) and (b) illustrates the mapping of those channels.

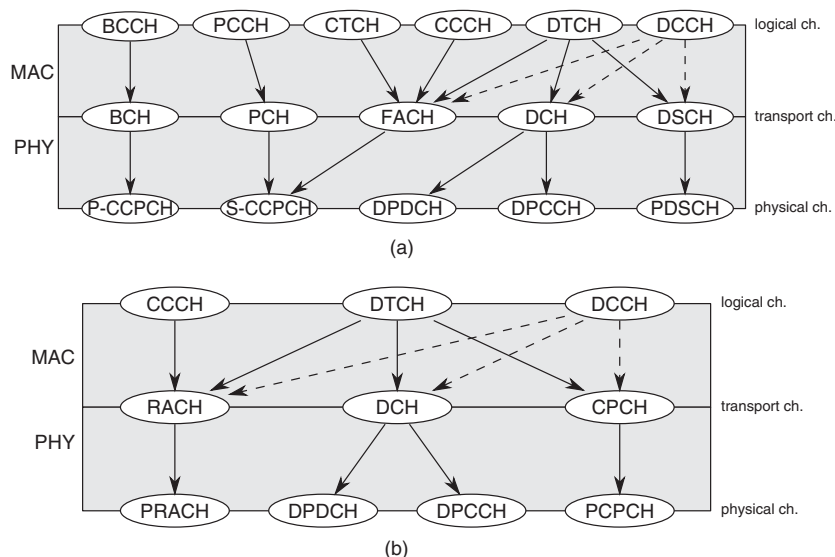


Figure 2.3. Mapping Upper-Layers into Lower-Layers. (a) Downlink. (b) Uplink. (extracted from [3])

The power control is one of the key features of WCDMA, and can be performed by two algorithms: open loop power control, used to set the initial transmission power, avoiding an excessive use of power and a closed loop power control to adjust the Signal-to-Interference Ratio (SIR) for each link, thus not wasting channel capacity.

Soft handover can be performed by WCDMA, in order to improve the signal quality. In the downlink, the UE receives the same data several times and combines them to increase its quality. For the uplink, a cell can receive the same message from several cells and combine them to increase the quality. These improvements allow the UE to use less power, reducing the interference level. If the interference level is too high, the call will drop because it is not possible to decode the data.

After Release 99, Release 5 and Release 6 were published by 3GPP: High Speed Downlink Packet Access (HSDPA) and High Speed Downlink Packet Access (HSUPA), respectively. HSDPA is a UMTS packet air interface that allows higher downlink peak rates, provides lower latency with reduced Round Trip Delays enabling great interactive applications, has enablers for high-speed transmission at the physical layer and fast scheduling. In Release 99, the scheduler has a part task of the RNC, but in HSDPA the scheduler is located in the Node B. Soft Handover and Power control are not supported as the link adaptation is now performed by the adaptation of Modulation with the Coding Rate.

HSPDA introduces new channels: High Speed Downlink Shared Channel (HS-DSCH) is used for data and shared by several users; the High Speed Physical Downlink Shared Channel (HS-PDSCH) is used to carry the HS-DSCH; and the High Speed Shared Control Channel (HS-SCCH) and the High Speed Dedicated Physical Control Channel (HS-DPCCH) for DL and UL signaling, respectively.

The use of a high order modulation, 16-Quadrature Amplitude Modulation (16-QAM), was introduced along with the Quadrature Phase-Shift Keying (QPSK) to achieve higher throughputs. From a code domain perspective, HSDPA uses a fix Spreading Factor (SF) of 16, allowing multi-code transmission (up to 15 codes/UE), depending on the UE capability, and parallel transmission (up to 4 UE/TTI) of

different users. While the total number of channelization code with spreading factor is 16, the total number of code was set to 15, because there is a need to have code space availability for common channels, HS-SCCH and for the associated Dedicated Channel (DCH). Due to the fact that a single user can receive up to 15 multi-codes, the resulting potential peak data rate is 10.8 Mbps. However the maximum specified peak data rate for HSDPA is 14.4 Mbps, when higher order modulation is used with no coding (effective code rate of one) and with 15 multi-codes. Figure 2.4 shows the theoretical peak user data rates.

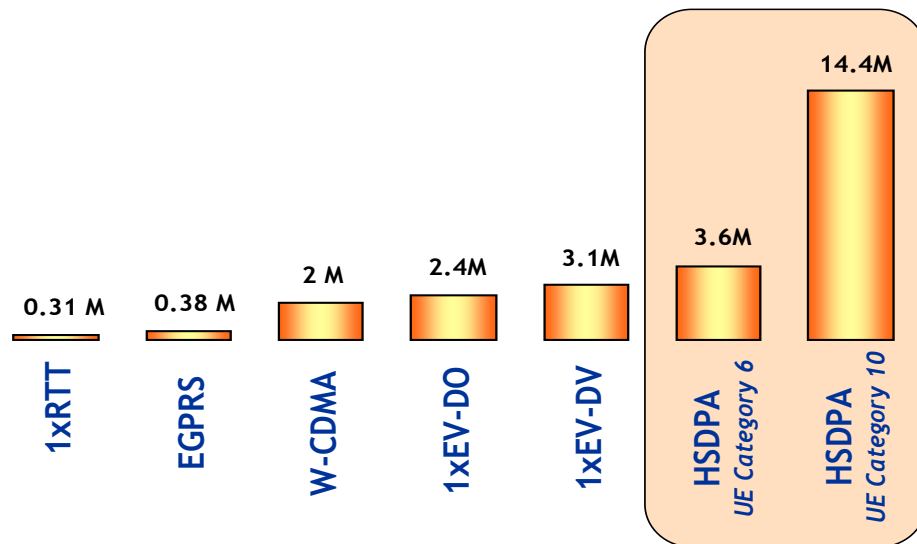


Figure 2.4. Theoretical Peak User Data Rates (extracted from [21])

Hybrid Automatic Repeat Request (HARQ) is also included in HSDPA for an increased speed of packet retransmission. This allows the UE to rapidly request retransmission of erroneous transport blocks until they are successfully received.

In Release 99, the radio transmissions were structured in frames of 10 ms. In this release, the supported Transmission Time Intervals (TTIs) were in the range of 10 to 80 ms. In HSDPA, the TTI was reduced to 2 ms, allowing a much faster scheduling and more often data transmissions over good radio links.

Adaptive Modulation and Coding (AMC) is a fundamental feature of HSDPA. It is used by the Radio Link Control (RLC) to optimize the user data throughput in the radio channel instead of using power control. Different combinations of modulation and channel coding rate can be used to provide different peak data rates, particularly when users experience more favorable channel conditions.

The HSDPA has enhanced the DL capabilities of UMTS. HSUPA was introduced by 3GPP to improve the UL data rate. The objective was to improve the performance of the uplink dedicated transport channels by scheduling the UL data rates of the UE depending on the interference and on the Node B processing resources, while increasing the radio interface robustness with the HARQ protocol associated with TTIs of 2 ms and 10 ms, keeping full compatibility with previous Releases (R99 and R5). HSUPA introduces the Enhanced Dedicated Channel (E-DCH). The main characteristics are fast

scheduling at Node B level, fast retransmission of data, QPSK modulation, uplink Noise Rise management in the Node B and uplink resource management in the Node B.

For HSUPA, a new set of channels were proposed: for DL, Enhanced HARQ Indicator Channel (E-HICH) indicates if the UL transmissions are well received, and Enhanced Absolute Grant Channel (E-AGCH) and Enhanced Relative Grant Channel (E-RGCH) indicate to the HSUPA UE (individually or per group) what are their allocated UL resources. In the UL, the Enhanced Dedicated Physical Data Channel (E-DPDCH) is responsible for carrying UL traffic and the Enhanced Dedicated Physical Control Channel (E-DPCCH) carries the UL signaling information. Scheduling in HSUPA is a multipoint-to-point procedure, therefore requiring a dedicated channel.

The scheduling has two major tasks: manages the E-DCH cell resources between UEs, and deals with uplink radio interferences.

For the HARQ mechanisms there are some differences between HSDPA and HSUPA. While in HSDPA the HARQ is a well-defined timing relationship between reception of the transport block and transmission of the acknowledgement by the Node B in HSUPA HARQ is based on synchronous retransmissions, where it has a maximum number of retransmissions configured per MAC-d flow and has a fixed number of Stop-and-Wait processes. In Table 2.3 we can see a comparison between HSUPA and HSDPA.

Table 2.3. Comparison between HSUP A and HSDPA (extracted from [22])

	Macrodiv	TTI	Modulation	Channel coding	Power control	HARQ	Fast scheduling	Fast link adaptation
<b>HSDPA</b>	Not supported	2 ms only	QPSK, 16QAM, 64QAM	Turbo	No	Supported	Supported	Supported
<b>HSUPA</b>	Supported	2 ms, 10 ms	BPSK and QPSK	Turbo	Yes	Supported	Supported but less reactive	Supported but less reactive

### 2.1.3 Coverage and Capacity

The planning and design of a WCDMA network must account for the distribution of the end users. The location of the users has great influence on the achievable coverage and capacity. Figure 2.5 illustrates some of the challenges faced by subscribers located indoors, served by outdoor macro cells.

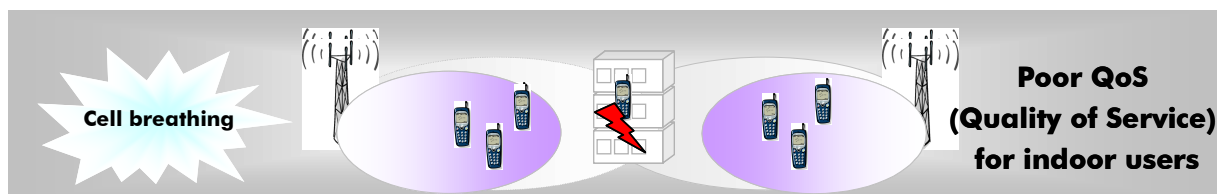


Figure 2.5. Indoor users served by outdoor macro cells (extracted from [23])

Providing service to indoor users will place disproportional high demands on the air interface resources of the outdoor macro cells (requiring a high proportion of the macro sites downlink power resources). The net effect is that the indoor coverage quality in such building is likely to be very poor and few subscribers will be supported.

With the success of IEEE 802.11 standard, also named as Wireless Fidelity (WiFi), femtocells base stations have been proposed, to extend macrocells coverage in indoor scenarios. Such solution ensures a greatly enhanced coverage quality and a corresponding higher number of subscribers support in indoor scenarios. Figure 2.6 shows indoor users served by a dedicated femtocell and the outdoor macro sites can support more subscribers.

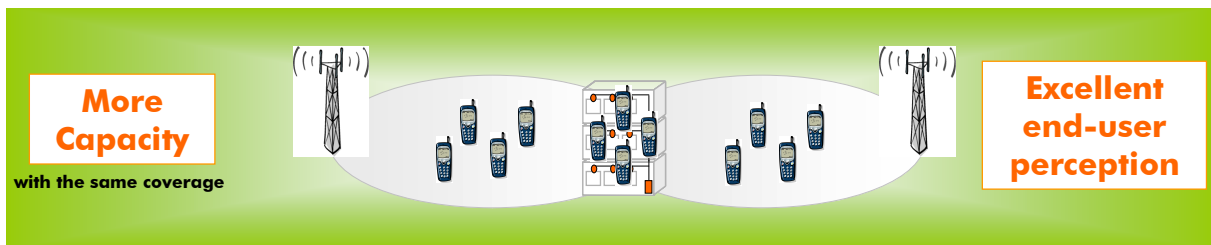


Figure 2.6. Serving indoor users with dedicated femtocells, and outdoor users with serving macrocell sites (extracted from [23])

Femtocells are small base stations directly installed by the customer in their home. With this kind of technology a customer can be assured of a high quality of service wireless data facility, with the advantages of voice support and UMTS mobility both indoors and outdoors.

Femtocells typically cover small areas and have fewer users, and because they have to be cheap [2], their output power and capacity are limited between 10 and 20 dBm and between four and thirty-two users [3], respectively. In Figure 2.7 one shows a comparison between femtocells and other type of cells, in terms of achievable range.

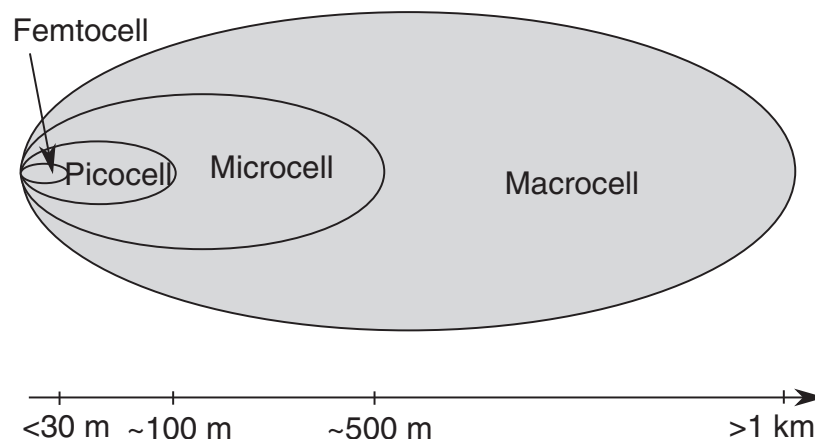


Figure 2.7. Comparison of cell sizes for different technologies (extracted from [3])

Within femtocell networks, outdoors users are connected to macrocells and when entering their home they automatically handoff their connection to their femtocell. This ensures a smooth communication

for the user and maximal coverage is obtained inside the home [10].

The main advantages of femtocells are the increase of coverage and network-capacity (number of cells are increased). For operators, femtocells are not only an efficient solution for increasing the indoor coverage, but also a cheap solution because customers pay for them. The alternative for increasing indoor coverage would be much more expensive for network operators, because they need to add more outdoor cells.

## 2.2 Mobility Management

One of the most challenging issues when deploying femtocells is the MM. In this chapter, an introduction to MM is given, methods for femtocells characterization are presented, access control is described, cell reselection and reselection is explained and cell handover is overviewed.

### 2.2.1 Introduction

MM is a very important feature for power consumption and signaling load reduction. The aim of MM is to track where subscribers are, allowing calls, SMS and other mobile phone services to be delivered to them. Femtocell to macrocell, macrocell to femtocell and femtocell to femtocell handovers have to be supported.

Apparently, no specific MM is necessary for femtocells, because they are expected to work within the existing network standards. However, its implementation breaks many aspects of the current network assumptions. This is mainly due to the following factors:

- Large number and high density of femtocells – The number of femtocells in the macrocell coverage is very large, and because the current neighbor cell list only allows having information 32 cells in it, it may not be sufficient to include all the femtocell information. There are only 512 Primary Scrambling Codes (PSC) shared within the network and it may not be sufficient to distinguish the cell identity of all the femtocells and macrocells.
- Dynamic neighbor cell lists – The neighbor cell list (NCL) is not stationary compared to the cell list within the macrocells. This is mainly due to the fact that users can either add or remove a femtocell, meaning that their locations are quite dynamic.
- Variant access methods – A femtocell can be in open, semi-open or fully closed access mode, which is configurable by the operators through the backhaul or by the user under the operator's supervision.
- User/Operator preference – A UE that approaches a femtocell coverage area, wants to assign the highest priority to the femtocell for best signal quality and cheaper billing package. For the operator, the fact that a UE is assigned to a femtocell means that macrocell load is reduced.

## 2.2.2 Femtocell Characterization

Signaling overhead between the macrocell users and femtocells will have a big impact on the performance of the network. The identifiers and mechanisms that characterize the aspects of femtocells are necessary for reducing the impact and enhancing the mobility procedures of supporting femtocells. With the help of the identifiers and mechanisms that distinguish a macrocell from a femtocell, the network can be treated as a two-layer network: macro-network and femto-network. Figure 2.8 illustrates this two-layer network.

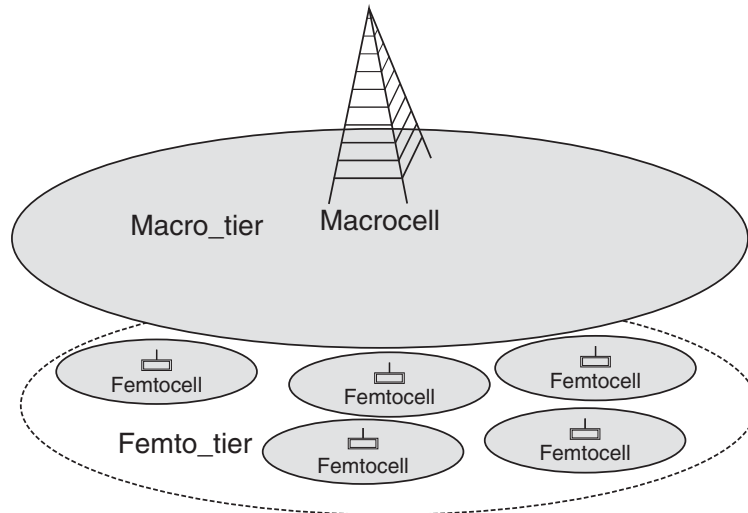


Figure 2.8. Two-layer network (extracted from [3])

Efforts can be made to enhance the mobility procedures and to reduce the signaling overhead between macro and femtocells. Reselection parameters can be configured to prioritize the femtocell users to camp on when they are entering the femtocell coverage area.

3GPP defines a special cell re-selection algorithm in a Hierarchical Cell Structure (HCS) environment [24]. With HCS, the reselection process will favor a smaller cell (with higher priority). This algorithm defines two layers: Macro or Femto/BS Router (BS). Figure 2.9 shows the priority levels for different kinds of cells.

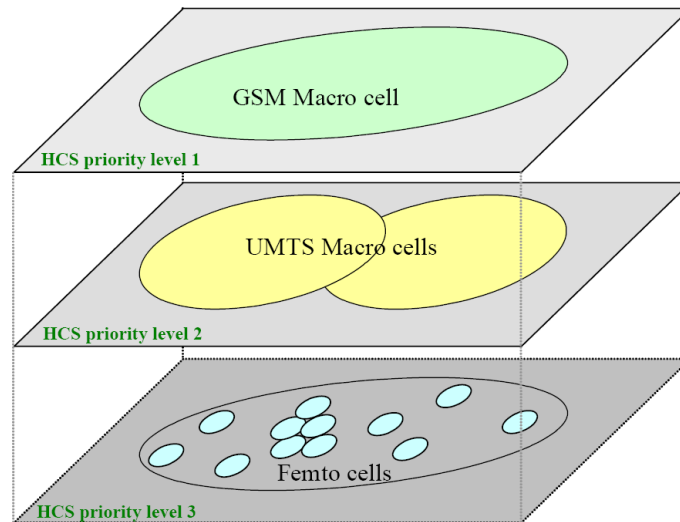


Figure 2.9. HCS priority levels for different kinds of cells (extracted from [25])

HCS can also consider the UE speed in the reselection process, which is given by the number of reselections that a UE performs in a given time. If a UE is moving in the coverage area of a single cell, it is considered to be static. If a UE is defined as moving, this reselection process will favor bigger cells, because a moving UE will go out of the coverage of the smaller cells quite fast, and therefore there is no real benefit of activating the HCS in this case. The HCS on the BS layer only makes sense if femtocells are deployed in-group and ensure a continuous coverage. This ensures that the UE does not leave the BSs coverage area, being possible to count the reselections between them to evaluate the speed. On the Macro layer, HCS makes more sense, as it gives some additional flexibility with additional timers. However, macro HCS could prevent an UE from reselecting a femtocell due to higher timers (the femtocell is not measured long enough).

Another method to distinguish femtocells from macrocells is the Separate Public Land Mobile Network (PLMN). Each operator is allocated one number or a number of PLMN IDs per country in which they operate. The PLMN ID consists of the Mobile Network Code (MNC) and the Mobile Country Code (MCC).

The femtocell is associated with one of the operator's PLMN IDs. The femtocell can have a separate PLMN ID, different from the PLMN ID of the macrocells, securing femtocell selection and minimizing the impact on macrocell users. Figure 2.10 shows a separate PLMN IDs network.

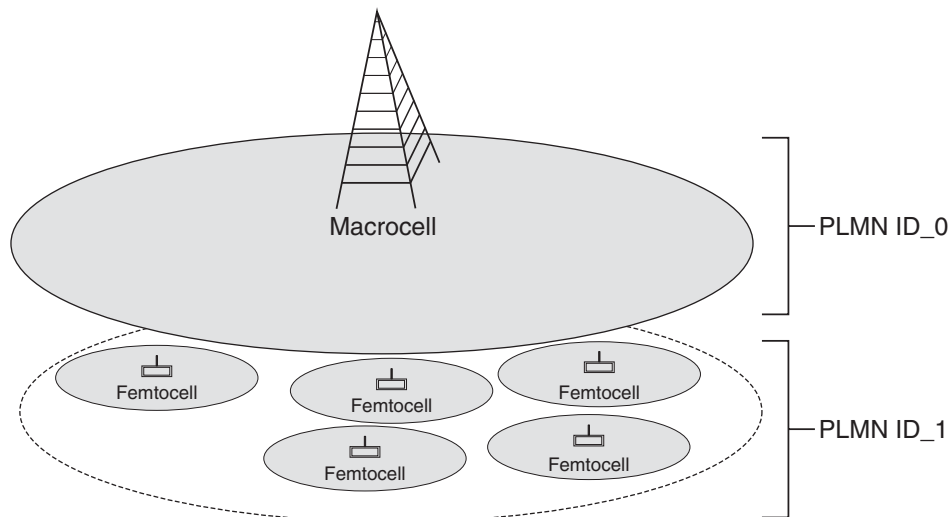


Figure 2.10. Separate femtocell PLMN ID (extracted from [3])

UEs that are not allowed to use a femtocell can be configured not to access the femtocell PLMN, resulting in better battery performance, and less signaling load towards the CN. A different PLMN ID allows the user to display the right network identifier, indicating to the user that he is camped in a femtocell.

In Release 8, 3GPP adopted, for UMTS, reserved frequency and PSC ranges. For better understanding of this method, only Closed Subscriber Group (CSG) cells are considered. Macrocells and femtocells may broadcast indications of one or more carrier frequencies used for CSG deployment. This information may be used for the UE that has no access to femtocells to avoid unnecessary measurements on that frequency. In UMTS the indications of which carrier frequencies are dedicated to CSG deployment can be signaled in the System Information Block (SIB) 11.

With shared carrier deployment, all CSG cells shall broadcast the reserved PSC range in their system information. This broadcast is only valid within the entire PLMN for 24 hours. The reserved PSC list may be signaled in the SIB 3 or SIB 11, being the first used by the CSG cell and the other by the macrocell. Figure 2.11 (a) and (b) shows how macrocells and femtocells are separated from each other by reserved PSCs, for both dedicated and shared carrier scenarios.

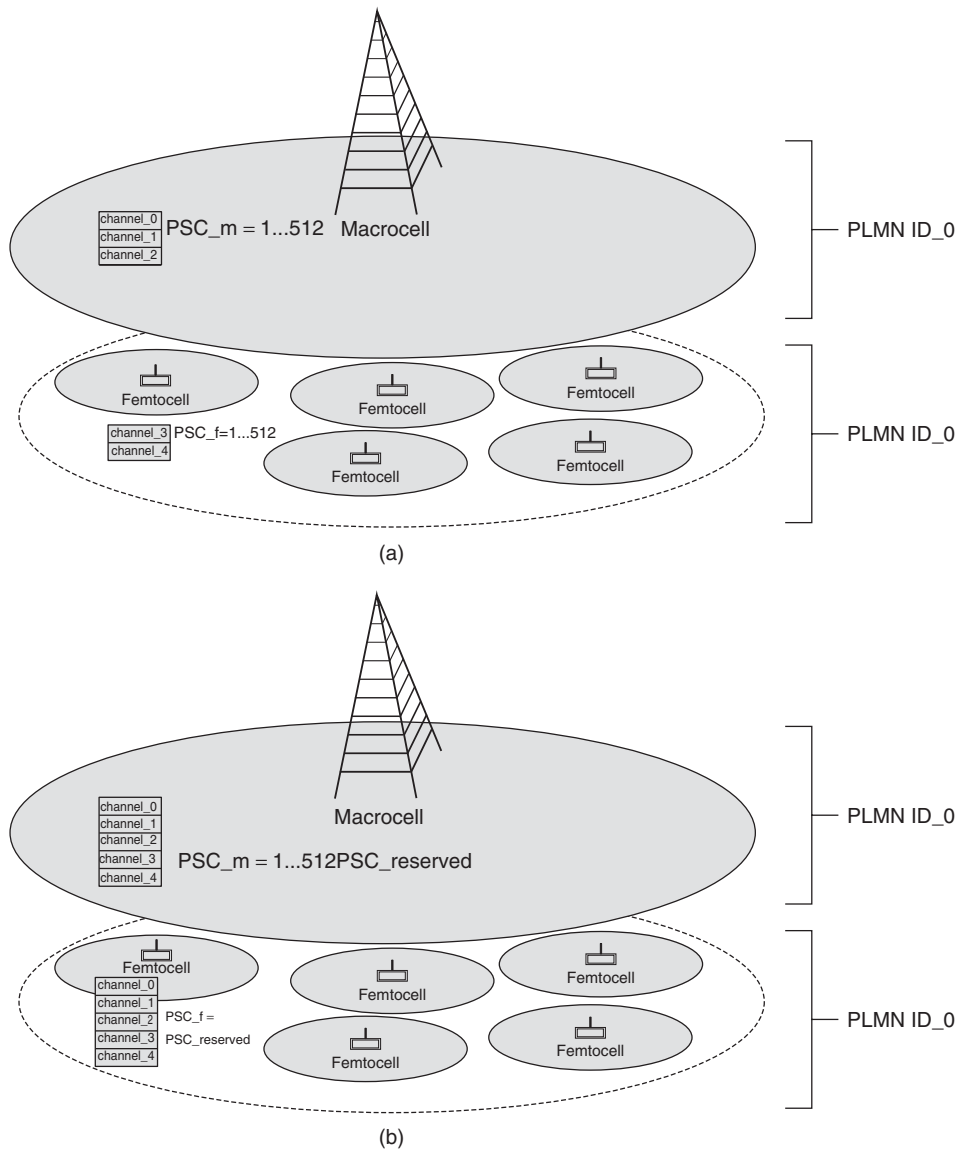


Figure 2.11. Separate femtocells from macrocells by means of dedicated frequencies or reserved PSCs. (a) Dedicated carrier. (b) Shared carrier. (extracted from [3])

### 2.2.3 Access Control

The access control mechanism plays an important role in mitigating cross-tier interference and handover attempts, which is why they have to be carefully chosen, depending not only on the customer profile but also on the scenario under consideration.

There are two situations when access control is triggered [15]. A common assumption is that access control is done by MM signaling, where each femtocell is assigned to a specific Location Area (LA) and UE's that are not allowed in a certain femtocell receive a negative response at location registration, being unable to camp normally in that femtocell. An alternative approach is to allow UE's, that are allowed to use femtocells to roam and camp, where they are not allowed [15]. In this

approach, access control would be triggered when data transmission service is requested. The non-allowed UEs would be redirected or handed over to an available macrocell.

Different access modes have been proposed: Closed access mode, where only a subset of users, defined by the femtocell owner, can connect to the femtocell. 3GPP referred to this model as the CSG, being the only featured access mode in release 8 [15]. Two other access modes have been presented by 3GPP in Release 9. The Open Access mode, where all users have the right to make use of any femtocell deployed by the operator, meaning that it operates as a normal cell. This mode is used to fill some indoor blind spots and some public hot spots and therefore the mobile network doesn't need to perform any specific UE access control; The Hybrid Access Mode is a combination of both open and closed access modes at the same time. This mode not only has a CSG ID, but also allows UEs that are not members to access the femtocell, having only a limited amount of resources available, reaching a compromise between the impact on the performance of subscribers and the level of access granted to non-subscribers. In Table 2.4, a comparison between the main features of closed and open access femtocells is presented.

Table 2.4. Comparison between Closed and Open Access femtocells (extracted from [26])

Closed access femtocells	Open access femtocells
Higher interference Lower network throughput Serves only indoor users Home market Easier billing	More handovers Higher network throughput Increased outdoor capacity SMEs, hotspots Security needs

## 2.2.4 Cell Selection and Reselection

Cell Selection and reselection are two basic mobility procedures in wireless mobile networks. Cell selection is performed in order to select a suitable cell to camp on, when the UE is powered on or followed by a recovery from lack of coverage. The UE selects a PLMN and the cell selection is performed under that PLMN. Cell reselection however, enables the UE to select a new serving cell when the cell reselection criterion is met.

In release 8, cell selection follows the strongest cell as the serving cell. By checking the CSG IDs against the UE's Allowed CSG List (ACL) during cell selection, the UE can avoid selecting an unauthorized femtocell as the serving cell. This procedure is called Automatic Cell Selection. In addition, manual CSG cell selection (release 8) can be used to enable the user to select a CSG ID. The UE is only allowed to select its serving CSG manually in idle mode. In connected mode, the manual cell selection is not supported, to avoid interruption to the current UE service. In release 9, non-CSG cells have to be taken into account. For open access femtocells, users do not need to check the CSG ID to camp on it, because this type of cells does not have the CSG ID. For hybrid access, the checking of the CSG ID has to be performed in order to distinguish whether the UE is in its CSG or not.

By introducing the CSG ID and UE autonomous search function in release 8, a femtocell-featured cell

reselection can now improve the reselection procedures for femtocells. This autonomous search function determines when and where to search for the allowed CSG cells, being disabled if the UE's CSG whitelist does not exist or is empty. The UE can now carry out cell measurements over suitable femtocells without knowing the NCL from the macrocell. Depending on the information broadcast by the network, the UE may select a cell from: the same FDD frequency (Intra-frequency), another FDD frequency (Inter-frequency) and another radio access technology (Inter-RAT). It shall be possible to UEs that are allowed to access a given CSG cell, to prioritize their camping towards the CSG cell when in the coverage of the CSG cells. Reselections to femtocell, from femtocell and between femtocells are described in [27].

## 2.2.5 Cell Handover

Cell handover enables the UE to transfer the service seamlessly from its serving cell to the target cell without terminating the service. Soft handover is not supported since there is no Iur interface for femtocells in the UTRA. Mobility from a macrocell to a femtocell from the network perspective is described in [7]. Handover to a femtocell follows the framework as specified in [7] and [28]. Handover to a femtocell is different from the normal handover procedure in three aspects:

- Proximity Estimation – in case the UE is able to determine, based on UE implementation, that it is near a CSG or non-CSG cell whose CSG ID is in the UE's CSG whitelist, the UE may provide to the Serving Radio Network Controller (SRNC) an indication of proximity. The CSG proximity indication may be used as described in [27].
- PSC/PCI Confusion – Since the cell size of the femtocell is typically much smaller than the cell size of macrocells, there can be multiple femtocells, within the coverage of the SRNC, that have the same PSC or Physical Cell Identity (PCI). In this case the SRNC is unable to determine the correct target cell for handover from the PSC/PCI included in the measurement reports messages (MRM) from the UE. This confusion is solved by the UE reporting the cell identity of the target femtocell.
- Access Control – If the target cell is a hybrid cell, prioritization of allocated resources may be performed based on the UE's membership status. Access control is done in a two-step process: The UE first reports the membership status based on the CSG ID received from the target cell and the UE's CSG whitelist; The network verifies the reported status.

Femtocells normally save the information of neighboring cells in their NCL by means of a self-configuration function. The handover from a femtocell to a macrocell is expected to be the same as the procedure specified by [28].

Release 8, expects that femtocells are to be deployed on home-based scenarios. In these situations, handover between femtocells rarely happens since the owner of the femtocell would not like the neighbor to camp on his femtocell. For enterprise or metro-zone scenarios, the femtocells usually belong to the same CSG. Both procedures of handover between femtocells are described in [27].

## 2.3 Propagation Models

### 2.3.1 Introduction

In mobile communications the surrounding environment is a key factor for both design and performance of the networks. Propagation models are divided into two categories: empirical and theoretical. The empirical ones are based in measurements that conduct to simple relationships between distance and attenuation. The advantage of these models is that they account for all the factors influencing propagation, but on the other hand, they need to be validated for different environments. The theoretical ones provide an approximation to the real environment, through assumptions that simplify the problem. The advantage of these models is that they allow for an easy change in parameters; however, when the scenario changes these models show low versatility. Nowadays, propagation models contemplate both approaches, which gives greater flexibility, in order to adjust they models to different scenario. These adjustment minimizes the error between the signal estimation and the reality. Another important aspects of propagation models is that it does not exist a model that can be applied in all scenarios and environments.

The selection of a model depends on the type of environment, because each type differs in some parameters: terrain ondulation, building density and height, open areas density, water areas density and vegetation. These environments are classified in three types: rural, suburban and urban. The rural environment is characterised by the large open areas, flat terrains without obstacles. Suburban type has terrains with few obstacles, i.e, small residential areas. The urban type is a highly dense environment, with buildings that have four or more floors, normally large cities and industrial areas.

Also it is important to point out the classification of cells, which is done according to their radius range and to the relative position of the BS antennas. For this type of classification is divided in four categories: large macro, small macro, micro and picocells. Although, femtocells are not under this classification, they can be seen as smaller picocells. Relevant for this work are small macro and picocells, since they are both used in urban scenarios. Small macro are built above roof-top level, which does not guarantee Line of Sight (LoS) in some areas, in the other hand, picocells, due to their usage of extending outdoor coverage into indoor areas, are always built under the roof- top. The coverage range of a small macro is between 0.5 and 3 Km and for picocells less than 200 m.

The characteristics that degrade the performance of an indoor models are quite different that the ones that degrade outdoor models, for this reason it is important to have these models in order to reduce the interference in this environment. Taking into account several parameters, such as building size variations, shape and strcture, construction materials and room layouts, becomes a complex multipath study. Therefore, these models are a suitable alternative, without the need of performing measures on site. The next section will give a detailed description of the existing models for both environments. For a correct analysis, the selected models take into account the fact that this work is dealing with UMTS urban small macro cells and indoor femtocells. For this reason two models were chosen as suggested in [29]: COST231 – Walfisch-Ikegami [30] for outdoor; COST231 – Multi-Wall [30] for indoor.

In order to estimate, i.e., the maximum loss that a system can tolerate due to propagation one needs to calculate the link budget. Annex A shows in greater detail the link budget calculations. However, one should introduce the generic path loss expression [20]:

$$L_p = P_{Tx} + G_{Tx} - P_{Rx} + G_{Rx} \quad [dB] \quad (2.1)$$

where:

- $L_p$  – Total path loss;
- $P_{Tx}$  – Transmitter output power;
- $G_{Tx}$  – Gain of the transmitting antenna;
- $P_{Rx}$  – Receiver power;
- $G_{Rx}$  – Gain of the receiving antenna;

This path loss can be obtained by the combination of outdoor and indoor losses, as Figure 2.12 shows:

$$L_p = L_{p_{ind}} + L_{p_{out}} \quad [dB] \quad (2.2)$$

where:

- $L_{p_{ind}}$  – Path loss attenuation given by the indoor model;
- $L_{p_{out}}$  – Path loss attenuation given by the outdoor model;

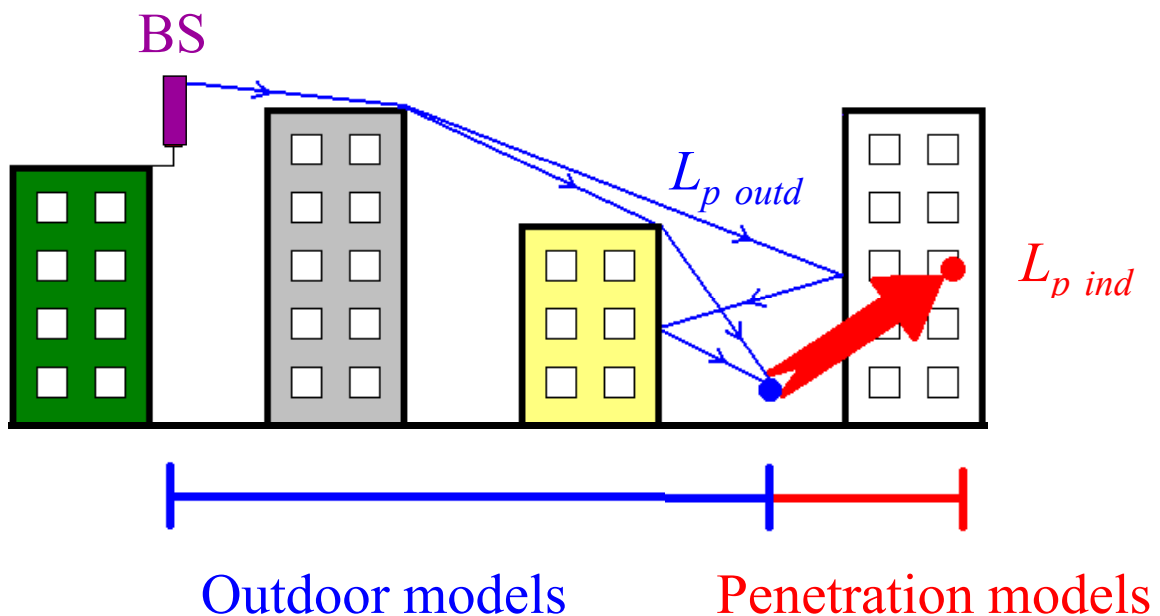


Figure 2.12. Illustration of indoor and outdoor losses (extracted from [20])

## 2.3.2 Outdoor and Indoor Models

For outdoor environments two models are suggested by [20], COST231 – Okumura-Hata and COST231 – Walfisch-Ikegami. The Okumura-Hata is based on Hata [31] and Okumura [32] models whereas Walfisch-Ikegami is based on Walfisch-Bertoni [33] and Ikegami [34] models. Both models were developed for urban, suburban and rural environments, however they have particularities: Okumura-Hata handles large distances, usually more than 5 Km, while Walfisch-Ikegami (WI) is used for small distances, less than 5 Km, in urban and suburban environments. Since this work is based on an urban scenario and from the fact that in this type of environments BS's are most of the times at less than 5 Km, WI was chosen over Okumura-Hata. WI is detailed in Annex B.

The WI takes into account the same assumptions of the Walfisch-Bertoni model in terms of urban structure. This urban structure is regular with equal height buildings and the propagation is being done perpendicular to the street axis which shown in Figure 2.13.

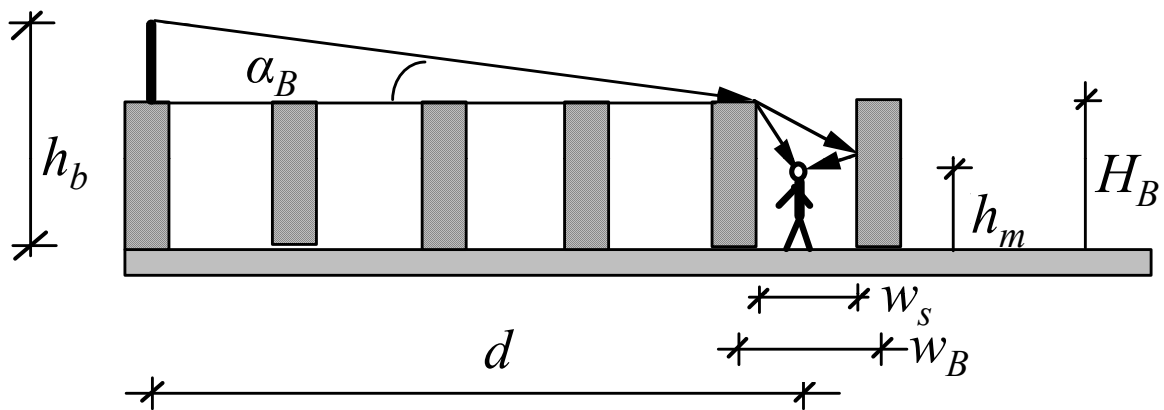


Figure 2.13. Urban Structure (extracted from [20])

For indoor models, COST231 considers three models [30]. The first model, one-slope model, assumes a linear dependence between the path loss and the logarithmic distance. The second one is the linear attenuation model, which assumes that the excess path loss is linearly dependent on the distance (meters) multiplied by attenuation coefficient added to the free space loss. Finally the Multi-Wall Model (MWM) gives the path as the free space loss added with losses that are introduced by wall and floors penetration that are in the direct path between the transmitter and the receiver.

One of the most interesting characteristics of the MWM is given by (2.3), which states that the total floor loss is a non-linear dependence of the number of floors penetrated. The average loss and wall and floor types are shown in Table 2.5.

$$L_p = L_{FS} + L_{glass} + \sum_{i=1}^l k_{wi} L_{wi} + k_f L_f \quad [dB] \quad (2.3)$$

where:

- $L_{FS}$  – Free Space loss between the transmitter and receiver;
- $L_{glass}$  – Glass loss Attenuation;
- $k_{wi}$  – Number of penetrated walls of type  $i$ ;
- $k_f$  – Number of penetrated floors;
- $L_{wi}$  – loss of wall type  $i$ ;
- $L_f$  – loss between adjacent floors;
- $l$  – number of wall types;

Table 2.5. Wall and floor types for MWM and weighted average loss (extracted from [35])

Loss category	Description	Factor [dB]
$L_f$	Typical floor structures (i.e. offices): hollow pot tiles, reinforced concrete, thickness type < 30 cm	2
$L_{w1}$	Light internal walls (<10cm): plasterboard, walls with large numbers of holes (e.g. windows)	10
$L_{glass}$	Typical glass	1

However, and due to the purpose of this thesis, two models that are used in this work should be introduced: the Path Loss Model for Outdoor to Indoor and Pedestrian Test Environment that is based in the WI model and the Path Loss Model for Indoor Office Test Environment which is derived from the MWM model are used in this work. These models are recommended by [36] and will be described in greater detail in Annex B.



## Chapter 3

# Fundamentals of Positioning

This chapter introduces the fundamentals of positioning, including basic concepts, infrastructures. The basic positioning methods are detailed. Also, precision and accuracy errors are illustrated. Finally, the state of the art is given.

## 3.1 Basic concepts

Positioning is a process of obtaining the spatial location of a target. There are various positioning methods, which differ in the number of parameters, such as quality, overhead and so on. In general, the following elements are used to determine the position of a target:

- One or several experimentally determined parameters (observables).
- A positioning method.
- A descriptive or spatial reference system.
- A positioning infrastructure.
- Protocols that coordinate the positioning process.

The observables are the basic data of any positioning method and usually reflect the spatial relationship between the target and a single or a number of fixed points in the surrounding environment, with well known coordinates. They are obtained from measurements, e.g, angles, ranges, range differences or the target velocity. By utilizing signals, normally denoted as pilot signals or simply pilots, these measurements are performed.

After the required number of observables has been collected, the target's position can be obtained from the coordinates of the fixed points and the results of the measurements. The calculation of the position is usually based on a specific method, which depends on the type of observables used. An overview of the basic positioning methods, their respective observables and measurement methods is presented in Table 3.1.

The positioning methods require a descriptive or spatial reference system to obtain the location of the target. The selection of this reference system strongly depends on the chosen method. Some systems provide descriptive locations in terms of cell identifiers, room numbers and floors; others give spatial coordinates based on WGS-84, UTM or alternative reference systems.

Because of the inability of a target to autonomously derive its position, a distributed infrastructure that implements positioning is required. Figure 3.1 illustrates the different components of such a typical infrastructure. Each target must be equipped with a terminal, which corresponds to the entity whose position needs to be located. BS's are required for most positioning methods, either to perform measurements or to assist the terminal in doing them. Furthermore, they are fixed points of well-determined coordinates against which the spatial relation of a terminal can be measured. The infrastructure components need to be coordinated and controlled by protocols in order for positioning to be achieved.

Table 3.1. Overview of positioning methods (adapted from [14])

<b>Positioning method</b>	<b>Observable</b>	<b>Measured by</b>
<b>Proximity sensing</b>	Cell-Id, coordinates	Sensing pilot signals
<b>Lateration</b>	Range	Travelling time or Path loss of pilot signals
	Range difference	Travelling time difference or Path loss difference of pilot signals
<b>Angulation</b>	Angle	Antenna arrays
<b>Dead reckoning</b>	Position	Any other positioning method
	Direction of motion	Gyroscope
	Velocity	Accelerometer
	Distance	Odometer
<b>Pattern Matching</b>	Visual images	Camera
	Fingerprint	Received signal strength

Because of the inability of a target to autonomously derive its position, a distributed infrastructure that implements positioning is required. Figure 3.1 illustrates the different components of such a typical infrastructure. Each target must be equipped with a terminal, which corresponds to the entity whose position needs to be located. BS's are required for most positioning methods, either to perform measurements or to assist the terminal in doing them. Furthermore, they are fixed points of well-determined coordinates against which the spatial relation of a terminal can be measured. The infrastructure components need to be coordinated and controlled by protocols in order for positioning to be achieved.

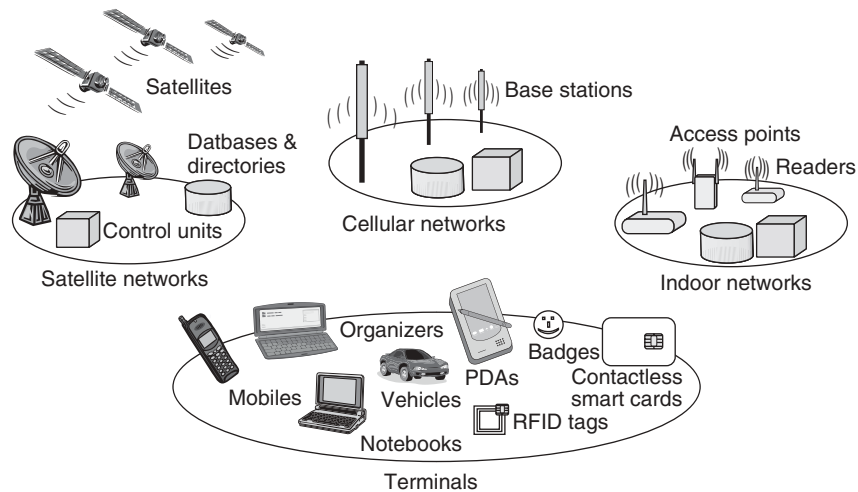


Figure 3.1. Positioning infrastructures (extracted from [14])

There are several criteria for evaluating the quality of the positioning methods and of the calculated position:

- Accuracy and precision – They are the most important parameters. Accuracy refers to the closeness of several position fixes to the true but unknown position of a target. Precision reflects the closeness of a number of position fixes to their mean value.
- Yield and consistency – The yield of a positioning method is its ability to obtain position fixes in all environments, while consistency is a measure of stability of accuracy in different environments.
- Overhead – It can be classified as signaling and computational overhead. The former refers to the waste of processing power that occurs in the control units or databases of the network and at the terminal; the later reflects the amount of messages that are exchanged between the terminal and infrastructure as well as within the network, to control positioning.
- Power consumption – It is only important at the terminal, since mobile devices normally have short power resources and high power consumption is at the expense of standby and talktimes. Power consumption is correlated with signaling and computational overhead, for positioning.
- Latency – Refers to the time period between a position request and the subsequent delivery of a position fix.
- Roll-out and operational costs – Roll-out costs and operational costs are related to the installation and complexity of a positioning infrastructure, respectively.

As presented in Table 3.1 and due to the scope of this thesis, only the methods using path loss, cell-id and coordinates are exploited. The reason for this selection comes from the parameters that were selected to develop the algorithm, which will be detailed in the next chapter.

## 3.2 Positioning Infrastructures

Positioning and positioning infrastructures in cellular networks are generally classified into three classes according to: (i) integrated and stand-alone infrastructure; (ii) network and terminal-based positioning and satellites; and (iii) cellular and indoor infrastructure.

An integrated infrastructure is a wireless network used for both communications and positioning purposes. This type of network was initially designed for communications. But through the reuse of BS's, mobile devices and protocols for location and MM, it is also able to perform positioning. The selection of an integrated infrastructure has the advantage that the network does not need to be built from scratch. But, on the other hand, the capacity of the network for user traffic decreases.

A stand-alone infrastructure is a network that works independently of the cellular network. GPS is the archetypal of this type of infrastructure, but indoor solutions have also been developed. The drawbacks of this approach are the high rollout and operating costs and the additional requirement of new software or equipment for target location.

The distinction between network-based and terminal-based positioning is only made because in the former the measurements and position calculation are carried out by the BS and in the latter by the UE. Alternatively, a hybrid approach called terminal-assisted network-based positioning can be used, where the UE performs the measurements and then transmits the results to the network for position calculation. A reverse configuration, network-assisted terminal-based positioning, is also available but is rarely used. The advantages of network-based over the terminal-based systems are that older devices can be located without updating need, and the fact that subscribers usually refuse to change a device just to use new network features.

Another criterion to classify positioning systems is to consider the type of network in which they are implemented and operated. In this case three categories are distinguished: (i) satellite positioning; (ii) cellular positioning; and (iii) indoor positioning.

Satellite positioning is usually used to cover vast geographical areas, and thus satellite positioning can pinpoint the location of a target on a whole continent or even the entire world. The main advantages of strategies based on satellite positioning are the higher accuracy of position fixes and the global availability of satellites. On the other hand, Non-Line of Sight (NLoS) between transmitter and receiver, especially in indoor environments, can cause poor accuracy and satellite receivers have high power consumption.

Cellular positioning relies on cellular networks like GSM or UMTS, to obtain the positions of subscribers. In this case, location management procedures are used, which frequently have insufficient accuracy and inappropriate location formats like cell and location-area identifiers. To improve these deficiencies network operators have extended their networks, by introducing auxiliary components and protocols. One such strategy consists in the use of several positioning methods in parallel, in order to improve availability and accuracy. These methods are normally network-based so that older devices, incapable of positioning, can be integrated in the system. Unlike satellite

positioning, cellular networks operate around a country, with very good availability in terms of yield, enabling almost permanent indoor positioning. One drawback of this type of positioning strategy, if high accuracy is required, is the fact that it degrades capacities used for voice or data transmissions, due to the increasing signaling overhead.

Indoor positioning is based on radio, infrared or ultrasound technologies for short-range communications and is normally realized by a stand-alone infrastructure or in conjunction with Wireless Local Area Networks (WLAN). The benefits of this approach are that utilizes low power consumption devices and for short-ranges high accuracy is achieved. There is, however, a lack of open, well-specified systems, such as in GPS or cellular positioning, due to standardization issues.

### 3.3 Basic Positioning Methods

In this section basic positioning methods will be introduced. Only proximity sensing and lateration will be described in greater detail, due to the scope of this thesis.

#### 3.3.1 Proximity Sensing

Proximity Sensing is a method that estimates the position of the target by using the BS coordinates that are received either on uplink pilot signal, if positioning is network assisted, or on downlink pilot signal, for terminal assisted positioning. Figure 3.2 (a) illustrates a cell configuration with an omnidirectional antenna and Figure 3.2 (b) shows a configuration with sectorized cell with a directional antenna. In this method the position of the target is assumed to be the known position of the BS that sends or receives the pilot signals. This approach is implemented according to different standards. Some of them are based on recommendations from official standardization authorities and others are operator- or vendor-specific solutions.

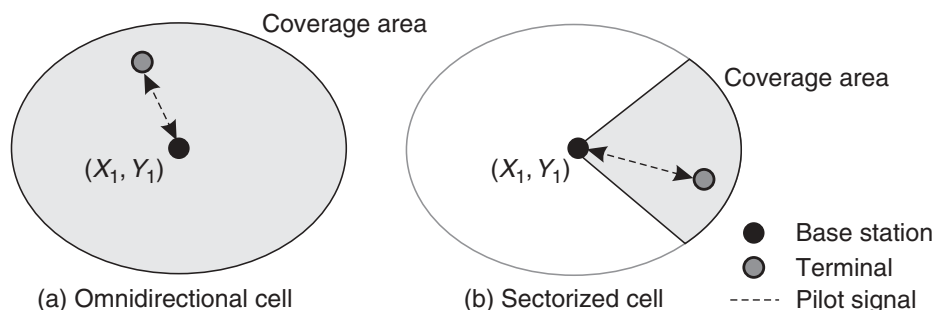


Figure 3.2. Proximity Sensing (extracted from [14])

This method, in cellular systems, is known as Cell of Origin (CoO), Cell Global Identity (CGI) or simply Cell-ID. It can be applied in two situations: (i) in an ongoing connection, where the target position is simply given by the coordinates of the serving BS (network-based variant); (ii) in idle, where the

terminal listens to a broadcast transmission of the nearby BS's and from there a receiver identifier of the position fix can be obtained by contacting a remote database that performs a mapping of the identifiers to BS's coordinates. To avoid signaling overhead, operators can include in the broadcast messages the BS's coordinates. Because this approach is terminal-based, it may be subject to standardization. There are, however, various proprietary solutions.

Proximity sensing has been very popular in cellular networks, because it requires simple modifications to the existing infrastructure and causes fewer signal overheads, when compared to other methods. The major problem is the degree of accuracy, which is strongly dependent on the cell radius that can vary from 100 m in urban areas to tens of kilometers in rural areas [37]. As such, this method does not fulfill many LBS and emergency services requirements [38]. It constitutes, however, a good potential solution when an indoor positioning system is in view, because, in this case, the technologies used imply a limited coverage range.

### 3.3.2 Lateration

In lateration, the observables may be either an absolute range or a range difference. For positioning at least three BS's are needed. The observables are used to set-up a system of  $n$  non-linear equations, where  $n$  represents the number of BS's, for position estimation. For  $n = 3$ , lateration is called trilateration. Circular lateration is normally selected if the observables consist of absolute ranges; hyperbolic lateration is used in conjunction with difference ranges. Both observables can be obtained by performing time measurements or Received Signal Strength (RSS) measurements. Both range measurements are subject to errors. They are therefore designated pseudo ranges to stress the fact that they differ from the true position with a certain potential error. This uncertainty is mainly due to inaccurate clock synchronization and both refraction and multipath propagation of the signals. The accuracy normally increases with the number of observables available.

#### Circular Lateration

As mentioned before, Circular Lateration is calculated through absolute ranges. If Circular Lateration uses time measurements it is called Time of Arrival (ToA). Figure 3.3 shows a 2-D solution of this method. Knowing the range between a terminal and a BS one can limit the position of the target to a circle of radius  $r_1$  around the BS (Figure 3.3a). When two BS's are considered (Figure 3.3b), the position of the target is limited to the two points originated by the intersection of the circles centered on the BS's. Figure 3.3c shows that the position of the target can be reduced to a point, when a third BS is considered. For a 3-D geometry, instead of circles, each range defines a sphere around the BS's. The intersection of two spheres defines a circle, and the intersection of three spheres restricts the position of the target to two points. In most cases, one of these points corresponds to an unrealistic location (normally a point in the water), whose elimination allows a definite positioning of the target. This unambiguous positioning can alternatively be achieved by adding a fourth BS. The calculation of the target's position is based on Pythagoras theorem. Assuming that  $(X_i, Y_i)$

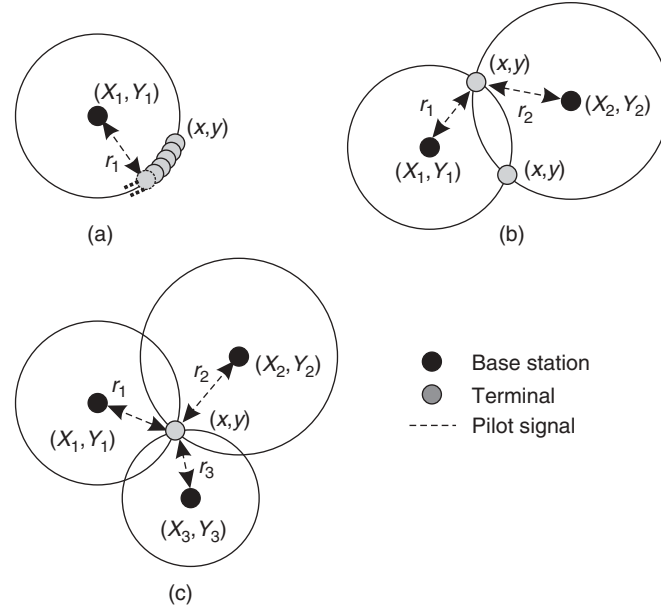


Figure 3.3. Circular Trilateration in 2D (extracted from [14])

Cartesian coordinates of the  $i$ th BS and  $(x, y)$  are the corresponding coordinates for unknown position of the target, then the range  $r_i$  between the  $i$ th BS and the target is given by:

$$r_i = \sqrt{(X_i - x)^2 + (Y_i - y)^2} \quad i = 1, 2, 3, \dots, k \quad [\text{meters}] \quad (3.1)$$

where:

- $r_i$  – distance between the  $i$ th BS and the target (in meters);
- $(X_i, Y_i)$  – cartesian coordinates of the  $i$ th BS (in meters);
- $(x, y)$  – cartesian coordinates of the target (in meters);

In general, the BS (known) coordinates and the target's (unknown) positioning are expressed as latitude and longitude. In this case the application of (3.1) requires firstly the conversion of the elliptical coordinates of the BS into Cartesian coordinates and secondly the reverse conversion of the calculated Cartesian coordinates of the target.

The determination of  $(x, y)$  relies on an iterative process of least square fits. The first step is to transform the non-linear equations into a system of linear equations. This can be implemented in two ways. The first one uses a reference BS, to compute all the equations. Consider the set of equations corresponding to a series of  $n$  circles defined by the position of  $n$  BS's:

$$\begin{aligned} r_1^2 &= (X_1 - x)^2 + (Y_1 - y)^2 \\ r_2^2 &= (X_2 - x)^2 + (Y_2 - y)^2 \\ &\vdots \\ r_n^2 &= (X_n - x)^2 + (Y_n - y)^2 \end{aligned} \quad [\text{meters}] \quad (3.2)$$

Expanding all equations in (3.2) and subtracting the first one from all the others leads to:

$$\begin{aligned}
(X_2 - X_1)x + (Y_2 - Y_1)y &= \frac{1}{2}[(X_2^2 - X_1^2)x + (Y_2^2 - Y_1^2)y - (r_2^2 - r_1^2)] \\
(X_3 - X_1)x + (Y_3 - Y_1)y &= \frac{1}{2}[(X_3^2 - X_1^2)x + (Y_3^2 - Y_1^2)y - (r_3^2 - r_1^2)] \\
&\vdots \\
(X_n - X_1)x + (Y_n - Y_1)y &= \frac{1}{2}[(X_n^2 - X_1^2)x + (Y_n^2 - Y_1^2)y - (r_n^2 - r_1^2)]
\end{aligned} \tag{3.3}$$

The system of (3.3) can then be expressed in matrix form:

$$Ax = h \quad [\text{meters}] \tag{3.4}$$

where:

$$A = \begin{bmatrix} X_2 - X_1 & Y_2 - Y_1 \\ X_3 - X_1 & Y_3 - Y_1 \\ \vdots & \vdots \\ X_n - X_1 & Y_n - Y_1 \end{bmatrix} \tag{3.5}$$

$$h = \frac{1}{2} \begin{bmatrix} (X_2^2 - X_1^2) + (Y_2^2 - Y_1^2) - (r_2^2 - r_1^2) \\ (X_3^2 - X_1^2) + (Y_3^2 - Y_1^2) - (r_3^2 - r_1^2) \\ \vdots \\ (X_n^2 - X_1^2) + (Y_n^2 - Y_1^2) - (r_n^2 - r_1^2) \end{bmatrix} \tag{3.6}$$

$$x = \begin{bmatrix} x \\ y \end{bmatrix} \tag{3.7}$$

The second method involves a Taylor series expansion combined with a least squares procedure. A first estimation of the target's position denoted  $(\tilde{x}, \tilde{y})$  needs to be initially computed. A correction vector needs to be applied to the estimated position. Applying the Taylor series to the function of the pseudo range,  $p_i$ , to the  $i$ th BS, leads to:

$$p_i = \sqrt{(X_i - x)^2 + (Y_i - y)^2} = p_i(\tilde{x} + \Delta x, \tilde{y} + \Delta y) \quad i = 1, 2, 3, \dots, k \quad [\text{meters}] \tag{3.8}$$

- $p_i$  – measured pseudorange between the  $i$ th BS and the target (in meters);

For the position fix, only the first order expansion is determined as:

$$p_i(\tilde{x} + \Delta x, \tilde{y} + \Delta y) = p_i(\tilde{x}, \tilde{y}) + \frac{\partial p_i}{\partial x} \Delta x + \frac{\partial p_i}{\partial y} \Delta y \quad [\text{meters}] \tag{3.9}$$

Solving the partial differentials in this equation yields:

$$\frac{\partial p_i}{\partial \tilde{x}} = \frac{-X_i + \tilde{x}}{\sqrt{(X_i - \tilde{x})^2 + (Y_i - \tilde{y})^2}} = a_i$$

$$\frac{\partial p_i}{\partial \tilde{y}} = \frac{-Y_i + \tilde{y}}{\sqrt{(X_i - \tilde{x})^2 + (Y_i - \tilde{y})^2}} = b_i$$
(3.10)

Substitution of (3.10), (3.9) leads to:

$$p_i(\tilde{x} + \Delta x, \tilde{y} + \Delta y) = p_i(\tilde{x}, \tilde{y}) + a_i \Delta x + b_i \Delta y \quad [meters]$$
(3.11)

- $p_i(\tilde{x}, \tilde{y})$  – pseudorange between the estimated position and the position of the  $i$ th BS (in meters);

Let  $\Delta p_i$  denote the difference between the pseudorange,  $p_i(\tilde{x}, \tilde{y})$  and the observed pseudorange, then (3.11) becomes:

$$\Delta p_i = a_i \Delta x + b_i \Delta y \quad [meters]$$
(3.12)

where (3.12) can be expressed by (3.4):

$$A = \begin{bmatrix} a_1 & b_1 \\ a_2 & b_2 \\ \vdots & \vdots \\ a_n & b_n \end{bmatrix}$$
(3.13)

$$h = \begin{bmatrix} \Delta p_1 \\ \Delta p_2 \\ \vdots \\ \Delta p_n \end{bmatrix}$$
(3.14)

$$x = \begin{bmatrix} \Delta x \\ \Delta y \end{bmatrix}$$
(3.15)

A 3-D solution can be obtained by adding the z coordinate to all the above equations. For both methods, if the number of BS's equals three the solution of (3.4) is expressed by:

$$x = A^{-1}h \quad [meters]$$
(3.16)

If more than three BS's are involved a solution can be found by using a least-squares method:

$$x = (A^T A)^{-1} A^T h \quad [meters]$$
(3.17)

To provide better accuracy and reduce the number of iterations it is possible to set-up a covariance matrix Q of the observation, which is applied to (3.17):

$$x = (A^T Q^{-1} A)^{-1} A^T Q^{-1} h \quad [\text{meters}] \quad (3.18)$$

As a consequence of the uncertainty associated with the difference between the pseudo range and the actual range, the intersection of the three circles does not give a definite point but a span area of a size. This area depends on the degree of accuracy of the range measurements. Figure 3.4 illustrates the potential error that results from inaccurate range measurements. One disadvantage of this method is the necessity for clock synchronization between the transmitter and the receiver. Thus, a fourth transmitter is usually required.

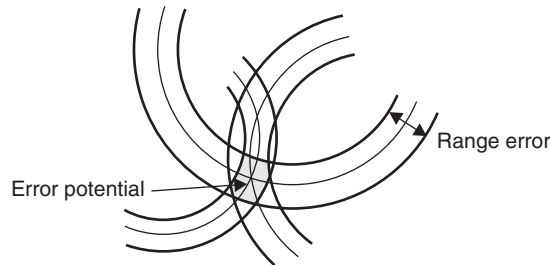


Figure 3.4. Potential error of Circular Lateration (extracted from [14])

## Hyperbolic Lateration

Hyperbolic Lateration uses range differences instead of absolute ranges. It is termed Time Difference of Arrival (TDoA) in cellular networks, because it uses time differences between BS's to obtain the range differences. The set of all points, between two fixed points, for which the difference in the range is constant defines a hyperbola. Figure 3.5 shows a 2-D representation of this approach. As illustrated in Figure 3.5 (a), the difference range between two BS's limits the target's position to a hyperbola. If another range difference between one of the two BS's and a third is determined, the intersection of the two hyperbolas gives the target's position, as illustrated in Figure 3.5 (b).

As for Circular Lateration, a system of linear equations can be defined, where each equation expresses the range difference with regard to a particular pair of BS's.

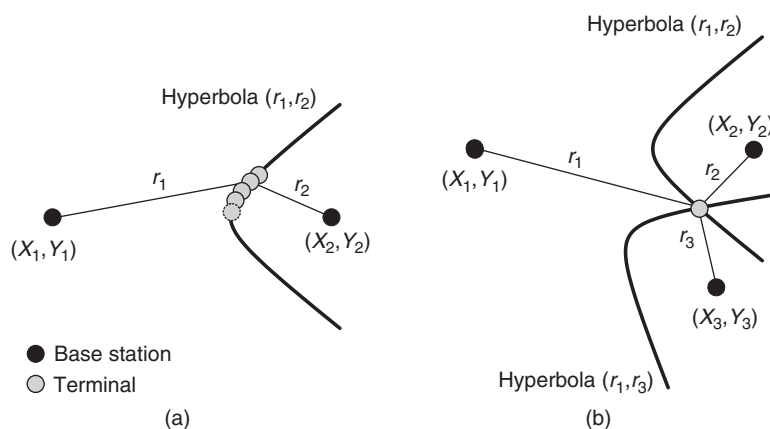


Figure 3.5. Hyperbolic Lateration in 2D (extracted from [14])

Normally, a reference BS is selected and all range difference measurements are expressed relative to it. The system of linear equations is given by:

$$d_{ij} = r_i - r_j = \sqrt{(X_i - x)^2 + (Y_i - y)^2} - \sqrt{(X_j - x)^2 + (Y_j - y)^2} \quad [meters] \quad (3.19)$$

where:

- $d_{ij}$  - difference between the ranges  $r_i$  and  $r_j$  of the  $i$ th and  $j$ th BS's with  $i \neq j$  (in meters);
- $r_j$  - distance between the  $j$ th BS and the target (in meters);
- $(X_j, Y_j)$  - cartesian coordinates of the  $j$ th BS (in meters);
- $(x, y)$  - cartesian coordinates of the target (in meters);

To compute a solution, the major difference between Circular and Hyperbolic Lateration, results from the coefficient of matrix A. If the reference base is indicated by  $i = 1$  the coefficients are as follows:

$$\begin{aligned} \frac{\partial d_{1j}}{\partial \tilde{x}} &= \frac{-X_1 + \tilde{x}}{\tilde{r}_1} - \frac{-X_j + \tilde{x}}{\tilde{r}_j} = a_i \\ \frac{\partial d_{1j}}{\partial \tilde{y}} &= \frac{-Y_1 + \tilde{y}}{\tilde{r}_1} - \frac{-Y_j + \tilde{y}}{\tilde{r}_j} = b_i \end{aligned} \quad (3.20)$$

with:

$$\tilde{r}_i = \sqrt{(X_i - \tilde{x})^2 + (Y_i - \tilde{y})^2} \quad i = 1, 2, 3, \dots, k \quad [meters] \quad (3.21)$$

where:

- $\tilde{r}_i$  - range between the target and the  $i$ th BS with regard to the estimated position (in meters);

Instead of  $\Delta p_i$  in (3.12), the system of equations now expresses the deviation,  $\Delta d_{ij}$ , between the range difference of the  $j$ th BS relative to the target's observed position on one hand and the range difference based on its estimated position on the other hand. To solve the system of equations for three BS's it is necessary to use (3.16). If the number of BS's exceeds three the solution relies on (3.17). As mentioned before (3.18) is applied in order to improve the accuracy. To obtain a 3-D solution it is necessary to add the z coordinate in (3.19)-(3.21). The intrinsic uncertainty of Hyperbolic Lateration due to inaccurate range difference measurements is illustrated in Figure 3.6.

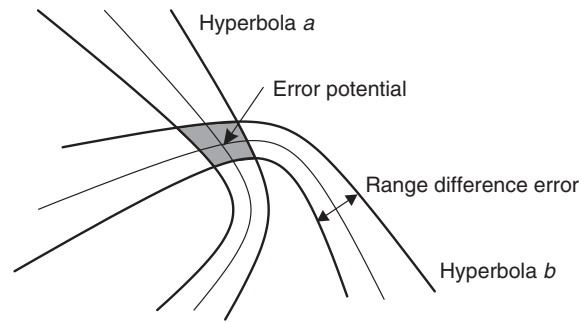


Figure 3.6. Potential error of Hyperbolic Lateration (extracted from [14])

### 3.3.3 Other Methods

In addition to Lateration a number of other methods can be use for position estimation. Angulation uses the angles between the target and the BS's, as the observables to estimate the target's location. This method is also known as Direction of Arrival (DoA) or Angles of Arrival (AoA). Its main drawback is the requirement that the handset or BS be equipped with antenna arrays. It is preferably to install, in BS's, this antenna array system over every handset because it is easier. The angle of a pilot signal is measured at the BS therefore restricting the target's position to a line that intersects both the target and the BS. To obtain the target's position it is necessary to take into account the angle of a second BS as shown in Figure 3.7.

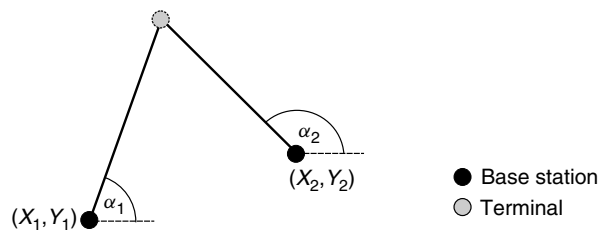


Figure 3.7. Angulation in 2D (extracted from [14])

Angulation may suffer from bad resolution of antenna arrays, and hence the observed angle is rather a rough approximation of the actual angle. The more the target is closer to the BS the more accurate this approximation will be. However, if NLoS exists between the transmitter and the receiver, problems with multipath propagation will arise. Therefore, the greater the number of available measurements the better the accuracy of the target positioning. Figure 3.8 illustrates the potential error resulting from these effects.

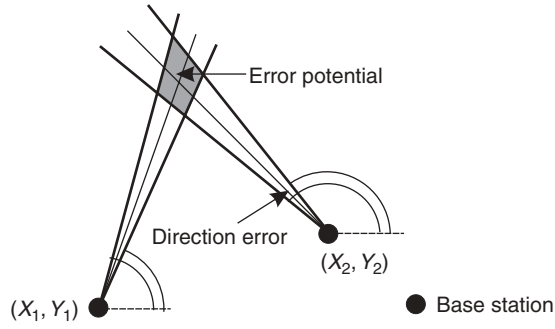


Figure 3.8. Potential error of Angulation (extracted from [14])

The angle for the  $i$ th BS is expressed as

$$\alpha_i = \tan^{-1}\left(\frac{Y_i - y}{X_i - x}\right) \quad [rad] \quad (3.22)$$

where:

- $\alpha_i$  – angle of the arriving pilot signal at the  $i$ th BS;

As for Lateration, a least square fit is used for the approximate solution and a Taylor series is applied for linearization, The mathematical expressions of these steps are analogous to (3.9)-(3.12), where the observed angles are expressed as a function  $\varphi(x,y)$  of an estimated position and a correction vector  $[\Delta x, \Delta y]$ ,

$$\varphi_i(x,y) = \tan^{-1}\left(\frac{Y_i - y}{X_i - x}\right) = \varphi_i(\tilde{x} + \Delta x, \tilde{y} + \Delta y) \quad [rad] \quad (3.23)$$

where:

- $\varphi(x,y)$  – observed angle of the arriving pilot signal at the  $i$ th BS;

and the partial differentials of the Taylor series expansion are given by:

$$\begin{aligned} \frac{d\varphi_i}{d\tilde{x}} &= \frac{\sin\varphi_i}{r_i} = a_i \\ \frac{d\varphi_i}{d\tilde{y}} &= -\frac{\cos\varphi_i}{r_i} = b_i \end{aligned} \quad (3.24)$$

The solution of the system is then achieved through (3.18).

Another method relies on pattern matching. The main principle consists in observing the scene where the positioning is to be applied and draw conclusions about the target's location from the observation. Pattern matching is classified as optical and nonoptical.

Optical version, also known as scene analysis, compares visual images of a site generated by a camera with each other. This scene analysis can be subdivided into static and dynamic. In static

scene analysis, position is estimated by comparing the observed images with stored images, while for dynamic scene analysis position estimation is achieved through differences of successive images taken on a scene.

In nonoptical pattern matching, also known as fingerprinting, other physical quantities are taken into account. Two steps are executed in this case. The first step involves having the site of interest covered by a grid and for each point of it the observer collects RSS measurements from multiple BS's, resulting in a vector of RSS values, also called the fingerprint. The next phase is to compose a sample vector of RSS values, at the current position, and then report them to a server. The server tries to match the received samples with the fingerprint thus estimating the target's position [39].

This approach overcomes different problems like, NLoS, shadowing and multipath effects. Another advantage is the fact that in some systems, terminals may require no or minor modifications. The major disadvantage is the requirement of databases to store fingerprints.

A hybrid method is another approach. This comes from the combination of all the positioning methods mentioned earlier. The main motivation is to provide higher accuracy, which is, for example, necessary for meeting accuracy standards defined by national authorities to enhanced emergency services [38]. One hybrid approach is to combine Hyperbolic Lateration with Angulation which provides better accuracy than using them separately [40].

### 3.4 Accuracy and Error Sources

As mentioned above, measurement errors lead to an intrinsic uncertainty in positioning. Various national and international authorities have defined a number of standards for assessing the uncertainty of positioning for survey and mapping purposes. Most of them are based on the concepts of root mean squares (RMS) or standard deviations ( $\sigma$ ) [41].

Often accuracy is specified at a specified confidence level, meaning that a certain percentage of the measured samples have an error equal or smaller than the accuracy level reported. The most common levels are 68.27%, 95% and 95.45%.

For a one-dimension,  $x$ , the accuracy as measured by the root mean squares error (RMSE) is given by:

$$RMSE_x = \sqrt{\frac{\sum_{j=1}^n (x_j - x_t)^2}{n}} \quad [meters] \quad (3.25)$$

where:

- $x_t$  – true target's position;
- $x_j$  – estimated target's position;

For two-dimensions, the accuracy, also known as horizontal accuracy, is given by:

$$RMSE_{xy} = \sqrt{RMSE_x^2 - RMSE_y^2} \quad [meters] \quad (3.26)$$

If  $RMSE_x$  and  $RMSE_y$  are equal (3.26) can be rewritten as:

$$RMSE_{xy} = \sqrt{2RMSE_x^2} = \sqrt{2RMSE_y^2} = 1.4142RMSE_x = 1.4142RMSE_y \quad [meters] \quad (3.27)$$

If, however,  $RMSE_x$  and  $RMSE_y$  are not equal but  $\frac{RMSE_{min}}{RMSE_{max}}$  is between 0.6 and 1.0 (where  $RMSE_{min}$

is the smaller value between,  $RMSE_x$  and  $RMSE_y$  and  $RMSE_{max}$  is the corresponding larger value), the circular standard error may be approximated as:

$$RMSE_{xy} = 0.5(RMSE_x + RMSE_y) \quad [meters] \quad (3.28)$$

for a confidence level of 39.35%.

The most common error sources contributing to the positioning uncertainty are:

- Clocks – Inaccurate and instable clocks lead to errors in measured ranges or range differences. Even with mechanism of clock synchronization and mathematical models for eliminating offsets and drifts, there is always a certain potential error remainder.
- Ionospheric and thropospheric refraction – Atmosphere refractions are also a source of error. They result in small deviations of the speed of pilot signals from the speed of light. It is also possible to limit these errors to a certain degree according to mathematical models.
- Multipath propagation – As a consequence of multipath propagation, different copies of a signal may overlay at the receiver and distort the amplitude and phase of the signal. This may be a particularly serious problem if ranges are determined by RSS or phase measurements. Fingerprints of a certain scene may also be useless if the configuration of the scenes changes.
- NLoS – This error arises due to multipath propagation. If LoS exists the first arriving pulse of the pilot signal is assumed to have traveled in LoS and the subsequent pulses arrive from reflected paths. However, if NLoS exists the pulses arrive from reflected paths that may lead to enormous time delays and degraded RSS signals, thus inferring errors to range calculations. This is a major problem for angulation positioning because a reflected signal may arrive from practically any direction at the BS.
- Medium Access – If subscribers within a cell and neighboring cells are transmitting on the same carrier, near-far-effect and hearability problems may arise. The first effect results in a signal break to terminals that are further away from the serving BS due to the proximity of another terminal. In the worst case the signals of distant terminals are regarded as noise or interference when arriving at the serving BS. Hearability appears in the downlink, where the signals of farther BS's cannot be properly received of even heard by the terminal that is in the close distance of its serving BS. This may be a problem for lateration, where at least three BS's are necessary for position estimation.

- BS coordinates – It is a major problem in satellite positioning, where the satellites are exposed to perturbing forces in their orbital motion, thus deviating the satellites true position from the calculated one. In cellular networks, this can be avoided by accurate surveying.
- Bad geometry – A bad geometry of the BS's may lead to significant errors on range and angles measurements. This corresponds to situations where, for example, the BS's are arranged along a line or if they are arranged very close to each other. As a consequence, the different radio paths arrive at the terminal at very shallow angles, increasing the potential error.

The errors of all positioning methods for different environments are thoroughly discussed in [37].

### 3.5 State of the Art

In this section a brief overview of the state of the art is present, to show what has been done in this field up to now, to enhance the work done in this thesis.

Femtocells are a recent technology, their deployment started in 2007 in the United States and in 2010 in Europe, namely the United Kingdom, as stated in [42]. The Small Cell Forum published in 2012 a white paper [13] explaining four methods to determine a femtocell location. The Assisted Global Navigation Satellite System (AGNSS) is described by having an accuracy of less than 20 m with about 95% certainty by the use of “self-surveying” receivers. The “self-surveying” is a 24-hour survey period that is recommended, as it will average across all multipath scenarios for a given antenna given that the satellites return to almost the same positions in the sky after 24 hours. Furthermore, it is described that the multipath environment largely determines the accuracy of this method. The second method described is the Cellular Network Listen with its accuracy between 100 and 300 m. In this method it is necessary to have at least 3 BS's in order to apply the TDoA method. The Hybrid AGPS-Femto Sniff is also present in this white paper. This concept, as name already indicates, involves Assisted-GPS (AGPS) and femtocell sniffing. The sniffing mode operates whenever the AGPS fails to synchronize. With this method the accuracy would be from 20 m to 300 m for the sniffing mode and 50 – 300 m in the AGPS mode. Also, it is mentioned that the GPS has accuracy from 50 to 20 meters. Finally it is said that GPS receiver is deployed with or within each femtocell in the United States, due to good GPS signals in North American homes.

In [43], Pesyna, Wesson, Heath and Humphreys propose a Tightly-Coupled Opportunistic Navigation strategy to extend the penetration of AGPS femtocells in order to improve their weak-signal in indoor environments, due to standards and regulatory agencies that impose strict location requirements on femtocells. With this solution it was indicated that the femtocell could acquire and track GPS signals down to 5 dB-Hz, allowing the positioning accuracy provided by the GPS to be extended to the majority of residential femtocells deployment meeting the necessary requirements imposed by the cellular standards and regulatory agencies.

In terms of positioning solutions, based on time and power measurements, a variety of studies were made. Wang, Zhu and Liu proposed a WCDMA locating method that uses a Weighted Least Square (WLS) method in [44]. In this proposal they try to correct the location errors caused by the field measurements and distance calculations. Although the obtained results did not meet the FCC requirements this method has the advantage of not needing any modifications to the mobile network and phones. In [39], it is proposed a network-based positioning method without the need of modification to the mobile terminals. The main difference between this method and the prior one is that a set of pre-measured signals is stored in a location server in the network. The measured signals are then matched with the ones stored in the location server in order to obtain the location of the target. The results are promising being the accuracy of 70-90 m for 67% of the measurements and for 90% of the measurements 130-195 m, however this measurement does not meet the FCC requirements [11].

In [37], different approaches for positioning are given, whether it is for GSM or for UMTS. Angulation, Circular and Hyperbolic Lateration, Fingerprinting are all positioning methods that are overviewed. Three positioning mechanisms are detailed: (i) network-based (e.g Uplink Time Difference of Arrival, Database Correlation Method and Pilot Correlation Method); (ii) terminal-based (e.g GPS, AGPS and Observed Time Difference of Arrival); (iii) non-conventional (e.g Bluetooth, Positioning via WLAN and MyLocation by Google). Also, some methods are compared, in terms of accuracy and precision, for three different areas: rural, suburban and urban. Finally it is concluded that the GPS is the method with higher accuracy, between 5 and 30 meters. Nevertheless, it is explained the difficulty on implementing the AoA, that Lateration methods show better results than Cell-ID and that the AGPS due to its characteristics is the best fit for all environments and that it will dominate the positioning market in the future.

# Chapter 4

## Models and Algorithm Development

In this chapter a functional description of the proposed positioning algorithm is provided. The first section explains the models, for propagation and positioning that were used. After giving an overview of the algorithm, both propagation and positioning algorithms are presented in detail. The last section describes the algorithm assessments.

## 4.1 Models

To understand some of the theoretical decisions made in the proposed algorithm some assumptions were made mainly concerning the study case and the models. In this section both propagation and positioning models are explained.

The scenario in study was a real neighborhood with a very high density of buildings. To simplify, for outdoor propagation models, all streets were assumed being perpendicular to each other and having the same width. All buildings were considered to have the same characteristics, i.e, width, length, height and each floor with 3 m of height. In addition, in terms of floor penetration, for indoor propagation, three-story buildings were considered because most of them had actually three floors.

The algorithm was divided in two major parts: (i) if a UE does not know its position, there is the need to calculate it. This situation occurs, either because the UE does not have GPS capabilities or because it is in an indoor situation where the GPS is unavailable; (ii) after calculating the positions of at least three UE's or the three positions of the same UE in distinct periods of time, the femtocell receives those positions (by MRM) to calculate its location; The algorithm used to calculate the positions of the UE is based only in Circular Lateration or Hyperbolic Lateration. These two Lateration methods are used in the algorithm so that they can be compared. For the femtocell a hybrid approach is used, meaning that for different situations that will be explained in Section 4.1.2, it uses either Circular/Hyperbolic Lateration or RSS-based Circular Lateration. Also in this case the Circular and Hyperbolic Lateration is used for comparison reasons. Another difference between the positioning algorithms are the fixed points used. For positioning an UE, the fixed points used are BS's and to position a femtocell, the fixed points used are the UE's.

### 4.1.1 Propagation Models

Using the RSCP's that the UE receives from the surrounding BS's or a femtocell, the UE-BS and UE-femtocell distances can be calculated using a Path Loss Models.

In outdoor environments, Okumura-Hata model cannot be used because the distances between an UE and BS's are less than 5 Km [20]. WI model is used in these situations, where distance is less than 5 Km for urban and suburban environments. Therefore, the model selected was the COST231 – WI due to better path loss prediction and consequently better distance prediction, since it considers more parameters to describe the environment, namely buildings height, streets width, building separation and street orientation with respect to the direct radio path [20]. Another model that has been chosen for hybrid environments (Outdoor and Indoor) is the Path Loss Model for Outdoor to Indoor and Pedestrian Environment. The reasons for selecting this model were three: (i) outdoor UE's can be connected to the femtocell (active set), being both able to exchange MRM; (ii) the UE can be in an indoor environments and therefore being unable to calculate its position via GPS. In this case, there is

the need to use the outdoor BS's to calculate the UE coordinates; (iii) when the femtocell (indoor) enters in the sniffing mode, it can sniff the surrounding BS's (outdoor) in order to calculate its location. Furthermore, this mode is important if a change on the environment occurs, e.g, change in the location of the femtocell. The surrounding cells are normally outdoor BS, however they can be femtocells as well. This model is used in cases of NLoS and takes into account parameters like time delay-spread, geometrical and excess path loss, shadow fading, multipath fading characteristics and operating radio frequency, but describes the worse propagation case [36]. The total path loss between the transmitter and the receiver is given by (B.20). For this particularly case, a typical urban environment and assuming that  $\Delta h_b = -5m, \Delta hm = 10.5m$ ,  $x = 15m$  and  $b = 80m$ , the total path loss between the transmitter and the receiver, calculated by (4.1), which is a simple function that depends only on the distance between the transmitter and the receiver and frequency:

$$L_p = 40\text{Log}_{10}(R) + 30\text{Log}_{10}(f) + 49 \quad [dB] \quad (4.1)$$

where:

- $R$  – Distance between the transmitter and the receiver (in Kilometers);
- $f$  – frequency (in MHz);

Where  $L_p$  shall in no circumstances be less than the Free Space Path Loss (FSPL).

Being femtocells an indoor solution, it is necessary to have indoor path loss model to calculate the distance between the UEs and the femtocell, for an indoor environment. In Section 2.3.2 the indoor models are described. The path loss model used, for this environment, is the Path Loss Model for Indoor Office Environment that is based on the COST 231 model. The choice of this model was done based on the fact that a real scenario is in study and there was the need to simplify the model equations (Annex B.3), because some of the characteristics of the buildings were not known, i.e, typical floor structures, light internal walls and internal walls [36]. Another assumption made for this model is that number of penetrated floors is 3 instead of the 4 (average number), for moderately pessimistic environments calculations [36]. The simplified equation for the indoor path loss has the following form:

$$L_p = 37 + 30\text{Log}_{10}(R) + 18.3 * n \left( \frac{n+2}{n+1} \right)^{-0.46} \quad [dB] \quad (4.2)$$

where:

- $R$  – Distance between the transmitter and the receiver (in meters);
- $f$  – frequency (in MHz);
- $n$  – number of penetrated floors in the path;

Where, once again,  $L_p$  shall in no circumstances be less than the FSPL.

Nevertheless and only for outdoor environments, if the distance between the transmitter and the receiver is less than 20 meters, it is assumed that LoS exists between them and therefore the FSPL model is applied to compute the distance.

The path loss models are selected according to the type of environment in which the UE is. If a femtocell is the serving cell it is assumed that the UE is in an indoor environment, otherwise it is assumed that the UE is in an outdoor environment. This is a reasonable assumption because femtocells are very short-range BS's, meaning that when the femtocell is the serving cell the UE-femtocell distance is very short. Regardless these assumptions, the UE positioning and femtocell positioning use different pathloss models. When the femtocell is the serving cell and to locate the UE, the path loss model used is the Path Loss Model for Outdoor to Indoor and Pedestrian Environment, because the UE is in an indoor environment and the BS's are located in an outdoor environment. To locate the femtocell, in this situation, it is used Path Loss Model for Indoor Office Environment, because the UE and the femtocell are located in an indoor environment. For the situation where the femtocell is the non-serving cell, it is assumed that the UE is located in an outdoor environment and the path loss models used are COST 231 – WI, for UE positioning, and the Path Loss Model for Outdoor to Indoor and Pedestrian Environment, for locating the femtocell. Figure 4.1 illustrates how the algorithm chooses between path loss models.

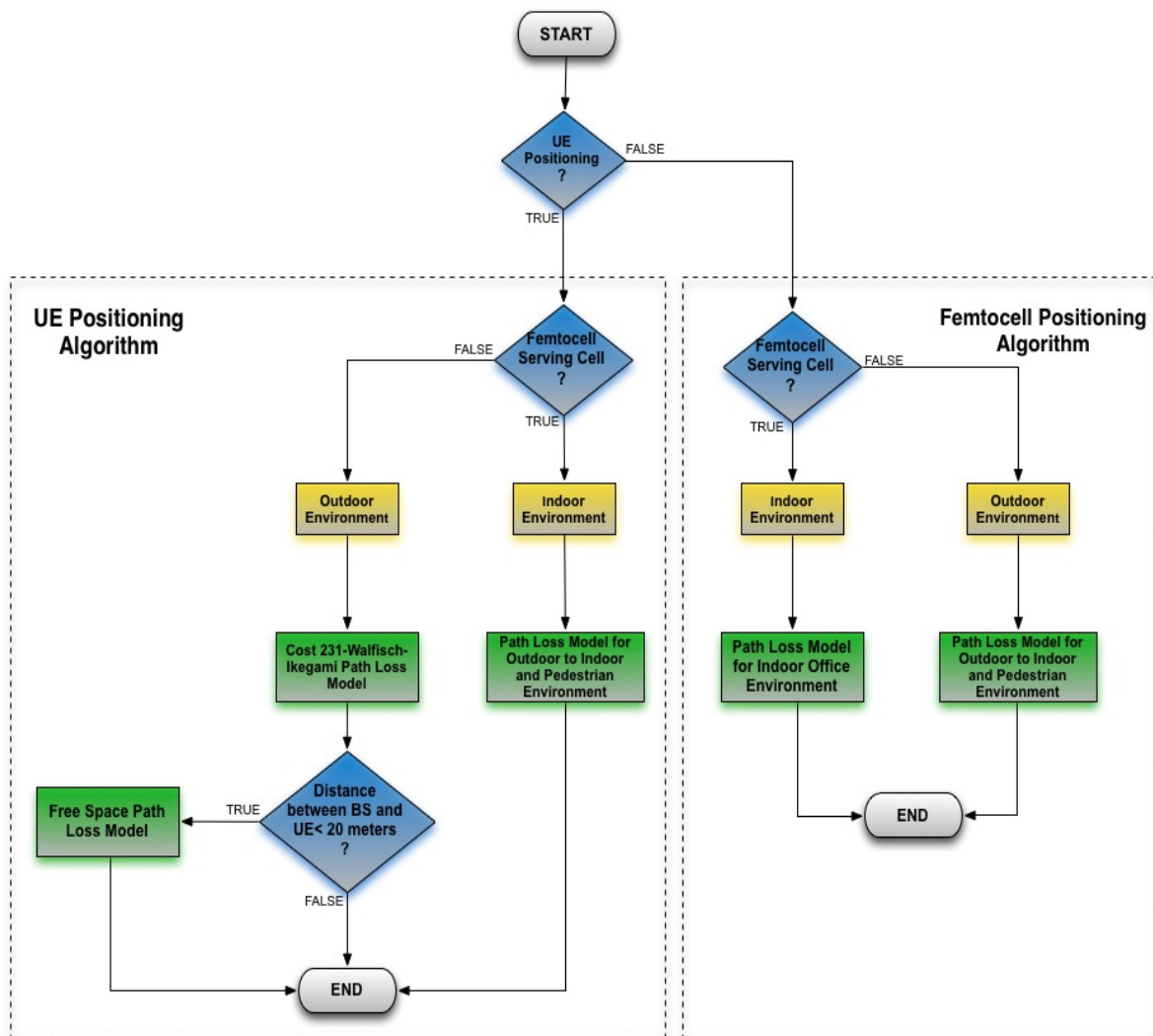


Figure 4.1. Path Loss Decision

The total path loss, to obtain the distances between BS and UE's and UE's and femtocell, is calculated according to (2.1). The transmitted power, in the Common Pilot Channel (CPICH) of the BS, is 33 dBm [45]. The typical antenna gains values for UE and BS were used, 0 dBi and 17 dBi, respectively [36],[46]. For the femtocell it was used the Equivalent Isotropic Radiated Power (EIRP) of 18.5 dBm [47]. For these reasons (2.1) becomes (4.3).

$$L_p = EIRP - RSCP + G_r \quad [dB] \quad (4.3)$$

where:

- $EIRP$  – Equivalent Isotropic Radiated Power;
- $RSCP$  – Received Signal Code Power (in dBm);
- $G_r$  – Receiver antenna gain (in dBi);

$$EIRP = P_t - L_c + G_t \quad [dBm] \quad (4.4)$$

with:

- $P_t$  – Transmitter output power (in dBm);
- $L_c$  – Losses in cable between the transmitter and antenna (in dB);
- $G_t$  – Transmitter antenna gain (in dBi);

## 4.1.2 Positioning Models

In Section 3.3 all positioning methods are presented. After a careful analysis, it has been concluded that only the three methods presented in Section 3.3.2 are used. These choices were made due to the data collected, which will be explained further in Section 4.2.1.

The selection between positioning methods, occurs when the environments change. The Circular or Hyperbolic Lateration is used when the environment in which the UE is an outdoor (femtocell is the non-serving cell). Otherwise, when the UE is in an indoor environment (femtocell is the serving cell) the RSS-based Circular Lateration is used.

For implementation of Circular and Hyperbolic Lateration, an approximation to a Taylor Series expansion was used, in order to calculate an initial estimation of the target's position. The distance between a target (e.g femtocell) and a fixed target (e.g UE) was calculated through (4.5), being the  $(x_{est}, y_{est})$  obtained by (4.6). The other method used was RSS Circular Lateration, where the distances were obtained directly through RSCP using one of the Path Loss Models described in Section 4.1.

$$d_{est} = \sqrt{(x_n - x_{est})^2 + (y_n - y_{est})^2} \quad n = 1, 2, \dots, k \quad [meters] \quad (4.5)$$

where:

- $d_{est}$  – estimated distance between the target and a fixed target;
- $x_{est}$  – x coordinate of the initial position (in meters);
- $x_n$  – x coordinate of the  $n$ th BS (in meters);
- $y_{est}$  – y coordinate of the initial position (in meters);

- $y_n$  – y coordinate of the  $n$ th BS (in meters);

$$\begin{aligned} x_{est} &= \sum_{n=1}^k x_n RSCP_n \\ y_{est} &= \sum_{n=1}^k y_n RSCP_n \end{aligned} \quad n = 1, 2, \dots, k \quad [meters] \quad (4.6)$$

with:

- $RSCP_n$  – RSCP of the  $n$ th fixed target (in dBm);

The positioning algorithm, which will be described in detail in the next section, was implemented using two distinct approaches, where for each one, two methods are used (i) For the first approach the position of the femtocell has been done according to (3.1)-(3.3) and (3.8)-(3.12) to obtain matrices  $A$  and  $h$ , therefore using only Circular Lateration (Taylor Series and RSS-based). For UE positioning only Circular Lateration (Taylor Series) is used; (ii) For the second approach, matrices  $A$  and  $h$ , were calculated with (3.19)-(3.21), instead of (3.8)-(3.10), and (3.1)-(3.3), using Hyperbolic Lateration and RSS-based Circular Lateration, to calculate the femtocell coordinates. For UE positioning only Hyperbolic Lateration was used. To obtain  $(x, y)$  both approaches use (3.16), only if the number of rows of matrix  $h$  is equal to two, or (3.17), if the number of rows is higher then 2. For better accuracy, one needs to take into account UE's error measurements and distance calculation errors, where (3.18) becomes (4.7).

$$x = (A^T E^{-1} A)^{-1} A^T E^{-1} h \quad [meters] \quad (4.7)$$

where:

- $E$  – Covariance of the Error Matrix;

$$e = h - Ax \quad (4.8)$$

with:

- $e$  – Error Matrix;

Distance limitations are taken into account for accuracy improvement. All distance above 1.2 km, for UE's positioning, and 200 meters, for femtocell positioning, are discarded. Another improvement was the creation of a square area surrounding the UE and the femtocell, depending on which positioning module is being used. When calculating the UE's location, if a BS is outside that area, it is discarded and not used for positioning calculations. Also the same procedure is applied when calculating the femtocell coordinates, being the difference between the two the fixed points used. Therefore all the UE's that are outside the surrounding area of the femtocell are discarded for positioning calculations. For the UE positioning this area is 2000 x 2000 square meters. The area for femtocells is much lower, limited to 600 x 600 square meters. Figure 4.2 illustrates these improvements.

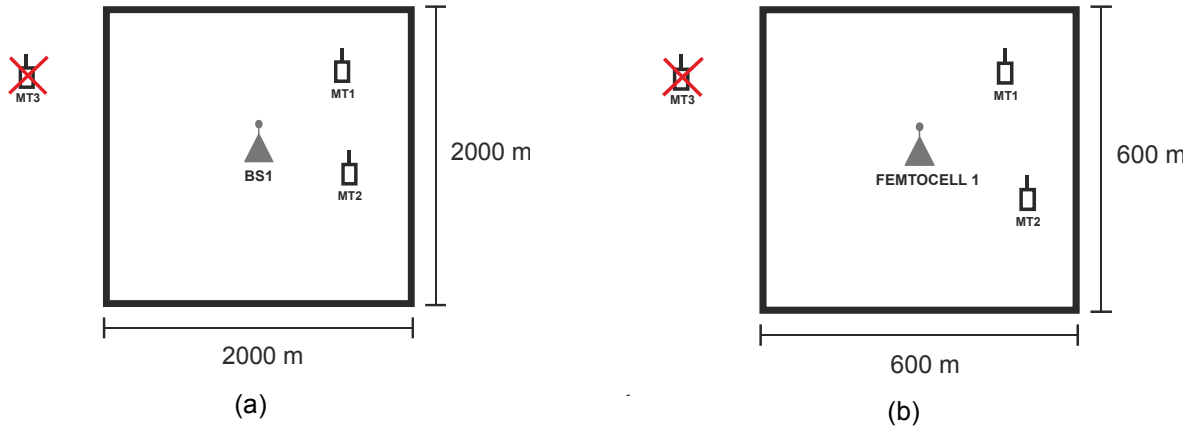


Figure 4.2. Area and distance limitations (a) UE (b) Femtocell

Another important aspect is the fact that for the Circular and Hyperbolic Lateralation the areas limitations are calculated through (4.9) and (4.10) for RSS-based Circular Lateralation:

$$\begin{aligned} |x_n - x_{est}| < 1000 \wedge |y_n - y_{est}| < 1000 \\ |x_n - x_{est}| < 300 \wedge |y_n - y_{est}| < 300 \end{aligned} \quad n = 1, 2, \dots, k \quad [meters] \quad (4.9)$$

where:

- $x_n$  – x coordinate of the  $n$ th BS (in meters);
- $x_{est}$  – x coordinate of the target initial position estimation (in meters);
- $y_n$  – y coordinate of the  $n$ th BS (in meters);
- $y_{est}$  – y coordinate of the target initial position estimation (in meters);

$$\begin{aligned} |x_n - x_{ref}| < 1000 \wedge |y_n - y_{ref}| < 1000 \\ |x_n - x_{ref}| < 300 \wedge |y_n - y_{ref}| < 300 \end{aligned} \quad n = 1, 2, \dots, k \quad [meters] \quad (4.10)$$

where:

- $x_n$  – x coordinate of the  $n$ th BS (in meters);
- $x_{ref}$  – x coordinate of the reference BS (in meters);
- $y_n$  – y coordinate of the  $n$ th BS (in meters);
- $y_{ref}$  – y coordinate of the reference BS (in meters);

## 4.2 Algorithm Development

In this section the algorithm developed will be explained. First an overview of the algorithm will be given. Both UE's and femtocell positioning modules will be described in detail along with how the data used is processed.

## 4.2.1 Algorithm Overview

The algorithm was developed in MATLAB R2012a [48]. Two modules, one concerning the UE's positioning and the other the femtocell positioning compose the algorithm. Due to the thesis scope, only UE's that had a PSC that belong to a femtocell, in their active set or neighbor set lists, were considered. The UE's positioning is only done if its coordinates could not be obtained, either because the UE does not possess GPS capabilities or the GPS could not perform it, e.g, indoor environments. Inside of each positioning module exist an algorithm to estimate the target's initial position, a module that obtains the necessary distances between UE's and BS, based on the RSCP's and according to one of the path loss models described in Section 4.1.1 and the distance estimation, between BS and the estimated initial position of the target. Figure 4.3 shows an overview of the proposed algorithm.

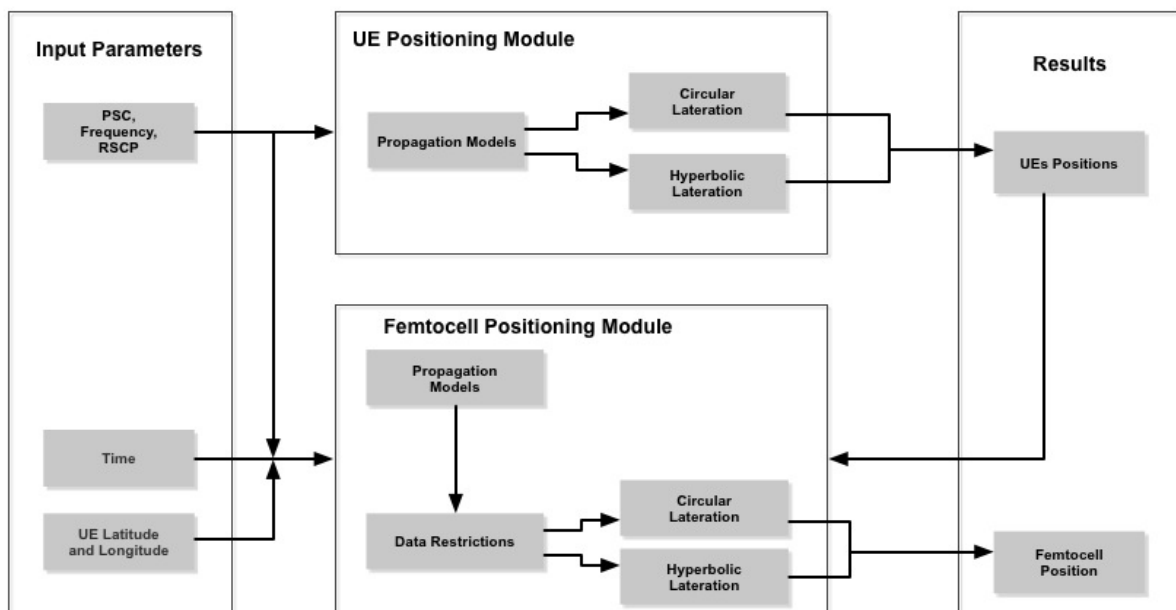


Figure 4.3. Algorithm architecture

The data is collected with TEMS Investigation [49], then passes through the MapInfo Professional [50], for data selection, and exported directly, in a Comma-Separated Value (.csv) file, to be read in Matlab. MapInfo Professional is also responsible for reading the log files exported by TEMS Investigation, which Matlab is not capable. Furthermore, it is also used to make a first selection of the data, using SQL queries. These queries are written in order to select only the data that has valid coordinates and valid PSC's. After the data being selected a spreadsheet is exported, so that this data could be readable by Matlab.

The algorithm receives the input parameters via the MATLAB Import Wizard, which imports a spreadsheet into a variable defined by the user. The advantages of this importing method are: (i) allows you to assign the data in each column as a variable; (ii) eliminates the need to know the format of the spreadsheet, unlike other import functions, like 'csvread' or 'xlsread'. An important aspect of this algorithm is that it is developed to be implemented in a femtocell or in a UE, making it irrelevant to

develop a GUI interface. The output parameters are directly given in the MATLAB Command Window and save into a variable on the Workspace, for further usage, namely for the algorithm assessments, which are explained in Section 4.3.

The structure chosen allows for a simpler and isolated implementation of the different modules, particularly for UE or femtocell positioning. Another important aspect is that it allows for a comparison between positioning methods, between Circular and Hyperbolic Lateration, using the same data in both cases.

The UE positioning module, in terms of path loss, receives BS's parameters as input, namely frequencies, Scrambling Codes (SC), and RSCP's, for distance calculation. In terms of positioning calculation it receives BS's features as well, specifically,  $x$  and  $y$  coordinates, distance estimated, distance calculated through path loss models, and the initial position estimation for the UE. The femtocell-positioning module, receives UE's features instead. The main difference between UE and femtocell distance calculations is that it does not receive the UE's height, because it was considered being constant. The positioning was calculated with same input features used for the UE.

## 4.2.2 UE Positioning Algorithm

The purpose of this module is to obtain the UE location. As explained before, this module is only used if the UE does not have a GPS device or if the GPS is unable to obtain its position. If the UE does not possess its location it is assumed that the values for both  $x$  and  $y$  coordinates are zero. In this algorithm only Hyperbolic and Circular Lateration are used. Figure 4.4 shows the structure of the algorithm.

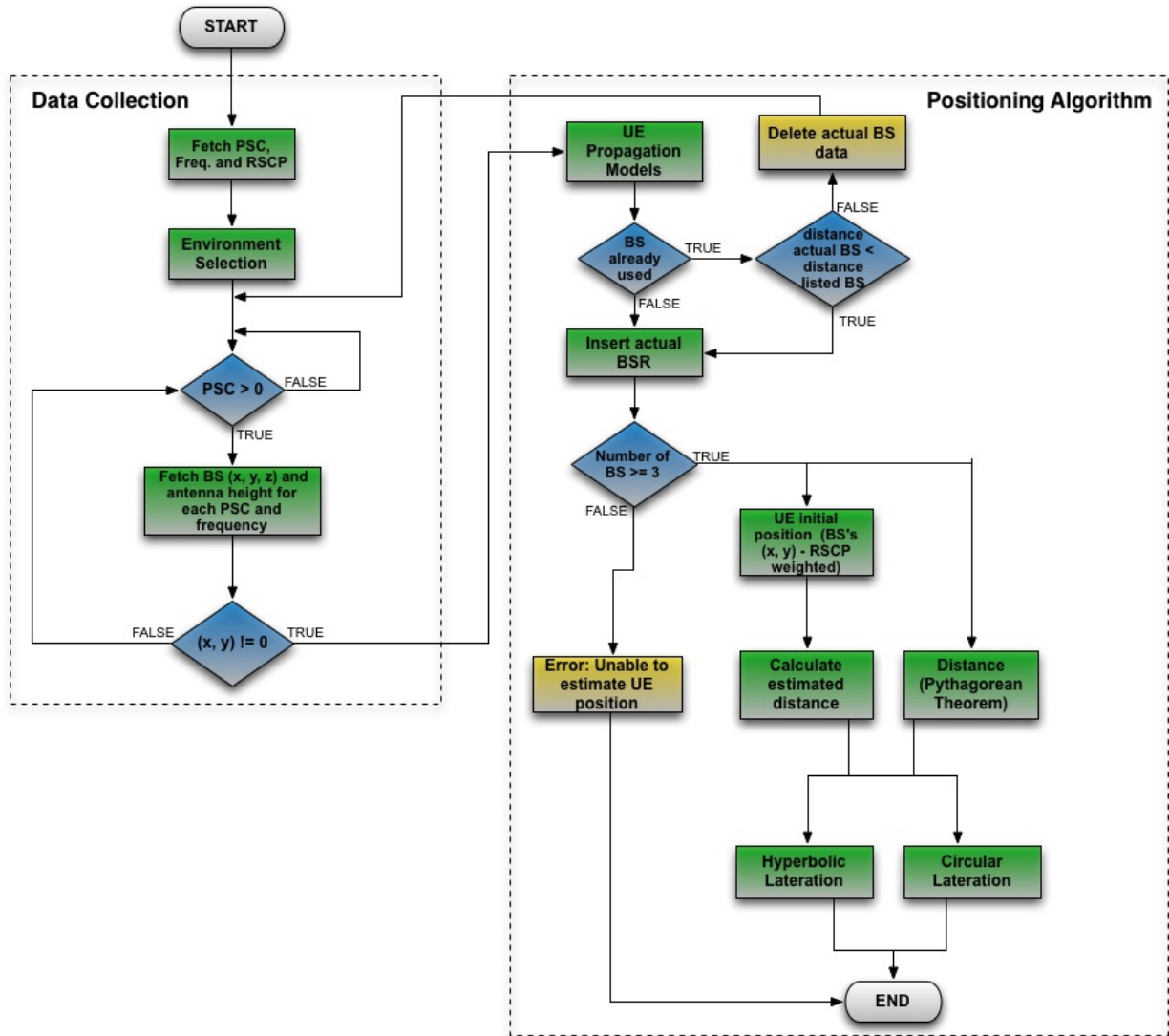


Figure 4.4. UE Positioning Module

The first feature of this algorithm is that it has a BS coordinates database. The input parameters of this database are the SC and frequency of the BS. The frequency parameter was added as an input, mainly because there are SC's in different frequencies and the same SC can be used in different cells, with different geolocations. With these parameters the algorithm can obtain the latitude, longitude and the antenna height of the BS's. The antenna height is a parameter that is used in the path loss model to calculate the distance between the BS and the UE. Another important aspect regarding the BS's distances is that they are all considered being in the  $(x, y)$  plan, therefore using the Pythagoras theorem as shown in Figure 4.5.

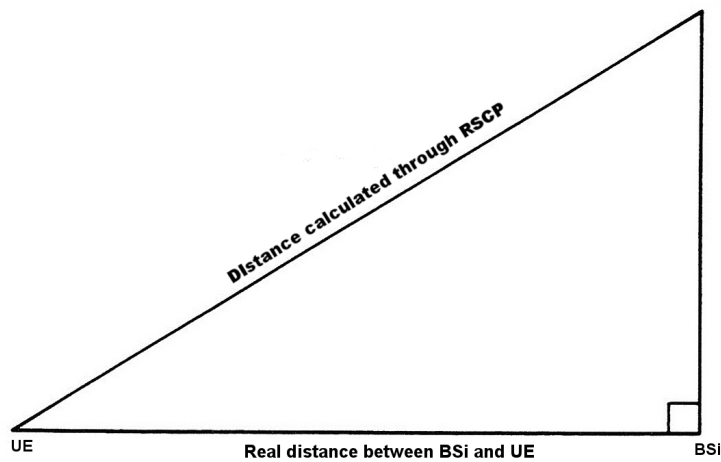


Figure 4.5. Pythagoras theorem applied to the distance between an UE and a BS

The most important feature of this module is that it only considers BS's from different cell sites. If more than one BS from the same site is available on the active or neighbor set lists, the algorithm selects the one with higher value of RSCP, which in practical terms for positioning calculations is equivalent to saying that BS closest to the UE is chosen. With this method of selecting the BS's that are in the same cell site, the error between the position calculated and the actual position of the target is reduced, as it is directly proportional to the distance.

For Hyperbolic Lateration, a reference BS has to be chosen. This selection is made based on the RSCP of each BS. The BS chosen is always the one with higher RSCP, due to the fact that is assumed to be the one closest to the UE. Nevertheless if the serving cell is a femtocell and due to the fact that a femtocell does not support soft handover, the reference BS is assumed to be the one with higher RSCP in the neighbor set list.

The output results of this algorithm are used for the femtocell-positioning algorithm, which will be explained in the next section. A particular aspect of the output results is that they can assume the value "Not a Number" (NaN), which is considered, as an error if three or more valid sites do not exist.

### 4.2.3 Femtocell Positioning Algorithm

This module is used to obtain the femtocell geolocation. This module uses the UE's position either obtained by the positioning algorithm or by the GPS device. In Figure 4.6 one shows the structure of the algorithm.

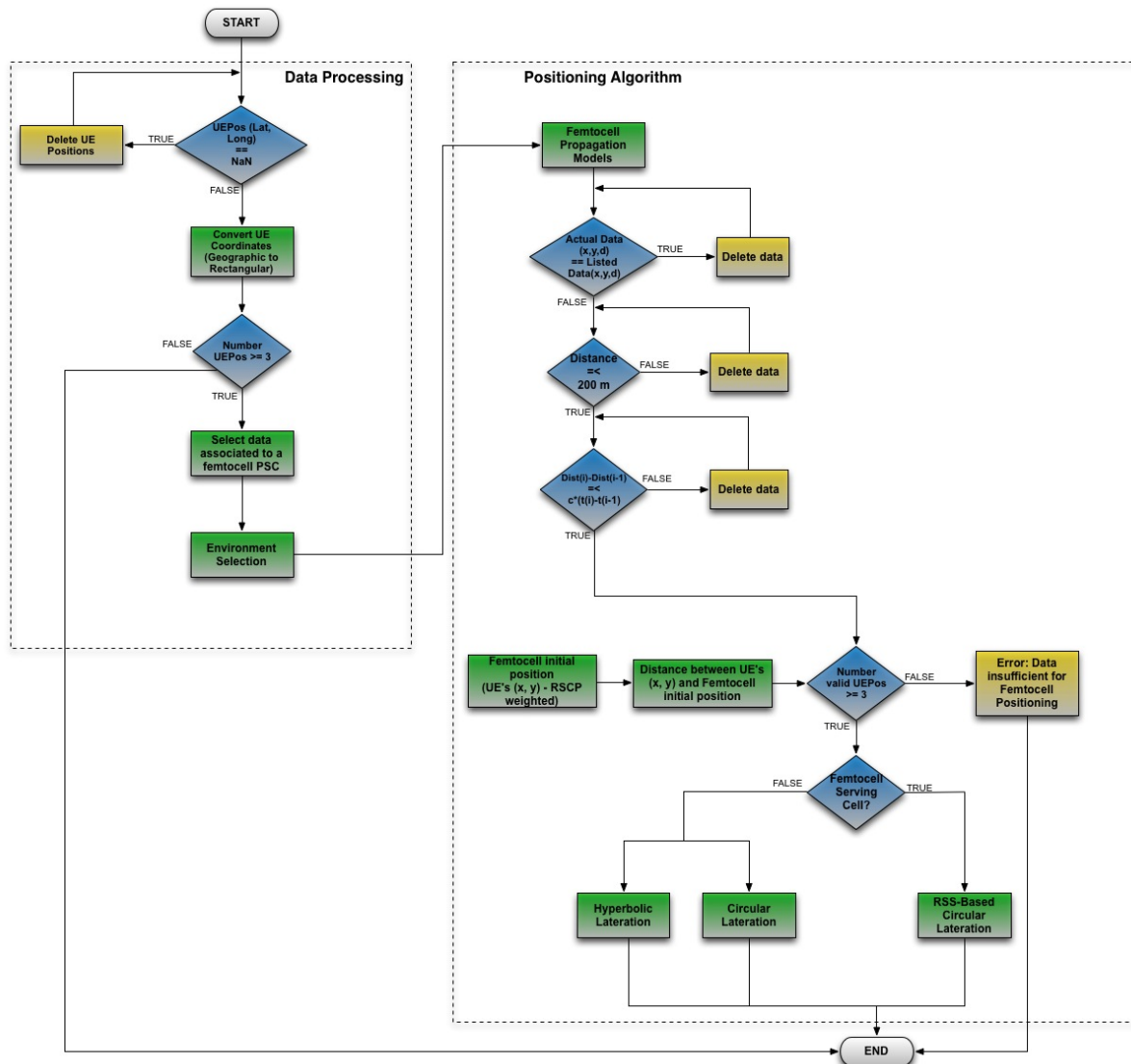


Figure 4.6. Femtocell Positioning Module

Before starting these module there is the need to erase all UEs, for which the positions could not be obtained. After erasing the data regarding them, the first features of it, as explained before, is to verify that there are available at least three valid positions for an UE or for three distinct UE. In addition, if only a UE is used, it is necessary to verify that the available positions are geographically different from each other.

Knowing that three valid UE positions exist, the femtocell data received by the UEs is then processed. The second feature is to organize the data received by the UE, regarding the femtocells. This consists in obtaining the corresponding SC, frequency, RSCP, x and y positions of the femtocell and the time at each the data was collected. The third feature corresponds to the environment selection and the path loss models, where the distance between the UE and the femtocell is obtained, which are both explained in Section 4.1.1.

Two important features of this module are related to data discarding. After obtaining the distances calculated through the path loss models, there is the need to discard all distances that are above 200

meters, which corresponds to maximum coverage range of the femtocells in study. The parameter time is also used for data discarding, where UEs are assumed to be moving at a maximum velocity of 3 km/h. To simplify, if you have two UEs,  $UE_n$  and  $UE_{n-1}$ , the difference between the calculated distances must not exceed the difference between the times of the two multiplied by the maximum admissible velocity. This situation is described by (4.11).

$$(d_n - d_{n-1}) \leq (t_n - t_{n-1})v_{max}, \quad n = 1, 2, \dots, k \quad [meters] \quad (4.11)$$

where:

- $d_n$  – distance between the  $n$ th UE and the femtocell (in meters);
- $d_{n-1}$  – distance between the  $(n-1)$ th UE and the femtocell (in meters);
- $t_n$  – data collection time of  $n$ th UE (in seconds);
- $t_{n-1}$  – data collection time of  $(n-1)$ th UE (in seconds);
- $v_{max}$  – maximum admissible velocity for the UEs (in meters per second);

Also, there is the need to estimate an initial position for the femtocell and to obtain the distances between the UEs and the initial position estimation, which are done in the same way as explained in Section 4.1.2.

Finally, after all data processing, if there are at least three valid positions, the positioning models are used. However, if the femtocell is the serving cell RSS-based Circular Lateration is selected, otherwise Circular and Hyperbolic Lateration are the selected models. Also for Hyperbolic and RSS-based Circular Lateration a reference point has to be chosen. This selection is made by the same criterion that the one explained in the previous section, but using a UE as the reference point instead of a BS. If the number of positions available are insufficient for positioning, the algorithm sends error message and the outputs results comes as NaN, which as explained before, is assumed as an error and therefore no location for the target is obtained.

### 4.3 Algorithm Assessment

Prior to results analysis the algorithm was assessed, so the output parameters could be validated. These validations were made using Matlab and Excel. For this purpose, statistical parameters, such as the mean and standard deviation of the results were analyzed.

The error between the calculated location and the real location was computed using (4.12).

$$\Delta d = \sqrt{(x_{est} - x_{true})^2 + (y_{est} - y_{true})^2} \quad [meters] \quad (4.12)$$

where:

- $\Delta d$  - Difference between the estimated position and true location of the Target;

The mean and standard deviation error for the values calculated in (4.12) were obtained using (4.13)

and (4.14), as defined in [51].

$$\mu = \frac{1}{n} \sum_{i=1}^n (z_i - z) \quad (4.13)$$

where:

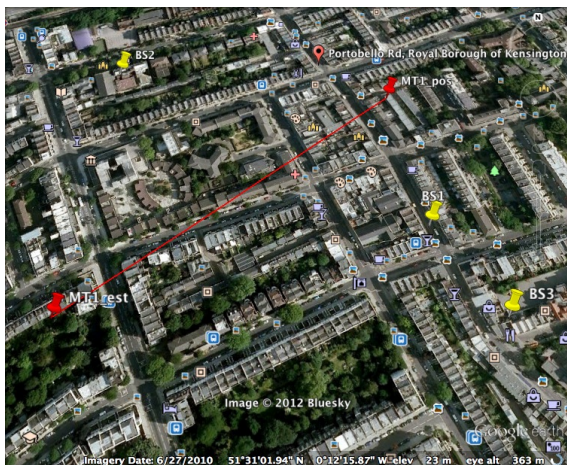
- $\mu$  – mean value;
- $n$  – number of samples;
- $z_i$  – target location sample  $i$ ;
- $z$  – target true location;

$$\sigma = \sqrt{\frac{1}{n} \sum_{i=1}^n (z_i - \bar{z})^2} \quad (4.14)$$

where:

- $\sigma$  – standard deviation value;
- $\bar{z}$  – average value of sample set  $z$ ;

To validate both algorithms the data used was very restricted, due to the fact that only measurements that had a femtocell PSC were of interest. The number of femtocells, used to validate the algorithm, was two. Being the scenario an urban environment the number of PSC from different sites was very reduced therefore preventing a precise validation. Another issue for validation was the absence of femtocell-positioning algorithms, which did not use GPS, to compare the results. Therefore, the results for the proposed algorithm were compared with the ones resulted from already developed UE's positioning algorithms. In Figure 4.7a and Figure 4.7b an example of the difference between the target's estimated and real positions (red pins) as well as the fixed points (yellow pins), for both algorithms.



(a)



(b)

Figure 4.7. Positioning Algorithm. (a) Femtocell. (b) UE.

Nowadays, most of the recent UEs have GPS capabilities and being the GPS one of the most accurate positioning methods [37], there was the need to compare the error in the position of the

femtocell when GPS was active and when it was not. Therefore, one of the tests concerning the geolocation of the femtocell is to use only the femtocell-positioning algorithm in order to obtain the position, without the need to resort to the UE positioning algorithm. The other test that has to be made is when the GPS is not active so both algorithms are used in order to obtain the femtocell geolocation.

Furthermore, a results analysis regarding the femtocell as the serving cell is needed for algorithm validation, with the average and standard deviation values determined. This test also validates the accuracy for when the Path Loss Model for Indoor Office Environment is used.

Additionally, a similar test to the previous one has to be also made for when the femtocell is either on the active set list, but not the serving cell, or in the neighbor set list. This test is of great importance for the algorithm validation as well, due to the fact that it validates the accuracy for when the Path Loss Model for Outdoor to Indoor and Pedestrian Environment is used. Another aspect of this test is that typically the RSCP of the serving cell is higher than all the other RSCP's in the active set list. Also the serving cell has always the higher power regarding all the cells in the neighbor set list. These aspects result in a degradation of the algorithm accuracy.

A test concerning the use of the UE positioning algorithms has to be done to see how the error achieved, by the UE positioning module, influences the result concerning the final location of the femtocell. Furthermore, this test has to be done by removing, one by one, the UE's that had their coordinates calculated through GPS. The error for femtocell geolocation will be greater the more the number of UE's, without GPS capabilities, used. There is the need to test the algorithm accuracy evolution, when more than three measurements are available. The first positioning point is an exception, because there is the need to have at least three valid points for geolocation. All the other measurements are added one by one so that a new location is calculated. All the estimated locations obtained for the femtocell are then computed one by one, regarding the femtocell true position, so that the location errors can be obtained.

Finally, a test regarding the RSS parameters has to be done in order to see which one has better accuracy in order to be used in the algorithm.



# Chapter 5

## Results Analysis

One important step in this thesis is the data collection that assesses the model developed. Therefore it is shown in this chapter, the results of the measurements done. First, a description of how the data was collected is presented. A description of the scenario in which these measurements were made is also given. The last section of this chapter presents the result analysis for three cases. The first case is a comparison between all the positioning methods used in the model development, the second an evaluation of the performance of the algorithm as the percentage of UE's with GPS capabilities decreases and the last one is an analysis concerning the selection of the RSS parameter.

## 5.1 Scenario Description

The reference scenario, where the measurements were made, is a road in London called Portobello Road. In this scenario some assumptions had to be made in order for the algorithm to work. The structure of the streets and the building characteristics were considered all the same. All the characteristics of the scenario are summarized in Table 5.1.

Table 5.1. Reference Scenario Characteristics

<b>Scenario</b>	Type	Dense Urban	
	Building Heights [m]	12	
	Buildings Separation [m]	56	
	Street Width [m]	12	
	Number of floors	3	
<b>System</b>	Frequency [MHz]	2127.4	
		2132.2	
	Number of femtocells	2	
	Tilt [°]	0	
	CPICH $P_t$ [dBm]	Macrocell	33
	$EIRP$ [dBm]	Femtocell	18.5
<b>UE Characteristics</b>	Height [m]	1.8	
	Antenna Gain [dBi]	0	

For the reference scenario, it was taken into account the values that better fit Portobello Road. The scenario type is a dense urban environment with 12 m of buildings height, 56 m of buildings separations and 12 m of street width. All the buildings were considered having 3 floors, each one with 3 m per floor and a pitched roof also with 3 m. The UE height considered was 1.8 m, due to the fact that it is the typical value for the human height. The environment had only users with pedestrian

mobility, being the value for their velocity 3 km/h. The users were walking randomly alongside the street.

The scenario uses sites with different numbers of antennas, and these antennas may be either above or below the buildings roof tops. The mechanical and electrical tilts of the antennas were not considered. The maximum CPICH transmission power is 33 dBm and a 17 dBi antenna gain, for microcells. Also, the femtocells that were considered in this scenario were positioned in an indoor environment, namely in shops, at their entrance. For the femtocells, EIRP was considered instead of the CPICH transmission power and its value is 18.5 dBm. For the UE's only the antenna gain was considered with a value of 0 dBi. All these values were already explained in Section 4.1.1.

## 5.2 Measurements

### 5.2.1 Overview

At the beginning, the idea was to collect various measures from two different scenarios, one dense urban and the other a suburban, but unfortunately this was not possible, due to the lack of different sites in the suburban scenario. For the measurements of the dense urban scenario, Alcatel-Lucent Portugal provided measurements that were made in Portobello Road, London. Figure 5.1 shows the scenario where the measurements were made.

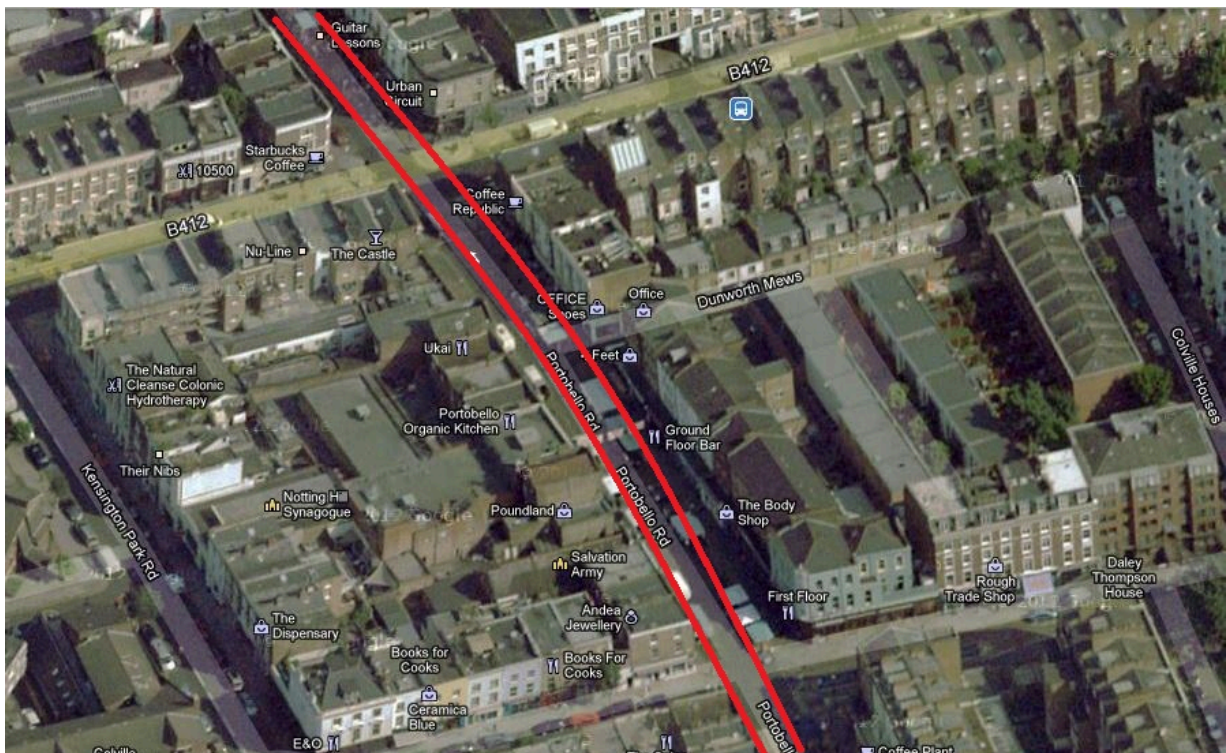


Figure 5.1. Side view of Portobello Road

Figure 5.2 shows all the equipment used for the measurements. Two UEs, two USB cables and one laptop compose the measurement set. The first UE is a Sony Ericsson W995 and was used to make phone calls; the other UE is a Sony Ericsson TEMS Pocket Z750i and was used as scanner. In Table 5.2 describe the UE's set up for the measurements.

Table 5.2. UE's set up

UE	Equipment Model	Test
MS1	Sony Ericsson W995	3G CS Call
MS2	Sony Ericsson TEMS Pocket Z750i	3G Scanner

Despite the use of two UE's, only the measurements obtained using the Sony Ericsson W995 were used. The reason for discarding the measurements made by the other UE, relies on the fact they did not had sufficient BS's for the algorithm to be tested.



Figure 5.2. Measurement Set

The software used to do the walk-test was TEMS Investigation 12.0. This software is an extremely versatile and portable engineering tool for measuring and monitoring the air interface of mobile networks air interface test tool. This solution eliminates the needs for multiple tools for all of a network operator's daily wireless network optimization tasks.

All measurements were performed in the idle and active mode of the UE, because the desired results can be obtained in both modes. The measurements were performed on an English mobile operator.

In order to perform the measurements, especially concerning the positions of them there was the need to configure TEMS Investigation. A detailed map of the place where the measurements were made had to be loaded in the software, alongside with some coordinates of specific points. The measurements were made along Portobello Road in both sides of the street. In some cases indoor measurements were performed, namely where femtocells were placed. Measurements alternated between voice calls (active mode) and no calls (idle mode). A map with some measurements points is described in Figure 5.3.

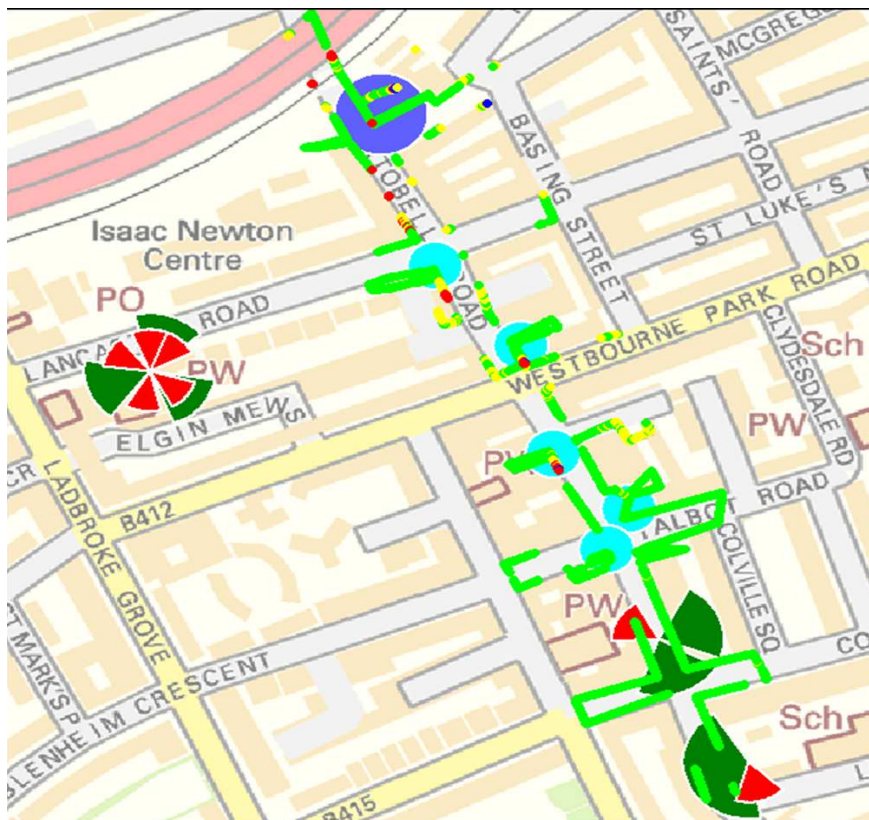


Figure 5.3. Map with some measurement points

All the measurements were recorded into a \*.log file for later usage. After extracting the data from the .log files of TEMS Investigation an extensive number of parameters were available. Being the scope of this thesis to treat only UMTS femtocells there was the need to extract only data concerning UMTS. A file with a \*.FMT extension was extracted from the software with the parameters of interest namely, SC, RSCP, UTRA Absolute Radio Frequency Channel Number (UARFCN),  $E_c/N_0$ , from both active set and neighbor set lists, and also Latitude and Longitude. By default, parameters like time and some messages that were exchanged between the UE and the network were also extracted. In order to reduce all the information retrieved from the program, some SQL queries were made in MapInfo Professional 11.5. MapInfo Professional is powerful software for mapping and analysis application providing geospatial data solutions [50]. The use of this solution was of great importance due to the fact that it allowed the data to be organized in tables and to select the important data extracted from

TEMS Investigation. A lot of the data collected did not have femtocell PSC's and for that reason they were eliminated. Due to this fact and as mentioned before, some SQL queries were done in order to select the rows of the table where femtocell PSC's were detected. After this selection, the resultant table is exported into a \*.csv file so that MATLAB could read the information.

## 5.2.2 Measurement Results

In this section, the measurements results are discussed. Measurement files show that a connection was established with a variable number of BS's depending on UE's position. Although, the UE received signals from several BS's only the BS's covering Portobello Road will be discussed in this section. In Table 5.3 an example of a measurement set extracted from TEMS Investigation into MapInfo Professional is shown.

Table 5.3. Example of a measurement set extracted from TEMS investigation

Parameter Name		Parameter Value			
Time		2:33:15 PM			
MS		MS1			
Frame_Number		Not Valid			
Messagem_Type		Combined DPCH SIR for Synch			
MS1_Latitude [Degrees]		-0.205263836			
MS1_Longitude [Degrees]		51.51640305			
MS1_SAN_SC [List Position]		[1]	[2]	[3]	[4]
		393	257	1	377
MS1_SAN_CPICH_RSCP	[List Position]	[1]	[2]	[3]	[4]
	[dBm]	-84	-93	-95	-96
MS1_SAN_UARFCN_DL [List Position]		[1]	[2]	[3]	[4]
		10661	10661	10661	10661
MS1_SAN_CPICH_Ec_No	[List Position]	[1]	[2]	[3]	[4]
	[dBm]	-9.5	-19	-22.5	-23.5

In Table 5.3 all the parameters used in the algorithm are shaded. Also, MS1\_SAN\_SC, MS1\_SAN\_CPICH\_RSCP, MS1\_SAN\_UARFCN\_DL and MS1\_SAN\_CPICH\_Ec\_No are viewed as lists. A position of each corresponds to information of a BS's, i.e., the position 1 in all lists corresponds to the actual value received by the MS1 from the BS with the SC 393.

To better understand the results, some additional information about these BS's such as location, SC, CPICH power, height and UARFCN, was required. The information containing these parameters is described in table 5.4. The UARFCN is used to obtain the frequency where the antennas are operating. Therefore, it is obtained by dividing the UARFCN by 5. For the site with the SC 208, 26, 257 and 258 the height is 19 m, also in this site there is a SC 256 with 18 m, the site with SC 393 has 7 m and the site with SC 377 as also 7 m. All of these BS's are microcells with a CPICH Power of 33 dBm. Also with the antenna heights the real distance between the UE and the BS's, in the (x, y) plan, could be obtained as explained in Section 4.2.2.

Table 5.4. Information of each site

Site	Latitude [Degrees]	Longitude [Degrees]	SC	CPICH Power [dBm]	UARFCN
Site 1	51.516843	-0.20854064	26	33	10637
			208		10637
					10661
			256		10637
			10661		
			257		10637
10661					
258	10637				
Site 2	51.515301	-0.20468095	377	33	10637
					10661
Site 3	51.514616	-0.20401608	393	33	10637
					10661

With the sites location, each BS's was drawn on a map. MapInfo Professional was used to draw Figure 5.4. With MapInfo Professional and the sites positions, it was easier to filter some measures that were obtained. These were mainly measurements that had only PSC's, in the active set and neighbor set lists, from the same site, e.g., a measurement where the UE is only receiving PSC's from site 1.

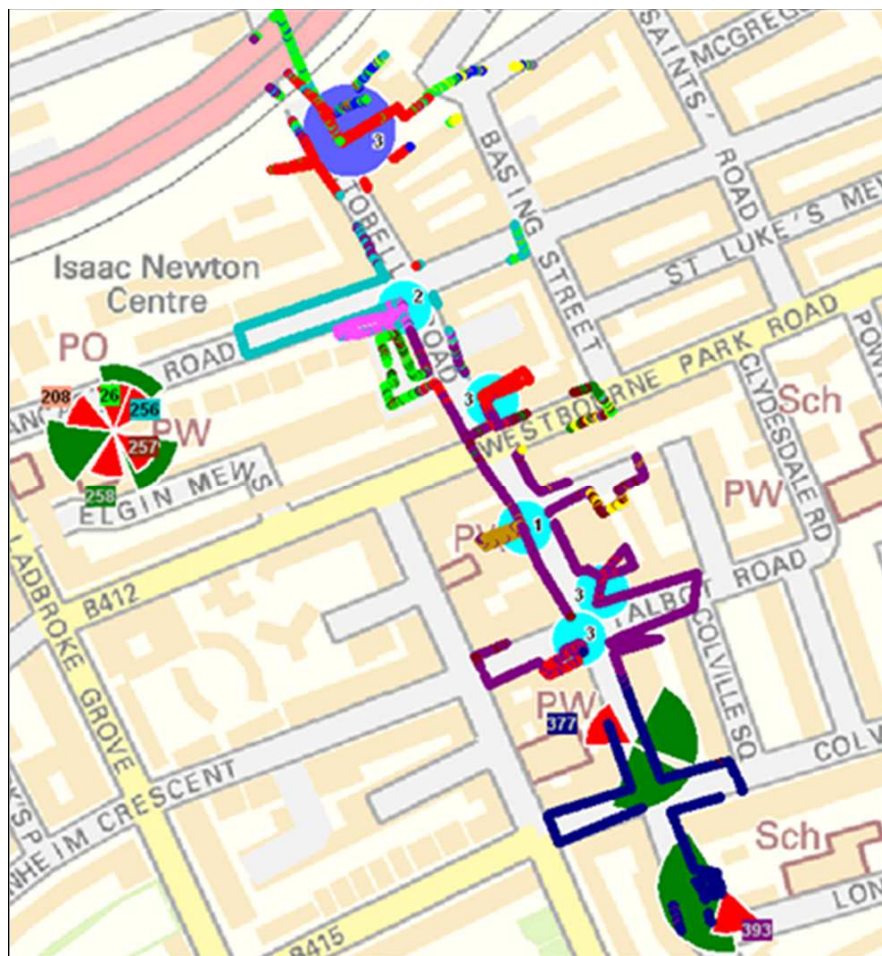


Figure 5.4. Detected BS's covering Portobello Road

While in Figure 5.4 the BS's are drawn as sectors, for the algorithm all BS's were considering using omnidirectional antennas. With this assumption, the azimuth of each antenna was not taken into account.

Being the reference scenario a real one, wall attenuation was considered being the same for all buildings. The main reason, for this assumption, comes from the fact that one could not know in which building the UE or the femtocell was situated, when testing the algorithm. Furthermore, being the femtocells a indoor solution, the operator cannot know where did the user put the equipment, being impossible to take into account the number of walls and floors that the signal had to penetrate along its path.

Finally after a careful analysis, results were obtained. Although the proposed algorithm is composed by three positioning methods, as described in section 4.2, a comparison between the three needs to be done. Figure 5.5 illustrates the comparisons between the three methods for when a femtocell is the

serving cell.

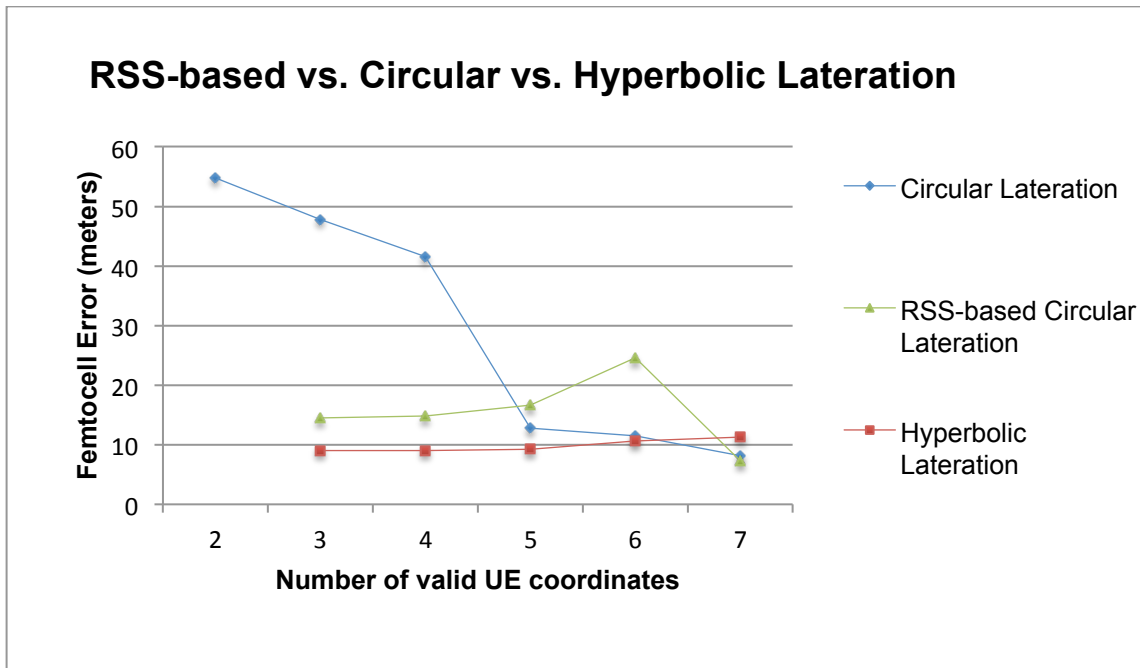


Figure 5.5. Location errors. Circular Lateration vs. Hyperbolic Lateration vs. RSS-based Circular Lateration

At first sight, it was easy to perceive that when a weak signal received by an UE, regarding either the femtocell or a BS was added to all the signals already obtained, that the distance error would increase several meters. Figure 5.6 shows this growth of the location error when a weak signal is used for Lateration and Table 5.5 shows the RSCP used to obtain those errors.

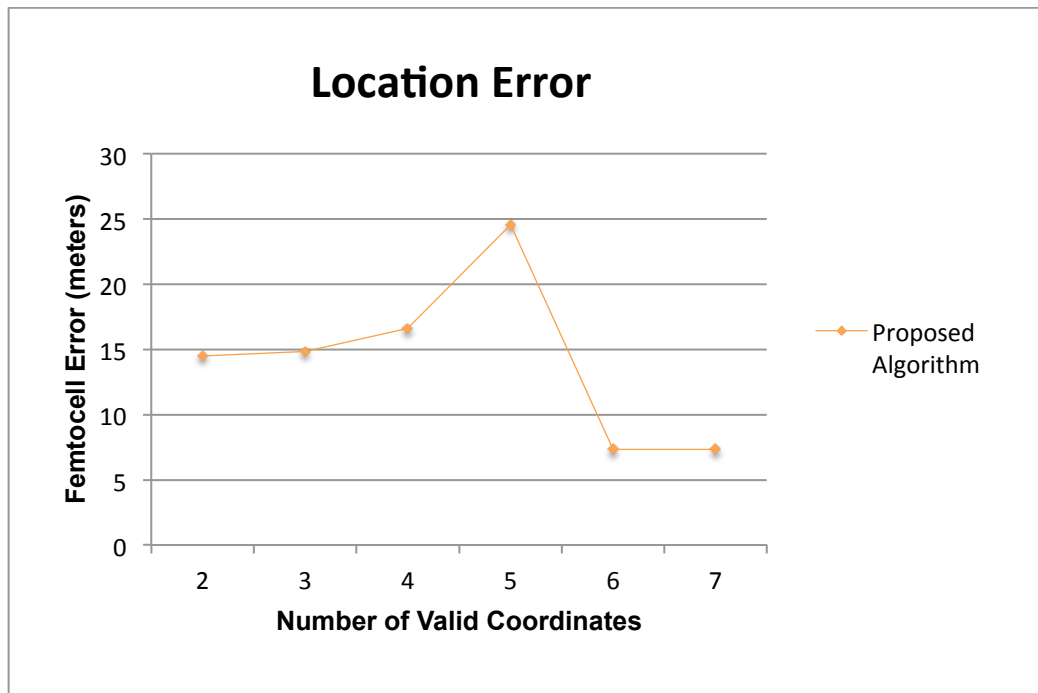


Figure 5.6. Location error regarding weak signals

Table 5.5. RSCP values used for Femtocell Location Error

Number of Coordinates	2	3	4	5	6	7
RSCP [dBm]	-50	-47	-46	-61	-44	-44

Another interesting thing concerns the fact that when a UE may be receiving a good signal from the femtocell, but is far away from it, in terms of its actual position, the location error may decrease. With Figure 5.6 one also shows the decreasing of the error if one of the UE's is far away from the femtocell in respect to the other UE's and in Table 5.6 the distance of all the UE's to the femtocell.

Table 5.6. Distance of all UE's in respect to the femtocell

Number of Coordinates	2	3	4	5	6	7
UE's real distances [Meters]	1.5784	2.2613	4.9903	21.7861	24.0536	1.8037
UE's distances calculated through a propagation model [Meters]	0.3954	0.3141	0.2909	0.9198	0.24947	0.24947

In Table 5.6, when the sixth UE is added to the calculations, the error for the position of the femtocell decreases. One of the reasons comes from the fact that the distance calculated through a propagation model can be much smaller than the real distance. Also, when the femtocell is the serving cell the method used is RSS-based Circular Lateration, however if the measurement being added is the one selected as the reference BS, the algorithm uses, only for this measurement, Circular Lateration. This means that  $N$  measurements will be used for calculations, instead of  $N-1$ , and the error is also reduced.

In conclusion, the geographic location of a femtocell is influence not only by a weak signal received, but also by the UE position with respect to the other UE's in the coverage area of the femtocell.

## 5.3 Result Analysis

In this section results obtained are presented. In the first part, the three methods, that were taken in to account in the previous chapter, are compared in order to see which are better suited for the proposed algorithm; in the second part, a comparison between the proposed algorithm in two distinct cases: (i) when all the UE's have their position calculated through GPS; (ii) when all the UE's have their position calculated through one of the proposed methods, meaning that the UE's do not have GPS capabilities. Also, an evolution of the algorithm performance is done by adding UE's that do not have GPS capabilities and removing the ones that have from the calculations; in the third part, an evaluation of which parameter for the received power has better performance is done, concerning the GPS dependency as well.

### 5.3.1 Positioning Methods

Being the proposed algorithm composed by two methods, there was the need to evaluate which of them had better performance, for different scenarios. First there was the need to do a comparison between Circular and Hyperbolic Lateration. The test was made using the two methods separately. Also a comparison between RSS-based Circular Lateration and the other two was done. Therefore two algorithms were constructed, one using RSS-based and Circular Lateration and the other also using RSS-based and Hyperbolic Lateration. All the tests made where done: (i) for when the femtocell was serving cell; (ii) for when the femtocell was the non-serving cell.

The main difference between the two is that Hyperbolic Lateration uses a reference point, which means that it uses  $N-1$  instead of using  $N$  system of equations. In Figure 5.7 one shows the results for both methods for when a femtocell is not he serving cell and Table 5.7 shows the mean values for the errors as well as their standard deviation. This test was made for situations where the femtocell was not the serving cell, to also test the propagation models used for when the UE is in and outdoor environment, as explained in Section 4.2. Also, the reason for the used of the RSS-based Circular Lateration will be explained later in this section.

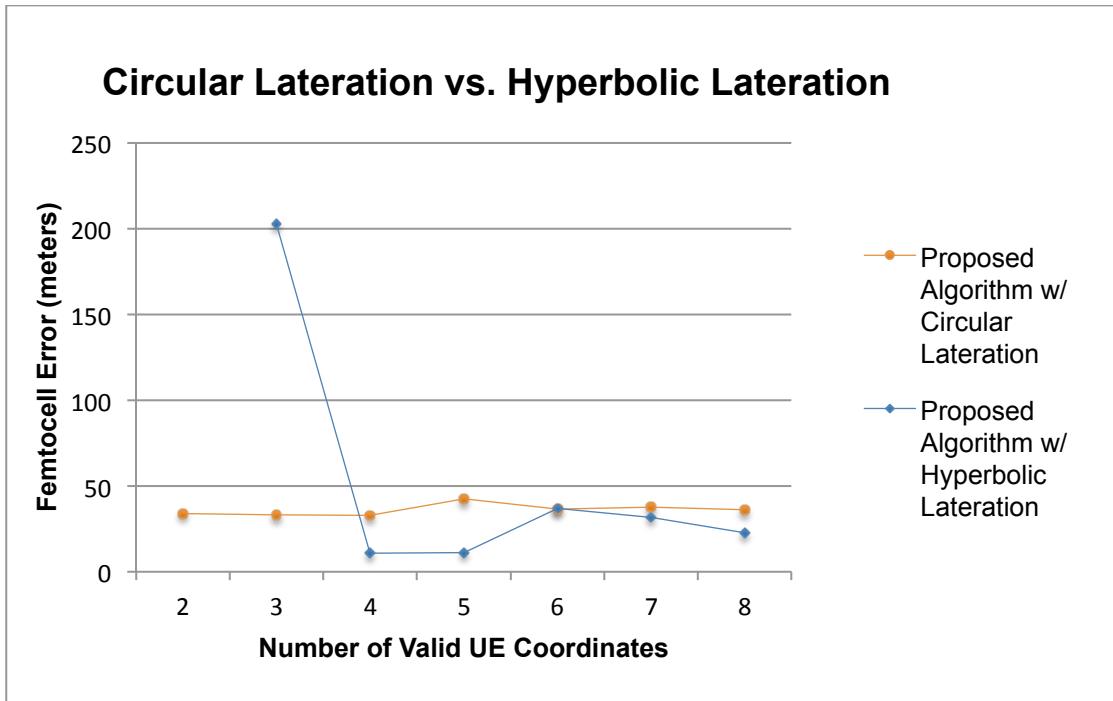


Figure 5.7. Circular Lateration Vs. Hyperbolic Lateration (Femtocell as non-serving cell)

Table 5.7. Mean Error and Standard Deviation

Proposed Algorithm	Mean Error [Meters]	Standard Deviation [Meters]
With Circular Lateration	36.1465	3.116
With Hyperbolic Lateration	52.7056	67.7438

In Figure 5.7 it can be seen that when Hyperbolic Lateration is used the location error of the femtocell is much more instable that the one when Circular Lateration is used. Also the mean value of the Proposed Algorithm with Hyperbolic Lateration is higher than the other one. The standard deviation is very high for the one using Hyperbolic Lateration. This value for the standard deviation comes from the fact that most the values obtained are not close to average error point.

Futhermore, when the femtocell is the serving cell the positioning model used is the RSS-based Circular Lateration and therefore the main difference between the proposed algorithm using Hyperbolic Lateration and the one using Circular Lateration is the total number of measurements used. As explained before, Circular Lateration uses one more point that Hyperbolic Lateration. In Figure 5.8 one shows the results for both methods. Also in Table 5.8 is shows the mean and standard deviation values.

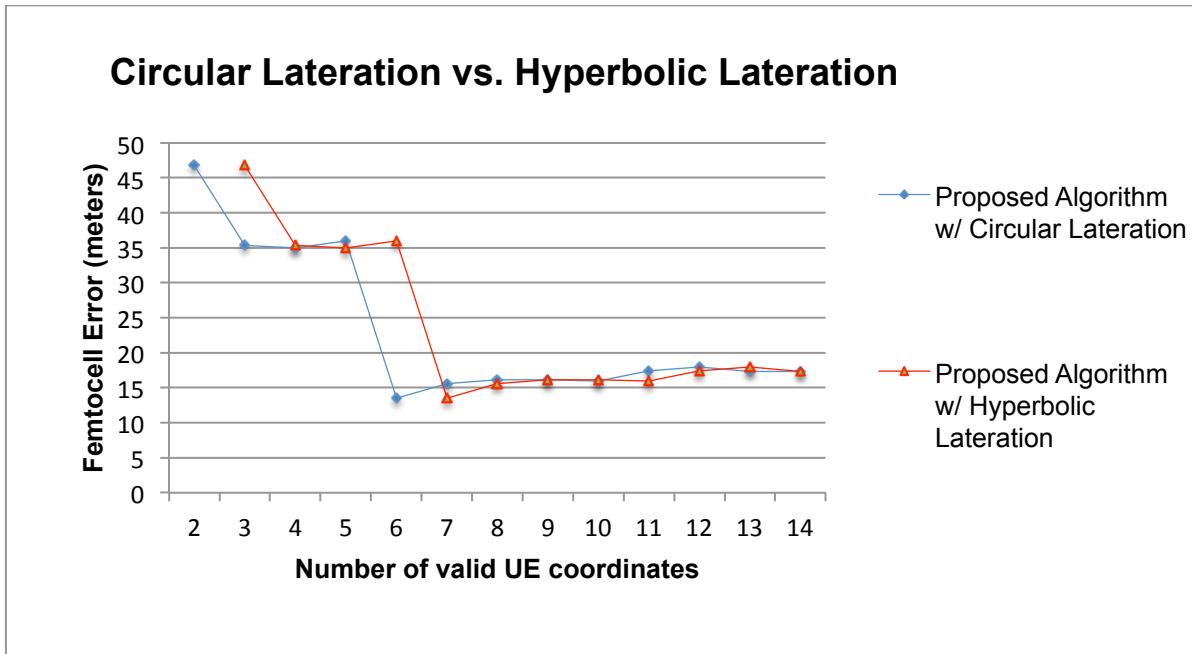


Figure 5.8. Circular Lateration Vs. Hyperbolic Lateration (Femtocell as Serving Cell)

Table 5.8. Mean Error and Standard Deviation

Proposed Algorithm	Mean Error [Meters]	Standard Deviation [Meters]
With Circular Lateration	23.1187	10.5175
With Hyperbolic Lateration	23.5986	10.8094

In Figure 5.8 it is described the difference between the two algorithms. In this figure one can see that the values for the positions are all the same, this comes from fact that positioning algorithm used, where in both cases is the RSS-based Circular Lateration. The major difference comes in the last point where in the algorithm that uses Hyperbolic Lateration it is non-existent. This non-existent point as explained before, is used for the reference BS, which in Circular Lateration it is not the needed. These two reasons explain why the values, in Table 5.8, are almost equal.

The proposed algorithm uses always the RSS-based Circular Lateration. The reason for selecting the method comes from the fact that it gives good results for when the femtocell is the serving cell, as shown in Figure 5.5. However, when the femtocell is not the serving cell the error for this positioning method becomes much bigger than the others. In this section only the mean error and standard deviation will be shown as the comparison between the three methods was done in section 5.2.2.

Table 5.9. Mean Error and Standard Deviation

Positioning Methods	Mean Error [Meters]	Standard Deviation [Meters]
RSS-based	15.5708	5.5117
Circular Lateration	29.4308	19.0637
Hyperbolic Lateration	9.8458	0.9046

Table 5.9 shows that the mean error and standard deviation of Hyperbolic Lateration is the smaller ones. Although, in Figure 5.5 one can see that RSS-based Circular Lateration, when all points are used in the calculations, has the smaller error between the estimated position and the real position. Also, the difference between the mean error and the standard deviation for this method and Hyperbolic Lateration is small.

So in conclusion, although the Hyperbolic Lateration is an adequate method for positioning, Circular Lateration gives better results. Also the Hyperbolic Lateration tends to be less accurate, when the RSCP signal begins to degrade. In addition, when the femtocell is serving the UE, the RSS-based Circular Lateration gives good results, also this method in comparison with the others has less calculations to be done, because it does not need a first estimation of the femtocell position as explained in Section 3.3.2.

### 5.3.2 GPS Dependency

In this section, it will be analyzed and shown, the results for the femtocell location, when the percentage of UE that do not have GPS capabilities, decreases. These simulations were made, where it was added one by one, UE's that did not have their position calculated through the GPS. Also, it will be shown, the evolution of the error for the location of the UE's.

One of the problems with the positioning of an UE's without the use of a GPS is that femtocells only support hard-handover. In other words, when a PSC of a femtocell is selected for the active set list of an UE that list only keeps that PSC and the others PSC's that were on the list before are moved onto the neighbor set list.

Although, nowadays, almost all the UE's have GPS capabilities some still do not have. For this reason it is necessary to calculate their position, in order to calculate the femtocell location. To locate the UE only Circular and Hyperbolic Lateration were used. The main reason relies on the fact that the distance between the UE and the fixed points (BS) are normally non-short range, i.e, macrocells, microcells, etc. Figure 5.9 shows a comparison between the Hyperbolic and Circular Lateration, for UE positioning. Also, it is illustrated in Figure 5.9, a mean error for all the UE's that needed to be located.

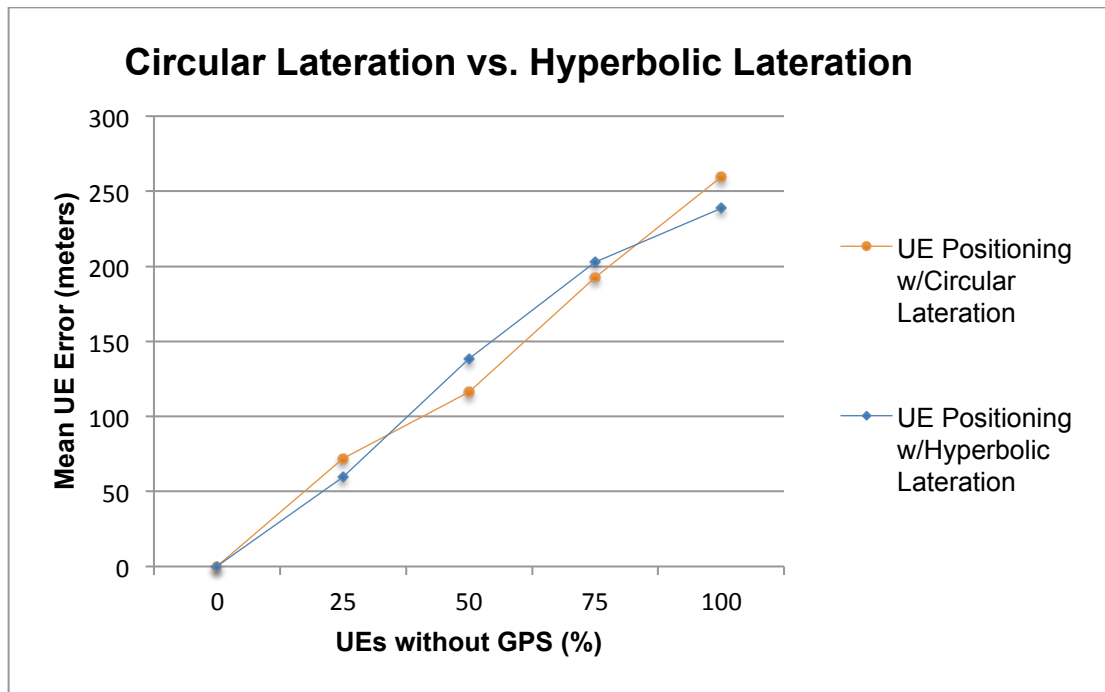


Figure 5.9. Mean error for UE's positioning. Circular Lateration Vs. Hyperbolic Lateration

Table 5.10. Mean Error and Standard Deviation for UE Positioning

Proposed Algorithm	Mean Error [Meters]	Standard Deviation [Meters]
With Circular Lateration	160.091	71.749
With Hyperbolic Lateration	159.72	68.139

Figure 5.9 we can see that the mean error to locate an UE's becomes greater as the number of UE's without GPS capabilities increases. The mean error was selected, in order to see that the larger the percentage of UE's that needed to be positioned, through the UE positioning module, the greater the error becomes. Also it is shown in Table 5.10 that the error and standard deviations for both algorithms are very closer. However when the percentage of UE's without GPS is 100%, Circular Lateration presents a worst performance than Hyperbolic Lateration. In Hyperbolic Lateration one can see that the error is not very linear, meaning that for the 50% and 75% it is more degraded than Circular Lateration. Furthermore, one can see in Table 5.10 that the accuracy of the two methods is almost the same. The main reason for which Hyperbolic Lateration was not selected to be implemented in the proposed algorithm, to locate the UE, comes from the fact that the final result for the femtocell location was worse than the one with Circular Lateration, which was the main goal of this thesis. Figure 5.10 shows the evolution of the error for the femtocell location as the percentage of UE's without GPS capabilities increases. Also, Table 5.11 it is shown the standard deviations and means errors for both algorithms.

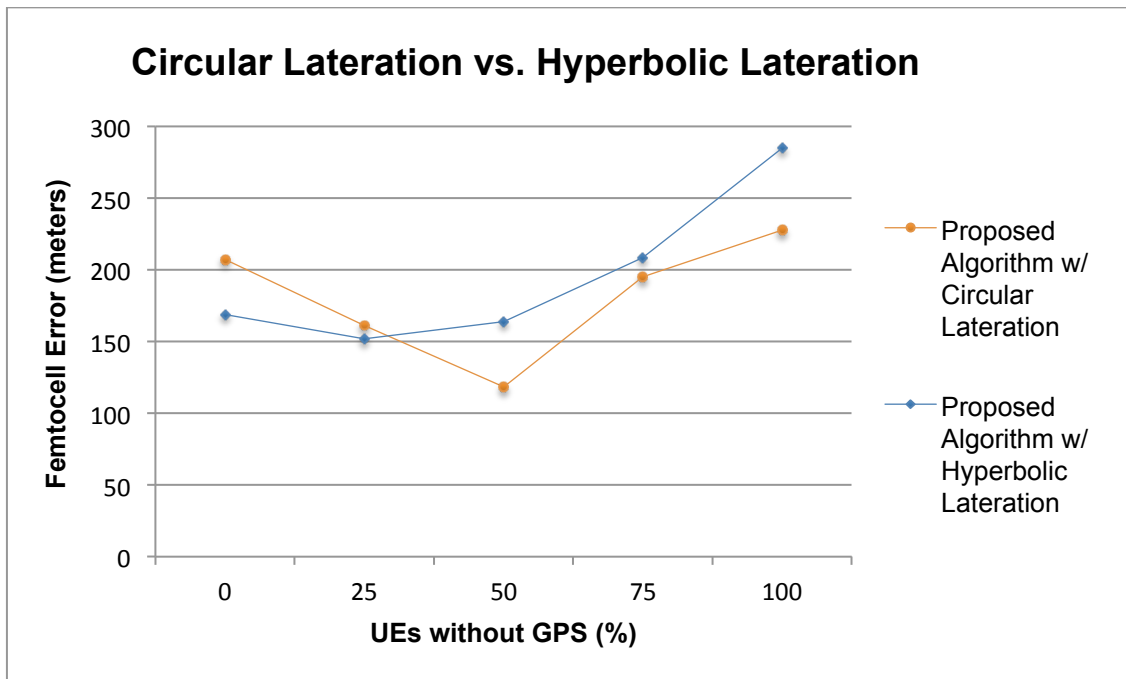


Figure 5.10. Femtocell location error as the percentage of UE's increases

Table 5.11. Mean Error and Standard Deviation (% of UE without GPS capabilities increases)

Proposed Algorithm	Mean Error [Meters]	Standard Deviation [Meters]
With Circular Lateration	181.764	38.359
With Hyperbolic Lateration	195.541	48.529

As presented in Table 5.11 the mean error for Hyperbolic Lateration is greater than the error for Circular Lateration as well as the standard deviation. Although the Hyperbolic Lateration as better performance in positioning the UE, when positioning the femtocell, using the results obtained from UE positioning, the overall performance decays. The reason for this degradation comes from the fact that the reference UE may have a large error, comparing to other UE's that are being used, or vice-versa. In other words, the positioning of all the UE will result in a significant dispersal relative to each other and therefore the result for the femtocell location comes with a larger error.

By comparing Figure 5.7 and Figure 5.10 one can see that the error is much higher for when it is used UE's that do not have GPS capabilities. This fact was already expected because an error is already associated when positioning a femtocell, when UE's do not have GPS capabilities are used. This error is associated to the positioning of the UE. Furthermore, when comparing Table 5.7 and Table 5.11 one can see that the values for the standard deviations are much higher for the case of Hyperbolic Lateration.

### 5.3.3 RSS Parameters

In this section an analysis will be made regarding the overall performance for the RSCP and Received Signal Strength Indication (RSSI) parameters. Also the GPS dependency will be discussed in order to sustain the selection, for the proposed algorithm, of the received power parameter to be used. The simulations regarding these two situations were made in the same conditions, in order to have a better analysis of both parameters. These parameters are used as inputs for the propagation models in order to calculate the distance. The major difference between the RSCP and the RSSI is that the second one takes into account the quality of the link. The relation between the RSCP and the RSSI is given by (5.1).

$$RSSI_i = RSCP_i - \left( \frac{E_c}{N_0} \right)_i \quad [dBm] \quad (5.1)$$

where:

- $RSSI_i$  – Received Signal Strength Indicator of BS<sub>i</sub>;
- $RSCP_i$  – Received Signal Code Power of BS<sub>i</sub> (in dBm);
- $\left( \frac{E_c}{N_0} \right)_i - E_c/N_0$  of BS<sub>i</sub> (in dBm);

In Figure 5.11, one shows a comparison between the proposed algorithm using the RSCP and RSSI.

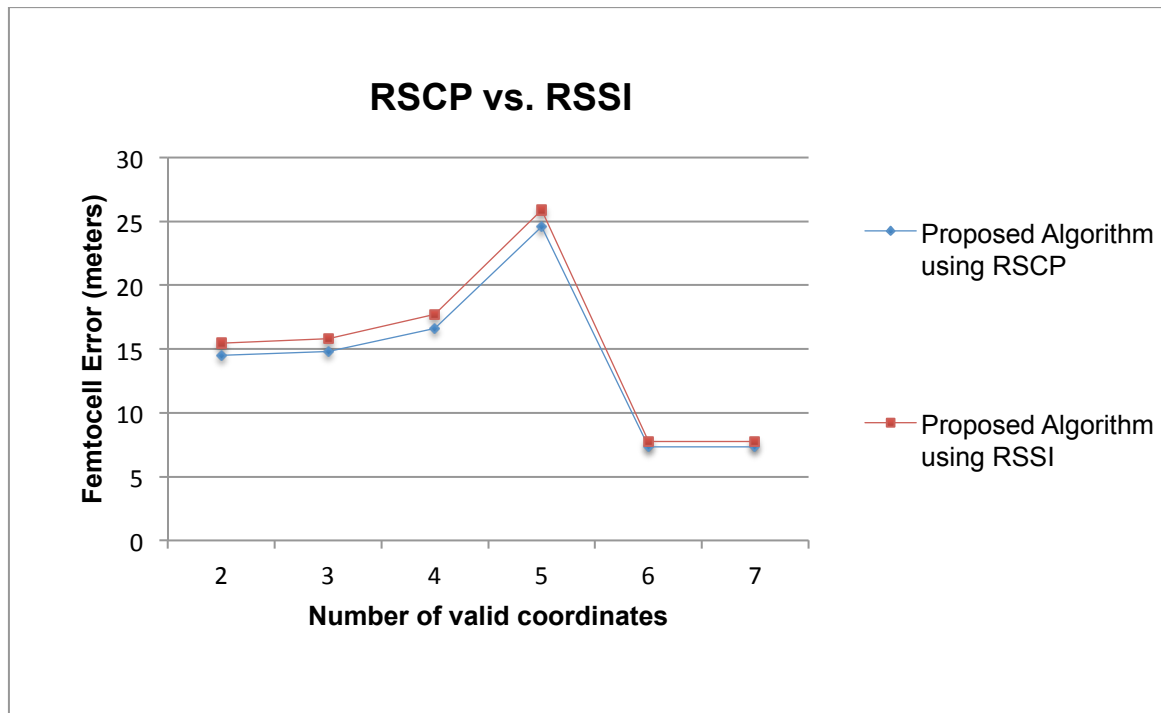


Figure 5.11. Proposed Algorithm. RSCP Vs. RSSI (Femtocell as Serving Cell)

In Figure 5.11 it is presented the error for the positioning of the femtocell using in one hand the RSCP parameter and in the other the RSSI. It can be seen that the results are very similar, although RSSI has worst performance along all the points. Also, in Table 5.12 it is shown the mean error and

standard deviation for this scenario, to better illustrate both performances.

Table 5.12. Mean Error and Standard Deviation

Proposed Algorithm	Serving Cell	
	Mean Error [Meters]	Standard Deviation [Meters]
Using RSCP	14.1981	5.8938
Using RSSI	15.0641	6.2134

When the femtocell is the non-serving cell, the algorithm using the RSSI parameter tends to have an irregular performance, meaning that for a fewer number of valid coordinates it has a better performance than for when all the valid coordinates are used. Unlike the RSSI parameter, RSCP has a much more regular performance and when all the valid coordinates are used it has a better error. This irregular performance of the RSSI can be seen in Table 5.13 by evaluating the value of the standard deviation which is three times more that the one for RSCP. However, the RSSI only has better performance in terms of mean error. This irregular performance is explained by the bad selection of the serving cell when the RSSI is applied, meaning that the interference caused from the neighboring cells and other sources may lead to this situation. The interference of neighboring cells and other sources can cause the  $E_c/N_0$  to be an irregular value, and influence the RSSI value, as we can see in (5.1).

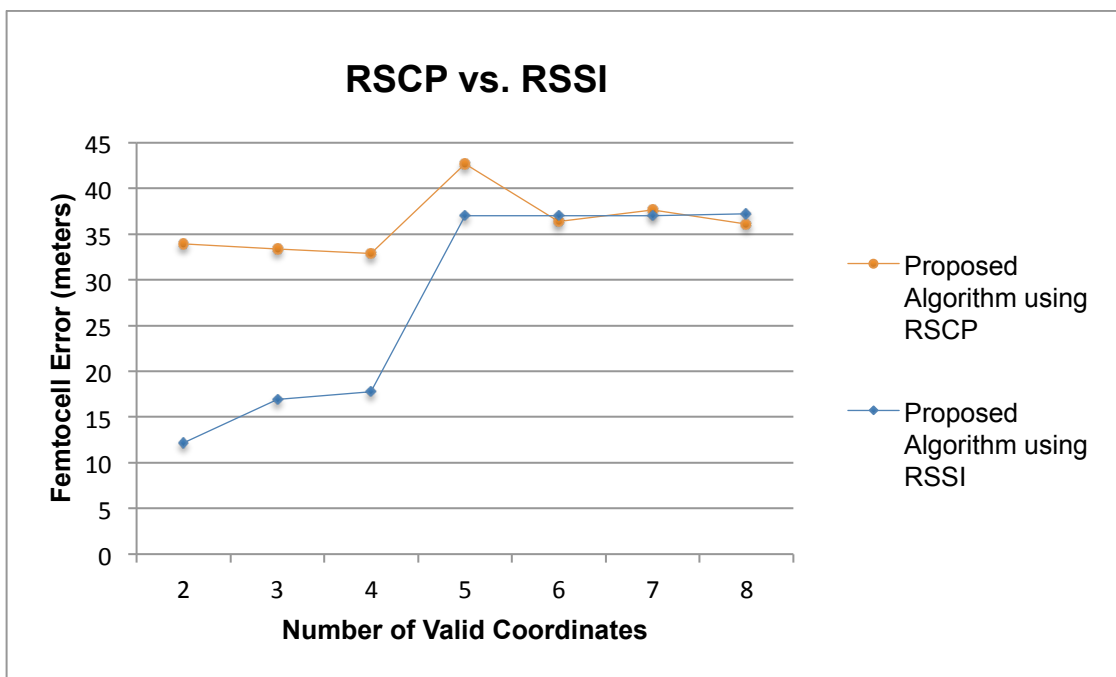


Figure 5.12. Proposed Algorithm. RSCP Vs. RSSI (Femtocell as Non-Serving Cell)

Table 5.13. Mean Error and Standard Deviation

Proposed Algorithm	Non-serving Cell	
	Mean Error [Meters]	Standard Deviation [Meters]
Using RSCP	36.146	3.116
Using RSSI	27.863	10.734

After a comparison, between the use of Hyperbolic and Circular Lateration in the previous section, there was not the need to compare both positioning methods using the two RSS parameters. This result analysis was done in order to see which parameter had better performance when calculating the UE and femtocell position for when the UE's did not had GPS capabilities. In Figure 5.13 it is presented, for the same scenario, the results for proposed algorithm when using the RSCP and the RSSI.

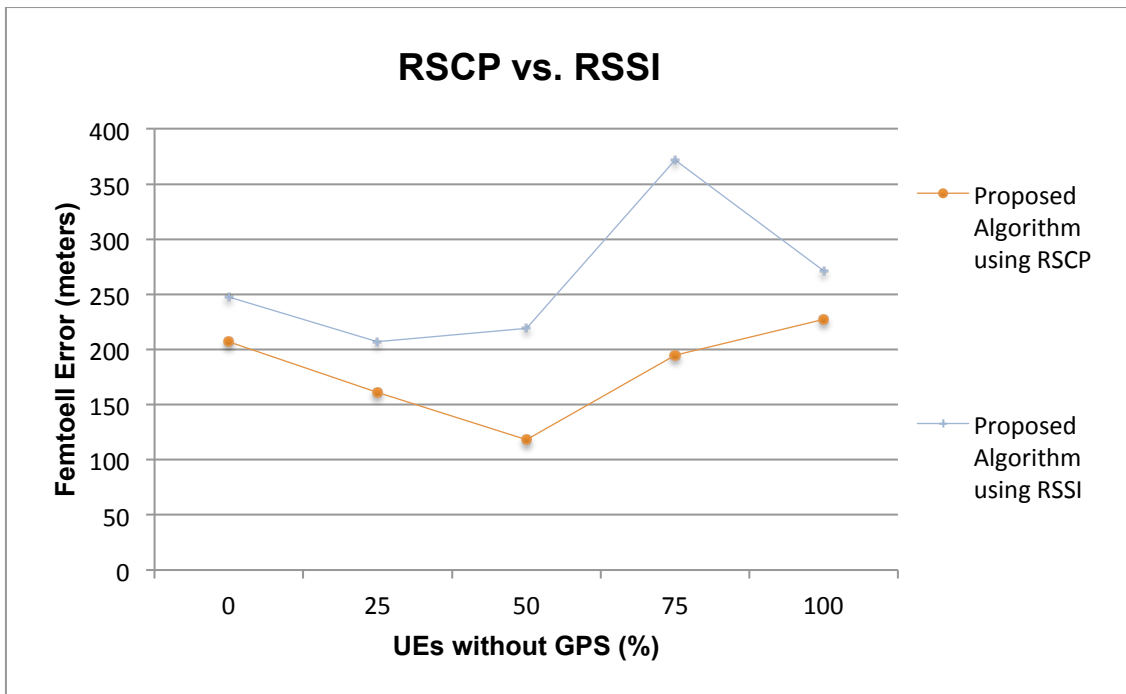


Figure 5.13. Proposed Algorithm. RSCP Vs. RSSI (GPS Dependency)

Table 5.14. Mean Error and Standard Deviation

Proposed Algorithm	GPS Dependency	
	Mean Error [Meters]	Standard Deviation [Meters]
Using RSCP	181.7638	38.3589
Using RSSI	263.385	58.5857

Figure 5.13 illustrates the dependency between the percentage of UE's that do not have GPS and the location error for the femtocell. Also, it can be seen that when RSSI is used the overall performance of the algorithm is much more degraded than when RSCP is used. As already explained for the situation where the femtocell is the non-serving, the algorithm may choose as the serving cell a cell that is not the actual serving cell. Furthermore, this bad selection may induce the algorithm to choose an inappropriate propagation model. In Table 5.14 are presented the mean errors and standard deviations for GPS dependency, which sustain that the RSCP has better performance than the RSSI.

# Chapter 6

## Conclusions and Future Work

In this chapter the context, structure, and main conclusions of this thesis are summarized and suggestions for future work are given.

The main objective of this thesis was the development of an algorithm for femtocell positioning, based on signal strength measurements and on the coordinates of the UE's connected to it. A precondition was the fact that the implementation of the algorithm should avoid costly modifications to the network. Positioning methods that used only signal strength parameters were therefore selected. On average, the proposed model was able to capture the location of femtocells obtained from a walk test to within 15-268 m.

Chapter 2 is focused on the description of femtocells in terms network architecture, radio interface, and coverage. Concerning network architecture and radio interface, the most relevant aspect is how the femtocells connect to the already existing network without the introduction of new components. Coverage is also a very important issue, because femtocells will be deployed in very large scale and it is necessary to optimize the network planning. The algorithm proposed in this thesis will allow a network operator to monitor femtocell locations. Based on this information he will be able to optimize the deployment of his outdoor cells. Chapter 2 further includes a description of propagation models, because they are the main tool to obtain the UE-femtocell and UE-BS distances, which are subsequently used for calculating the position of the target.

Chapter 3 includes an overview of the theory behind the positioning models. This chapter describes all the positioning methods that rely on RSS parameters. The main parameters used for assessment of the algorithm accuracy and error sources are also mentioned.

The details of the algorithm are presented in Chapter 4. The results of the validation tests, which also influenced the final version of the algorithm, are discussed in Chapter 5. The algorithm allows not only an estimation of femtocell coordinates but also the estimation of UE's positioning. The development strategy involved two parts: one concerning propagation models and another related to positioning models. Three propagation models were considered to estimate the UE-femtocell and UE-BS distances in different environments. The correspondence between the models and the possible scenarios is summarized in Tables 6.1 and 6.2.

When the UE is in an outdoor environment, the distance between the indoor femtocell and the UE is computed through the Path Loss Model for Outdoor to Indoor and Pedestrian Environments, as recommend by ETSI TR.101 [36]. COST231 Walfisch-Ikegami model estimates the distances between the UE and the surrounding BS's. When both the femtocell and UE are in an indoor environment, the propagation models used are the Path Loss Model for Outdoor to Indoor and Pedestrian Test Environment and the Path Loss Model for Indoor Office Test Environment. The first model is used to estimate the distance between the indoor UE and the outdoor BS's and the second model is used to estimate the distance between the indoor UE and the indoor femtocell. This model is also recommend by ETSI TR.101 [36]. To estimate the location of the femtocell two positioning models where selected: (i) when the femtocell is the non-serving cell the Circular Lateration model, which relies on an initial estimation of the target position, is used; (ii) when the femtocell is the serving cell, RSS-based Circular Lateration, which relies on the signal strengths that the UE receives from all surrounding cells at a given time, is applied. As detailed in Sections 4.1.2 and 4.2.3, some distance and time restrictions where assumed to improve overall accuracy of the femtocell positioning given by the algorithm.

Table 6.1. Correspondence between the propagation models and the scenarios for femtocell positioning

Environment		Model for the Calculation of Femtocell-UE Distance
Femtocell	UE	
Indoor	Outdoor	Path Loss Model for Outdoor to Indoor and Pedestrian Test Environment
Indoor	Indoor	Path Loss Model for Indoor Office Test Environment

Table 6.2. Correspondence between the propagation models and the scenarios for UE Positioning

Environment		Model for the Calculation of UE-BS Distance
UE	BS	
Outdoor	Outdoor	COST231 Walfisch-Ikegami
Indoor	Outdoor	Path Loss Model for Outdoor to Indoor and Pedestrian Test Environment

Only Circular Lateration was used for UE positioning because UE-BS distances are not short range. RSS-based Circular Lateration was not selected in this case since, as discussed in Chapter 5, it consistently led to poorer performance compared to Circular Lateration. The effect of using Hyperbolic rather than Circular Lateration on the accuracy of the model was also tested. The difference between Circular and Hyperbolic Lateration is that the former uses absolute ranges as observables and the latter difference ranges. The use of Hyperbolic Lateration led to an overall poorer performance of the algorithm.

As mentioned above, Chapter 5 is essentially devoted to a discussion of the results obtained in this work. The discussion was divided into three sections concerning the dependency of the femtocell location error on (i) the positioning methods, (ii) the GPS dependency, and (iii) the RSS parameters.

In the section on positioning methods (Section 5.3.1) a comparison of the two Lateration procedures is presented. At the end of this section a brief comparison of the two Lateration with the RSS based positioning method, in terms of mean error and standard deviation, is also given (see also Figure 5.5). This comparison showed that the RSS method performs slightly better than Circular or Hyperbolic Lateration for the short-range femtocell-UE distances typical of scenarios where the femtocell is the serving cell. The Lateration methods were compared for two situations:

- Femtocell as the serving cell. In this case, the calculation of the femtocell position was obtained by the RSS-based method using the point corresponding to the UE that receives the highest RSCP value as reference. A small improvement of the accuracy (2 % based on the mean error, see Table 5.8) of the positioning estimate could be obtained by adding an extra equation corresponding to Circular Lateration around the selected reference point to the computation (see also Figure 5.8). Hyperbolic Lateration was not considered in this case because, analogously to the RSS-based method, it requires a reference point.
- Femtocell as the non-serving cell. As shown in Figure 5.7, in general, Hyperbolic Lateration performs better than Circular Lateration. The latter method gives, however, more consistent results. Indeed, while Circular Lateration consistently leads to a positioning error of ~35 m, the error of hyperbolic lateration increases from ~11 m to ~203 m (1800 % increase) when the number of valid coordinates decreases from 3 to 2. Circular Lateration was therefore found to represent a better error/consistency compromise and was therefore selected for implementation in the algorithm.

Two other conclusions can be drawn from the results in this section: (i) if, for example, one of the signals received by an UE is considerably weaker than the others, and this signal is included in the calculations, the error of location of a femtocell will become larger; (ii) calculations that use a reference BS are much more sensitive (larger error oscillation) to the increase in the UE-femtocell distance than calculations that only use an initial estimation of the target's position.

Even today, not all UE's have GPS capabilities. For this reason it was necessary to evaluate the accuracy of the algorithm when the determination of UE location could not rely on GPS data. To overcome this problem the algorithm contains a module that, in the absence of GPS information, allows the estimation of UE positioning. Hyperbolic Lateration and Circular Lateration were tested for this purpose. As can be concluded from Figure 5.9 and Table 5.10, the performances of Circular and Hyperbolic Laterations are very similar. Circular Lateration was therefore selected to estimate UE location because, as mentioned above, it had already proven more consistent in terms of femtocell positioning error. Note, also, that when UE's without GPS capabilities were introduced in the calculation of the femtocell location, the obtained error did not always meet the FCC 911 requirements [11].

The RSS parameters also have an impact on the accuracy of the femtocell positioning. In this thesis, two types of RSS parameters were analyzed: the CPICH RSCP and the RSSI. The RSCP is one of the parameters used as a handover criterion [52] and is related with RSSI as defined in (5.1). The RSSI value corresponds to the total power received, which includes the interference from neighboring cells and other sources [18]. It can be concluded from Table 5.12 and Figure 5.11 that, when the femtocell is the serving cell and all the UE's have GPS capabilities the use of RSSI leads to a small degradation of the femtocell location error (~6%) relative to the use of RSCP. When the femtocell is the non-serving cell RSSI performs better but less consistently than RSCP (Figure 5.12 and Table 5.13). Finally, as illustrated in Figure 5.13 RSCP systematically gives smaller (19% to 91%) errors than RSSI independently of the percentage of UEs with GPS capabilities.

In closing, some suggestions for future work may be mentioned. The algorithm developed in this thesis can, in principle, become more accurate if an altitude coordinate, in addition to latitude and longitude, is considered. This 3D scenario is expected to improve the accuracy of the positioning estimates, because without an altitude coordinate it is, for example, impossible to discriminate femtocells located in different floor buildings. With better accuracy, the number of estimates that meet the FCC 911 standards should also increase. The development and validation of an algorithm for 3D geo positioning requires, however, that walk test measurements including latitude, longitude and altitude are performed. These data were not available for the present thesis. Another important aspect to better differentiate the cells is to have access to Cell IDs, in addition to the PSCs. Finally, it will be interesting to extend this study to LTE femtocells.



# Annex A – Link Budget

The calculation of the maximum path loss in a cell is a key factor for the estimation of the cell range, hence for a good cellular design. This calculation is called the link budget and throughout this thesis it is based in the 3GPP Release 99.

The total path loss can be calculated by [20]:

$$L_p = P_t + G_t - P_r + G_r = EIRP - P_r + G_r \quad [dB] \quad (A.1)$$

where:

- $L_p$  – Total path loss;
- $P_t$  – Transmitting antenna power (in dBm);
- $G_t$  – Transmitting antenna gain (in dBi);
- $P_r$  – Receiving antenna power (in dBm);
- $G_r$  – Receiving antenna gain (in dBi);
- $EIRP$  – Equivalent Isotropic Radiated Power (in dBm);

If diversity is used at the reception, its gains need to be taken into account. So,  $G_r$  in (A.1) is replaced by (A.2):

$$G_{r_{div}} = G_r + G_{div} \quad [dBi] \quad (A.2)$$

with:

- $G_{r_{div}}$  – Total gain, considering diversity (in dBi);
- $G_{div}$  – Diversity gain (in dBi);

The EIRP can be estimated for DL by (A.3) and for UL by (A.4):

$$EIRP^{DL} = P_{Tx} - L_c + G_t \quad [dBm] \quad (A.3)$$

$$EIRP^{UL} = P_{Tx} - L_u + G_t \quad [dBm] \quad (A.4)$$

where:

- $P_{Tx}$  – Transmitter output power (in dBm);
- $L_c$  – Cable loss attenuation between the transmitter and the BS antenna (in dB);

- $L_u$  – User body loss attenuation, which values can be [3, 10] dB for voice and [0, 3] dB for data (in dB);

The receiver power can be calculated by (A.5) for DL, and (A.6) for UL:

$$P_{Rx}^{DL} = P_r - L_u \quad [dBm] \quad (A.5)$$

$$P_{Rx}^{UL} = P_r - L_c \quad [dBm] \quad (A.6)$$

where:

- $P_{Rx}$  – Receiver input power;

Furthermore, in UMTS, the receiver sensitivity can be expressed as [20]:

$$P_{Rxmin} = N - G_p + SNR \quad [dBm] \quad (A.7)$$

where:

- $N$  – Total noise power given by (A.8) (in dBm);
- $G_p$  – Process gain (in dB), Table A.1;
- $SNR$  – Signal-to-noise ratio (in dB), Table A.1;

Table A.1. HSDPA and HSUPA processing gain and SNR definition (adapted from [53])

System	Processing gain	SNR
HSDPA	Fixed and equal to 16	SINR
HSUPA	$\frac{R_c}{R_b}$	$\frac{E_b}{N_0}$

The total noise power is given by [20]:

$$N = -174 + 10\log(\Delta f) + F + M_i \quad [dBm] \quad (A.8)$$

where:

- $\Delta f$  - signal bandwidth, in UMTS it is equal to  $R_c$  (in Hz);
- $F$  – Receiver noise figure (in dB);
- $M_i$  - Interference margin (in dB);

For sensitivity calculations, the  $E_b/N_0$  is obtained using  $E_c/N_0$  [20]:

$$\frac{E_b}{N_0} = \frac{E_c}{N_0} + G_p \quad [dB] \quad (A.9)$$

where:

- $E_b/N_0$  – Energy per bit to noise spectral density ratio (in dB);
- $E_c/N_0$  – Energy per chip to noise spectral density ratio (in dB);

Several margins have to be taken into account as defined by [20]:

$$M_p = M_{FSF} + M_{FFF} + L_{p_{ind}} - G_{SH} \quad [dB] \quad (A.10)$$

where:

- $M_{FSF}$  – Slow fading margin (in dB);
- $M_{FFF}$  – Fast fading margin (in dB);
- $L_{p_{ind}}$  – Indoor penetration losses (in dB);
- $G_{SH}$  – Soft handover gain (in dB);

Finally, the total path loss can be calculated by:

$$L_{p_{total}} = L_p + M_p \quad [dB] \quad (A.11)$$



# Annex B – Propagation Model

In this annex all the propagation models used in this work will be described. The first model that will be described is the COST231 – WI that is the most suited model for urban and suburban outdoor scenarios. The second model is the Path Loss Model for Outdoor to Indoor and Pedestrian Environment. This model is used for coverage efficiency and simple capacity evaluation. It is also used for spectrum efficiency evaluations in urban environments modelled through a Manhattan-like structure as described in [36], in order to evaluate the performance of Round-Trip Time (RTT) in microcell situations, which will be common in European cities for UMTS deployment. The Path Loss Model for Indoor Office Environment is the last model that will be described in this Annex. This model derived from the COST 231 indoor model presented in [30] and is recommend for this type of environments by [36].

## B.1 COST231 – Walfisch Ikegami

To estimate the path loss, the parameters used in this model are: building height ( $h_{Roof}$ ), street width ( $w_s$ ), building separation ( $w_b$ ) and street orientation with respect to the direct radio path ( $\varphi$ ) as shown in Figure B.1 and Figure B.2. This model distinguishes between LoS and NLoS. For LoS propagation ( $\varphi = 0$ ) the path loss is calculated through (B.1). For NLoS propagation the model is composed by three terms: free space loss ( $L_{FS}$ ), multiple screen diffraction loss ( $L_{msd}$ ) and roof-top-to-street and scatter loss ( $L_{rts}$ ). This situation is calculated by (B.2).

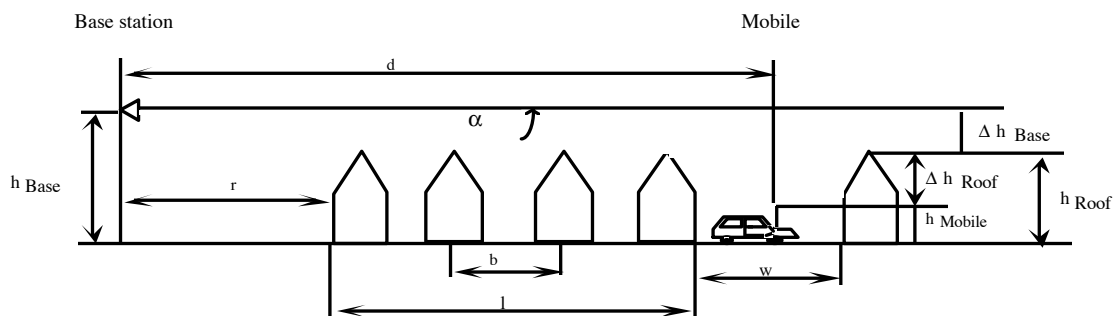


Figure B.1. Definition of the parameters used in the COST 231 – WI model (extracted from [30])

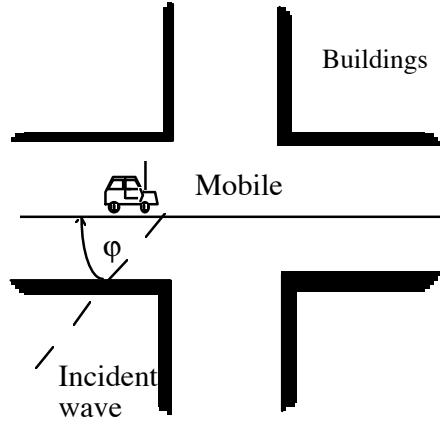


Figure B.2. Definition of the street orientation angle  $\varphi$  (extracted from [30])

$$L_p = 42.6 + 26\log_{10}(d) + 20\log_{10}(f), \text{ for } d \geq 0.02 \text{ Km} \quad [dB] \quad (B.1)$$

where:

- $d$  – Distance between the transmitter (in Kilometers);
- $f$  – Frequency (in MHz);

$$L_p = \begin{cases} L_0 + L_{rts} + L_{msd} & , \text{ for } L_{rts} + L_{msd} > 0 \\ L_0 & , \text{ for } L_{rts} + L_{msd} \leq 0 \end{cases} \quad [dB] \quad (B.2)$$

The free space loss is given by:

$$L_0 = 32.4 + 20\log_{10}(d) + 20\log_{10}(f) \quad [dB] \quad (B.3)$$

The term  $L_{rts}$  describes the coupling of the wave propagating along the multiple-screen path into the street where the UE is located. This term takes into account the street width and its orientation. It is based in the Ikegami model, however COST231 applies a different street-orientation function.

$$L_{rts} = -16.9 - 10\log_{10}(w_s) + 10\log_{10}(f) + 20\log_{10}(\Delta h_{Mobile}) + L_{ori} \quad [dB] \quad (B.4)$$

where:

- $\Delta h_{Mobile}$  - Difference between the roof height and the mobile height (in meters):

$$\Delta h_{Mobile} = h_{roof} - h_{Mobile} \quad (B.5)$$

- $L_{ori}$  - Street orientation loss (in dB):

$$L_{ori} = \begin{cases} -10.0 + 0.354\varphi & , \quad 0^\circ < \varphi < 35^\circ \\ 2.5 + 0.075(\varphi - 35) & , \quad 35^\circ \leq \varphi < 55^\circ \\ 4.0 + 0.114(\varphi - 55) & , \quad 55^\circ \leq \varphi < 90^\circ \end{cases} \quad [dB] \quad (B.6)$$

The  $L_{msd}$  parameter describes the loss between the BS antennas and the last rooftop. COST 231

extended this model for BS antennas that are located below rooftop levels with the use of an empirical function, based on measurements.

$$L_{msd} = L_{bsh} + k_a + k_d \log_{10}(d) + k_f \log_{10}(f) - 9 \log_{10}(w_b) \quad [dB] \quad (B.7)$$

where:

- $L_{bsh}$  - Losses due to the fact that BS antennas are above or below roof-top level (in dB):

$$L_{bsh} = \begin{cases} -18 \log(1 + \Delta h_{base}) & , \text{ for } h_{base} > h_{Roof} \\ 0 & , \text{ for } h_{base} \leq h_{Roof} \end{cases} \quad [dB] \quad (B.8)$$

with  $\Delta h_{base}$  being the difference between the BS antenna height and the roof-top height (in meters):

$$\Delta h_{base} = h_{base} - h_{Roof} \quad (B.9)$$

- $k_a$  – increase of the path loss for BS antennas below the roof-top of the adjacent buildings:

$$k_a = \begin{cases} 54 & , \text{ for } h_{base} > h_{Roof} \\ 54 - 0.8 \Delta h_{base} & , \text{ for } d \geq 0.5 \text{Km} \text{ and } h_{base} \leq h_{Roof} \\ 54 - 1.6 \Delta h_{base} d & , \text{ for } d < 0.5 \text{Km} \text{ and } h_{base} \leq h_{Roof} \end{cases} \quad (B.10)$$

- $k_d$  – control the dependence of the multi-screen diffraction loss versus distance:

$$k_d = \begin{cases} 18 & , \text{ for } h_{base} > h_{Roof} \\ 18 - 15 \frac{\Delta h_{base}}{h_{Roof}} & , \text{ for } h_{base} \leq h_{Roof} \end{cases} \quad (B.11)$$

- $k_f$  – control the dependence of the multi-screen diffraction loss versus frequency:

$$k_f = \begin{cases} -4 + 0.7 \left( \frac{f}{925} - 1 \right), & \text{for } \begin{cases} \text{urban} \\ \text{suburban} \end{cases} \\ -4 + 1.5 \left( \frac{f}{925} - 1 \right), & \text{for } \text{dense urban} \end{cases} \quad (B.12)$$

If the data on the structure of buildings and roads are unknown the following default values are recommend by [30]:

$$\left\{ \begin{array}{l} h_{\text{Roof}} = 3x\{\#\text{floors}\} + \text{Roof} - \text{height} \\ \text{Roof} - \text{height} = \begin{cases} 3\text{m} & \text{for pitched} \\ 0 & \text{for flat} \end{cases} \\ w_b \in [20,50] \\ w_s = \frac{w_b}{2} \\ \varphi = 90^\circ \end{array} \right.$$

The model is restricted to [30]:

$$\left\{ \begin{array}{l} f \in [800,2000] \\ d \in [0.02,5] \\ h_{\text{base}} \in [4,50] \\ h_{\text{Mobile}} \in [1,3] \end{array} \right.$$

The standard deviation of this model takes values in [4, 8] dB and the error increases when the BS height is much higher than the roof height as described in [30].

## B.2 Path Loss Model for Outdoor to Indoor and Pedestrian Environment

This model is intended for outdoor to indoor environments and pedestrian test environments and it is assumed a 1.5m mobile antenna height. In the general model the outdoor losses are described by (B.13):

$$L_p = L_{fs} + L_{rts} + L_{msd} \quad [dB] \quad (B.13)$$

where:

- $L_{fs}$  – Free space loss (in dB):

$$L_{fs} = -10 \log_{10} \left( \frac{\lambda}{4\pi d} \right)^2 \quad [dB] \quad (B.14)$$

- $L_{rts}$  – Diffraction loss from rooftop to the street (in dB):

$$L_{fs} = -10 \log_{10} \left[ \frac{\lambda}{2\pi^2 r} \left( \frac{1}{\theta} - \frac{1}{2\pi + \theta} \right)^2 \right] \quad [dB] \quad (B.15)$$

$$\theta = \tan^{-1}\left(\frac{|\Delta h_m|}{x}\right) \quad [dB] \quad (B.16)$$

$$r = \sqrt{(\Delta h_m)^2 + x^2} \quad [dB] \quad (B.17)$$

with  $\Delta h_m$  being the difference between the mean building height and the mobile antenna height and  $x$  the horizontal distance between the mobile and the diffracting edges.

- $L_{msd}$  – Loss due to multiple screen diffraction past rows of buildings (in dB):

$$L_{msd} = -10\log_{10}(Q_m^2) \quad [dB] \quad (B.18)$$

with  $Q_m$  being a factor that depends of BS antenna height relative to the mean buildings height [ref]

In this model  $L_{fs}$  and  $L_{rts}$  are independent of the BS antenna height, while in  $L_{msd}$  the BS antenna height strongly depends if it is above, below or at building heights.

However, if the BS antenna height is near the mean rooftop level:

$$Q_m = \frac{d}{R} \quad (B.19)$$

Finally, (B.13) becomes:

$$L_p = -10\log_{10}\left(\frac{\lambda}{2\sqrt{2\pi R}}\right)^2 - 10\log_{10}\left[\frac{\lambda}{2\pi^2 r}\left(\frac{1}{\theta} - \frac{1}{2\pi + \theta}\right)^2\right] - 10\log_{10}\left(\left(\frac{d}{R}\right)^2\right) \quad [dB] \quad (B.20)$$

When  $\Delta h_b = -5m$ ,  $\Delta h_b = 10.5m$ ,  $x = 15m$  and  $b = 80m$  (B.21) reduces to a simple function depending only on the distance between the transmitter and the receiver and the frequency.

$$L_p = 40\text{Log}_{10}(R) + 30\text{Log}_{10}(f) + 49 \quad [dB] \quad (B.21)$$

where:

- $R$  – Distance between the transmitter (in Kilometers);
- $f$  – Frequency (in MHz);

Also, for this model,  $L_p$  cannot be less than the free space loss. Furthermore, it is only valid for NLoS case and describes the worst-case propagation. It is assumed a log-normal shadow fading with a standard deviation of 10 dB and 12 dB for outdoor and indoor users, respectively, and an average building penetration loss of 12 dB with a standard deviation of 8 dB [36].

## B.3 Path Loss Model for Indoor Office Environment

This model, as mentioned earlier, derives from the COST 231 indoor model. This COST 231 indoor model is described by (2.3). However, the constant loss parameter and number of penetrated floors have the values as suggested by [36]:

$$\left\{ \begin{array}{l} L_c = 37 \text{ dB} \\ n = 4 \text{ is an average for indoor office environment. For capacity calculations in moderately pessimistic environments, the value can be modified to } n = 3. \end{array} \right.$$

Under the assumptions mentioned above and in Table 2.5, for office environment, the indoor path loss model has the following form:

$$L_p = 37 + 30\text{Log}_{10}(R) + 18.3 * n \left( \frac{n+2}{n+1} \right)^{-0.46} \quad [\text{dB}] \quad (\text{B.22})$$

where:

- $R$ – Distance between the transmitter and the receiver (in meters);
- $n$  – number of floors between the transmitter and the receiver;

For this model  $L_p$  shall in no circumstances be less than the free space loss. Also, it is expected a 12 dB log-normal shadow fading standard deviation and it is assumed a mobile antenna height of 1.5m [36].

# Annex C – Interference Management

In this annex, it will be described, how the femtocell manages interference. With the deployment of femtocells in macrocellular networks, two clearly separated layers appear in the network architecture, the macrocell layer and the femtocell layer. However, this two-layer topology brings new problems and creates new design challenges. One of the main challenges that a femtocell deployment faces is the interference. Interference-limited systems, such as CDMA, will be greatly affected by the presence of femtocells and therefore interference avoidance techniques, such as time hopping or power control are required. If interference avoidance techniques are not applied, dead zones may appear within the macrocell, causing the service to disrupt in the proximity of a femtocell. In this section the key concepts of interference are given, and several interference avoidance techniques are overviewed.

## C.1 Key concepts

Femtocells provide indoor coverage to the subscribers, but they also radiate towards neighboring houses as well as outdoors. Figure C.1 shows a two-layer network, where interference among the different elements in the network is illustrated.

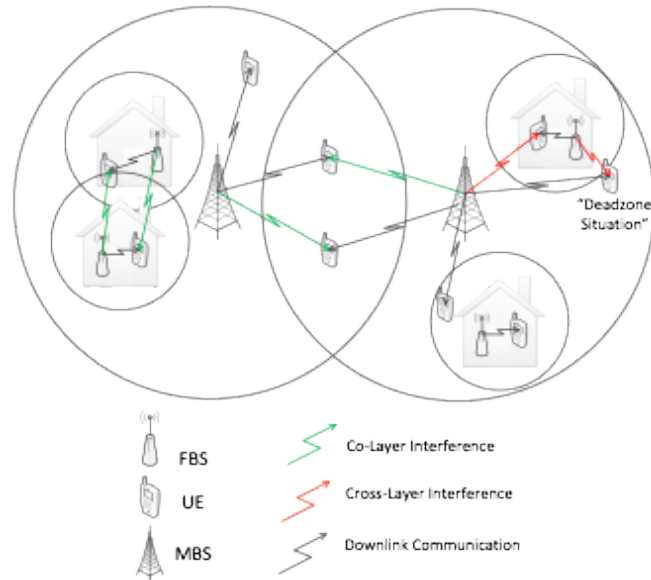


Figure C.1. Interference scenarios in a two-layer network (extracted from [54])

According to [3], interference can be classified as:

- Co-Layer – This type of interference is described as the unwanted signal received at a femtocell and sent from other femtocells, thus decreasing the quality of its communication. The name makes reference to the fact that all femtocells belong to the same network layer, unlike other elements like Node Bs. This kind of interference occurs mainly between immediate neighbors due to low isolation between house and apartments. Since femtocells can be deployed in three access modes, the impact of the co-layer interference will be different from each one.
- Cross-Layer – Occurs among network elements that belong to different layers of the network. This type of interference is a problem especially in two-layer networks where both femtocells and macrocells share the same frequency band.

As mentioned before, severe interference can lead to dead zones, which are areas where the Quality of Service (QoS) is significantly degraded. For this reason interference management is required in order to avoid these situations.

## C.2 Interference Cancellation

Interference Cancellation (IC) refers to any method that is used to minimize the effects of interference in receiver systems. The interest in these techniques in femtocell networks comes from the unavoidable presence of co-channel interference and the need for receiving systems that can operate in the presence of higher interference levels. The sources of co-channel interference can be femtocells and macrocells BS's as well as femtocells and macrocells UEs. The interfering source is important to be known because it will determine the optimal process for IC.

For UL, according to [3], there are five techniques to be used for IC:

- Filter Based - The main objective of this technique is to provide a filter that attenuates part of the spectrum of the input signal that is highly affected by interference. Mainly this technique attenuates regions of the spectrum where the SIR is very low and amplifies the parts where it is high. For these reasons, these filters need to be adaptive and change over time depending on the interference condition. One of the ways of doing this adaptation is with the Forward Linear Prediction (FLP).
- Multiuser Detection – These kind of techniques are based on the fact that each user has a certain signature waveform. For CDMA systems, this technique relies strongly on the orthogonality of the waveforms from different users, because each one makes use of a different spreading code. Two approaches were proposed: (i) Minimum Mean Square Error detector [55]; (ii) Successive Interference Cancellation (SIC) [56].
- Cyclostationary – This technique relies on the fact that the statistics of cyclostationary signals vary over a certain period of time. In the frequency domain, this translates into fluctuations of  $n$  frequency bands that are statistically dependent. Frequency Shift (FRESH) filters are used to combine frequency shifted versions of the input versions of the input signals and to the removal of interference when the desired signal is used as reference. However there is a need for blind adaptation of FRESH filters, because the desired signal is obviously not present at the receiving end.
- High Order Statistics – These methods are based on the use of signal statistics other than first order statistics. They proved to be quite successful for the purpose of source separation. The objective is to separate independent signals from their addition to others, which can be done effectively by using spatial diversity with array antennas. As an example of this technique, Blind Source Separation is based on the use of higher order statistics and it consists on separating the signals coming from multiple users using multiple outputs of an array antenna.
- Spatial Processing – The main idea of this technique is to assign different weights to the elements of the receiving antenna array so as to form beams in given directions. This way, the direction of the interfering signal can be attenuated, while the desired signal is amplified. Multiple Input Multiple Output (MIMO) can be applied for this purpose.

In the DL, IC techniques are implemented on the mobile terminal, but the objective is still to mitigate the effect of co-channel interference like in the UL.

### C.3 Interference Avoidance

IC techniques are usually expensive to implement, increasing the cost of the network. Due to this fact, interference avoidance is being considered as an approach with higher chances of success. In CDMA systems, time hopping has been proposed for reducing cross-layer uplink interference [3]. The basic

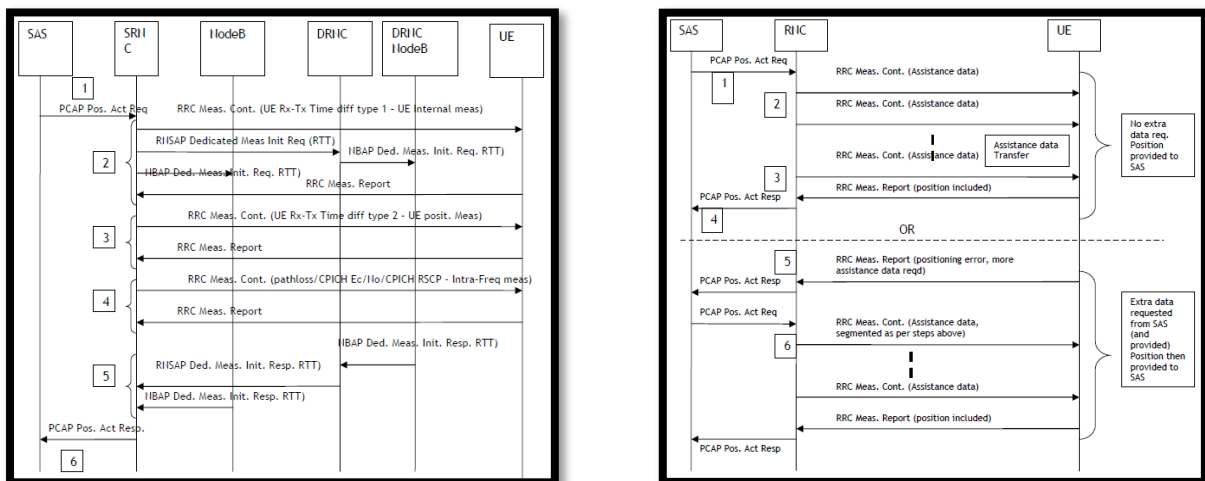
idea is to transmit during short periods and staying idle during the remaining period. In this approach it is assumed that femtocells and macrocells do not communicate. The moment of transmission is selected independently in the two-layers of the network, meaning that no procedure for synchronization of the transmission slots of different cells is needed. Each UE connected to the femtocell chooses for transmission one of the hopping slots whose length is  $T/N_{hop}$ .  $T$  is the time period of a CDMA transmission and  $N_{hop}$  is the number of hopping slots. This approach reduces the interference between different femtocells and between femtocells and macrocells by a factor of  $N_{hop}$ , according to [57]. If there are many UE's connected to the femtocell, the joint hopping is a good approach for reducing the outage probability in the uplink of the macrocells. In this approach all the users of the same femtocell transmit in the same time slot, thanks to the averaging aggregate interference in CDMA systems. Also,  $N_{hop}$  decreases interference between different femtocells since the selection of the transmission slot is independent between femtocells. Also in [57] it is proposed to other techniques: (i) the use of antennas with  $n$  sectors ( $N_{sec}$ ) is suggested as way of reducing the interference caused by UE's, connected to macrocells, in the uplink. In this approach the interference between femtocells and macrocells is decreased by  $N_{sec}$ ; (ii) the use of the femtocell exclusion region, which consists in silencing femtocells that are too close to a macrocell.

# Annex D – Positioning Procedures

In this annex gives a brief description of how does the UE reports its position to the network. In [28], the procedures for UE positioning are described. The procedures that will be explained in this annex will be between the UE and a BS, however it can be assumed that the messages flow will be almost the same between the UE and a femtocell.

The measurement control messages includes all the standard RRC messages such as the message type, the transaction identifier and the integrity check information. One of the elements of these messages is the UE positioning measurement. This UE positioning measurement includes the positioning configuration information, the reporting criteria (event triggered or periodic reporting) and the assistance data for the Observed TDoA and GPS measurements [28].

In Figure D.1 it is illustrated a message flow between the UE and the network.



(a)

(b)

Figure D.1. Message flow between the UE and the network. (a) UE based. (b) UE assisted. (extracted from [58])

The Serving Mobile Location Centre (SMLC) is the network element that handles location services. So the Stand Alone SMLC (SAS) is a server that determines, initiates and controls the procedures for

related to positioning requests of an UE by exchanging information with the RNC. These exchanges involve the UE positioning measurement data or UE position estimated data. However the RNC is responsible for determining, initiating and controlling the positioning method to be used for each request made by SAS. The Positioning Calculation Application Part (PCAP) is a protocol between the RNC and SAS that consists of elementary procedures. These procedures are shown in Figure D.2. The PCAP has the function of position calculation, information exchange and for reporting general error situations.

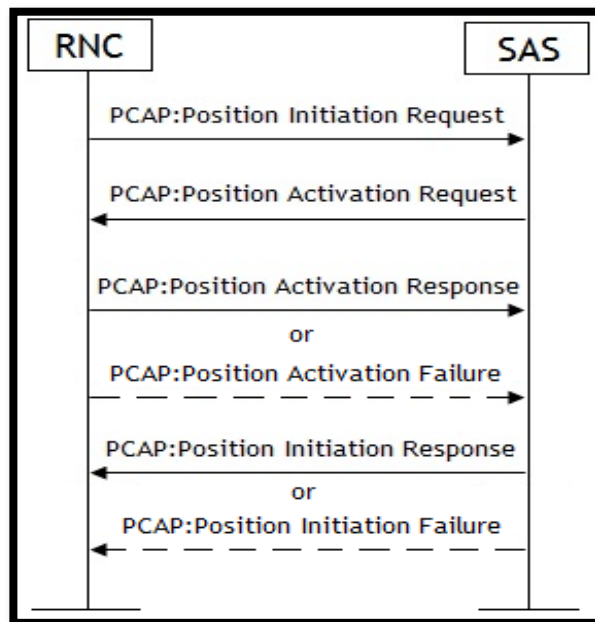


Figure D.2. Messages procedures between the RNC and SAS (extracted from [58])

In the UE based methods the UE position calculation is performed by the target itself based on measurements provide by the network or by the GPS. In the UE assisted method the UE position calculation is performed by the network based measurement reported by the UE and on data collected by the network. However, both methods depend always on the network and UE capabilities. The most common methods used for UE positioning are: (i) A-GPS, where the UE performs GPS measurements with the help of data provided by the network, however this method may be UE based or assisted; (ii) Cell-ID/RTT, where the UE uses measurements performed by the BS to calculate its location. This methods uses the UE's mobility algorithm, the BS geographical coordinates, time measurements and path loss measurements; (iii) Cell-ID, which uses only the geographical coordinates of the serving BS.

# Annex E – Additional Results

This annex shows additional simulation results. The results presented are for the reference scenario and for two different femtocells, which will be denoted by Femtocell 1 and Femtocell 2.

In Figure D.1 and Figure D.2 one can see the results of the algorithm, for when the two femtocells are the serving cells, for four different algorithms that were developed in this work: (i) Circular Lateration + RSS-based, using RSCP; (ii) (Circular Lateration + RSS-based, using RSSI; (iii) Hyperbolic Lateration + RSS-based, using RSCP; (iv) Hyperbolic + RSS-based, using RSSI; Also, it is shown in Table D.1 and Table D.2 the mean errors and standard deviations for all the algorithms.

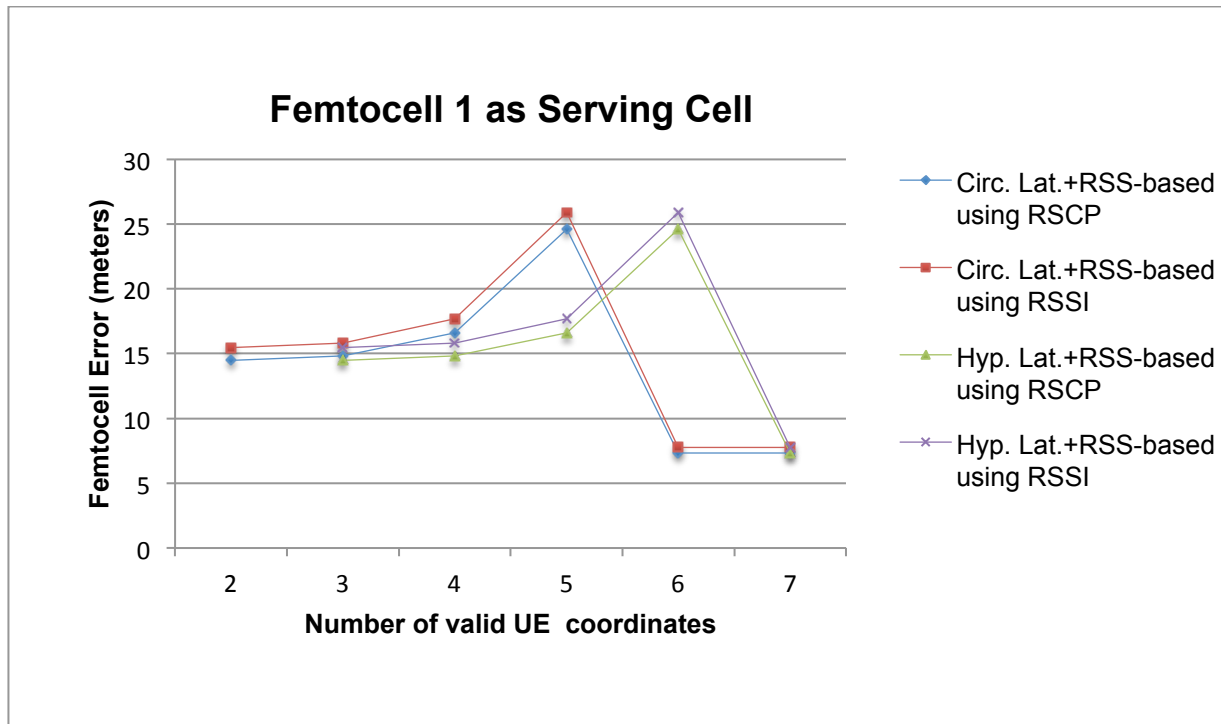


Figure E.1. Comparison between all the methods developed for when the femtocell is the Serving Cell (Femtocell 1)

Table E.1. Mean Error and Standard Deviation for Serving Cell (Femtocell 1)

Proposed Algorithm	Mean Error [Meters]	Standard Deviation [Meters]
Circ. Lat + RSS-based using RSCP	14.1981	5.8938
Circ. Lat + RSS-based using RSSI	15.0641	6.2134
Hyp. Lat + RSS-based using RSCP	15.5708	5.5117
Hyp. Lat + RSS-based using RSSI	16.5258	5.7887

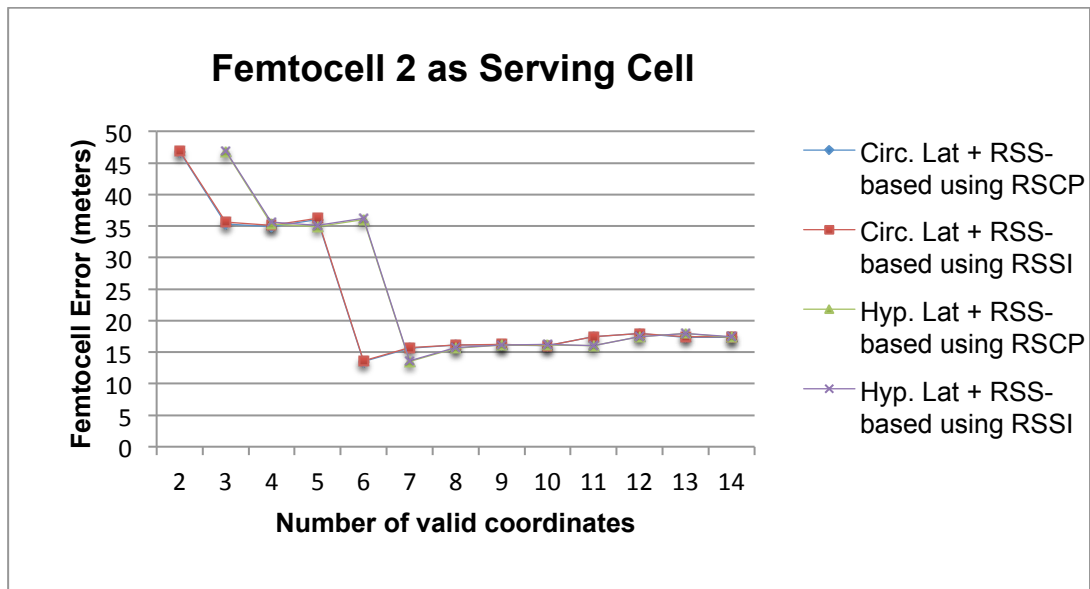


Figure E.2. Comparison between all the methods developed for when the femtocell is the Serving Cell (Femtocell 2)

Table E.2. Mean Error and Standard Deviation for Serving Cell (Femtocell 2)

Proposed Algorithm	Mean Error [Meters]	Standard Deviation [Meters]
Circ. Lat + RSS-based using RSCP	23.1187	10.5175
Circ. Lat + RSS-based using RSSI	23.2308	10.5707
Hyp. Lat + RSS-based using RSCP	23.5986	10.8094
Hyp. Lat + RSS-based using RSSI	23.7152	10.8629

In Figure D.1 and in Figure D.2 one can see that results are almost the same. However, and as explained in Section 5.2.2, the algorithms using Circular Lateration use one more measurement than the ones using Hyperbolic Lateration. With the use of this extra measurement the mean error for both algorithms is reduces and the standard deviation increases in Table D.1, however in Table D.2 the mean error also decreases, however is this case the standard deviation also decreases. This variation of the standard deviation, for both tables, derives from the extra measure, meaning that if the RSCP of the additional measurement is above the mean values of the others RSCP the standard deviation decreases, and vice-versa.

In Figures D.3 and Figure D.4 the same results are shown, however in this case the femtocells are not UE's the serving cell. Also, in Table D.3 and Table D.4 the mean error and standard deviation are shown.

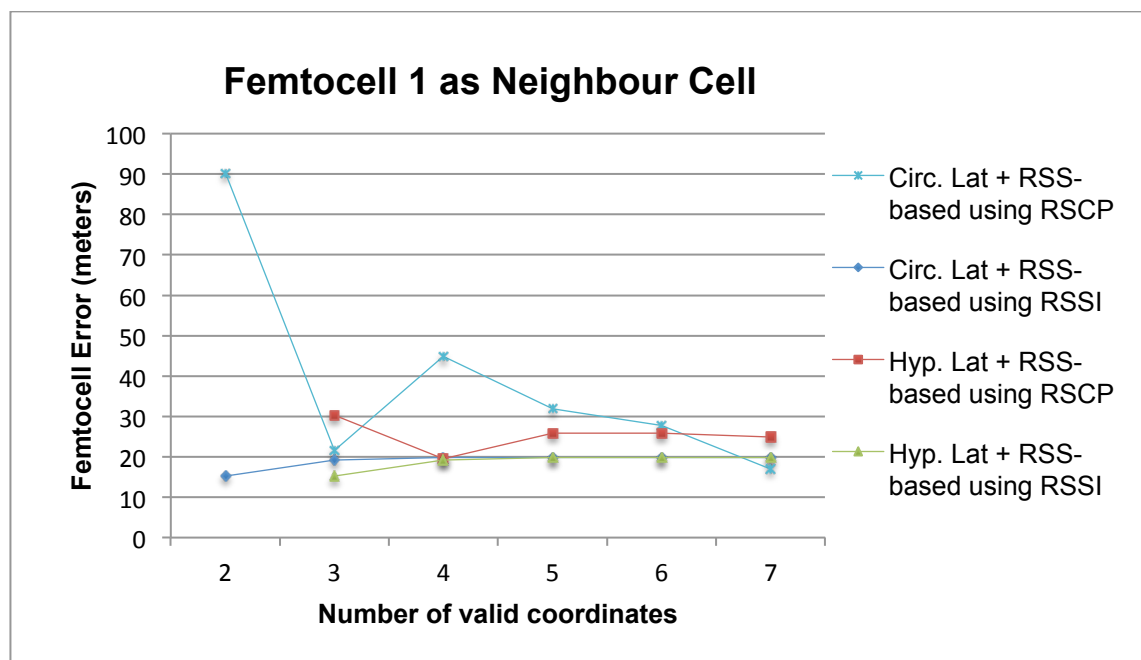


Figure E.3. Comparison between all the methods developed for when the femtocell is a Neighbor Cell (Femtocell 1)

Table E.3. Mean Error and Standard Deviation for Neighbor Cell (Femtocell 1)

Proposed Algorithm	Mean Error [Meters]	Standard Deviation [Meters]
Circ. Lat + RSS-based using RSCP	38.8503	24.5499
Circ. Lat + RSS-based using RSSI	18.9621	1.6864
Hyp. Lat + RSS-based using RSCP	25.3177	3.4643
Hyp. Lat + RSS-based using RSSI	18.7796	1.7925

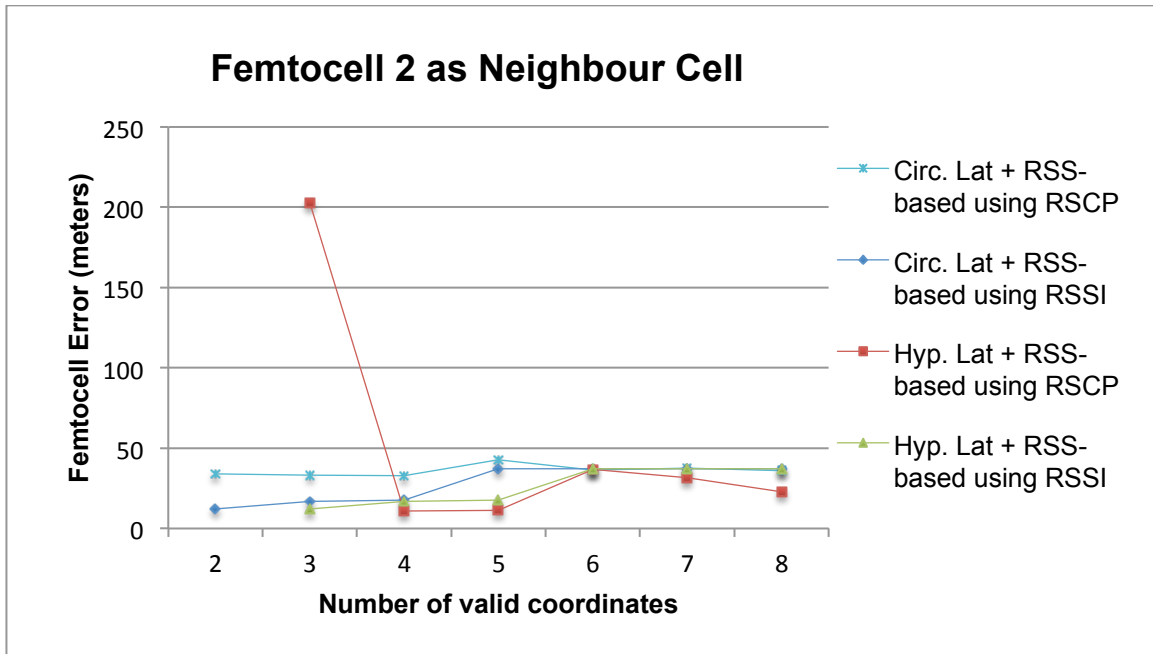


Figure E.4. Comparison between all the methods developed for when the femtocell is a Neighbor Cell (Femtocell 2)

Table E.4. Mean Error and Standard Deviation for Neighbor Cell (Femtocell 2)

Proposed Algorithm	Mean Error [Meters]	Standard Deviation [Meters]
Circ. Lat + RSS-based using RSCP	36.1465	3.116
Circ. Lat + RSS-based using RSSI	27.8629	10.7336
Hyp. Lat + RSS-based using RSCP	52.7056	67.7438
Hyp. Lat + RSS-based using RSSI	26.3392	10.8701

As illustrated in Figure D.3 the algorithms using Hyperbolic Lateralation have better performance than the ones using Circular Lateralation. Furthermore, the algorithms using RSSI have also better performance than the ones using RSCP as shown in Table D.3. However, the algorithm using Circular Lateralation and RSCP presents a better final result than all the others. Also, in Figure D.4 and Table D.4 the algorithms using RSSI have better performance, in terms of mean error, than the ones using RSCP, however the ones using RSCP present better final result and smaller standard deviations.

In Figure D.5 and D.6 it is illustrated the GPS dependency for both femtocells. In Table D.5 and Table D.6 mean errors and standard deviations are also shown.

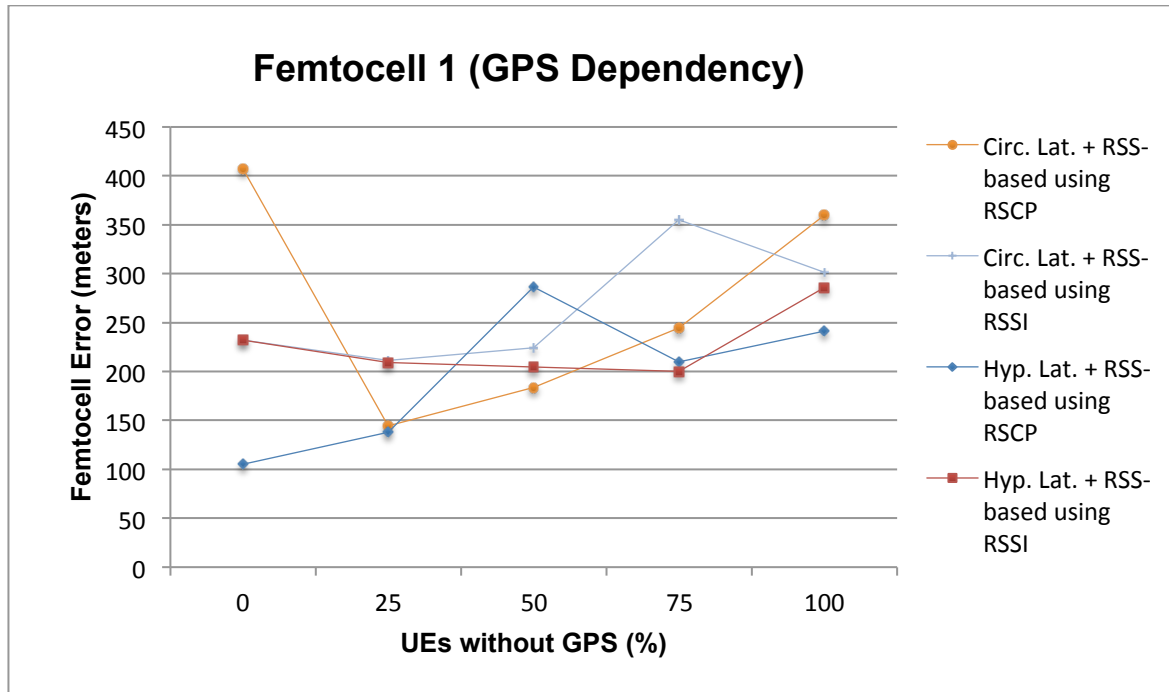


Figure E.5. Comparison between all the methods developed for GPS Dependency (Femtocell 1)

Table E.5. Mean Error and Standard Deviation for GPS Dependency (Femtocell 1)

Proposed Algorithm	Mean Error [Meters]	Standard Deviation [Meters]
Circ. Lat + RSS-based using RSCP	267.7651	100.7796844
Circ. Lat + RSS-based using RSSI	264.82454	54.84393114
Hyp. Lat + RSS-based using RSCP	196.14574	66.43668746
Hyp. Lat + RSS-based using RSSI	226.43646	31.60550577

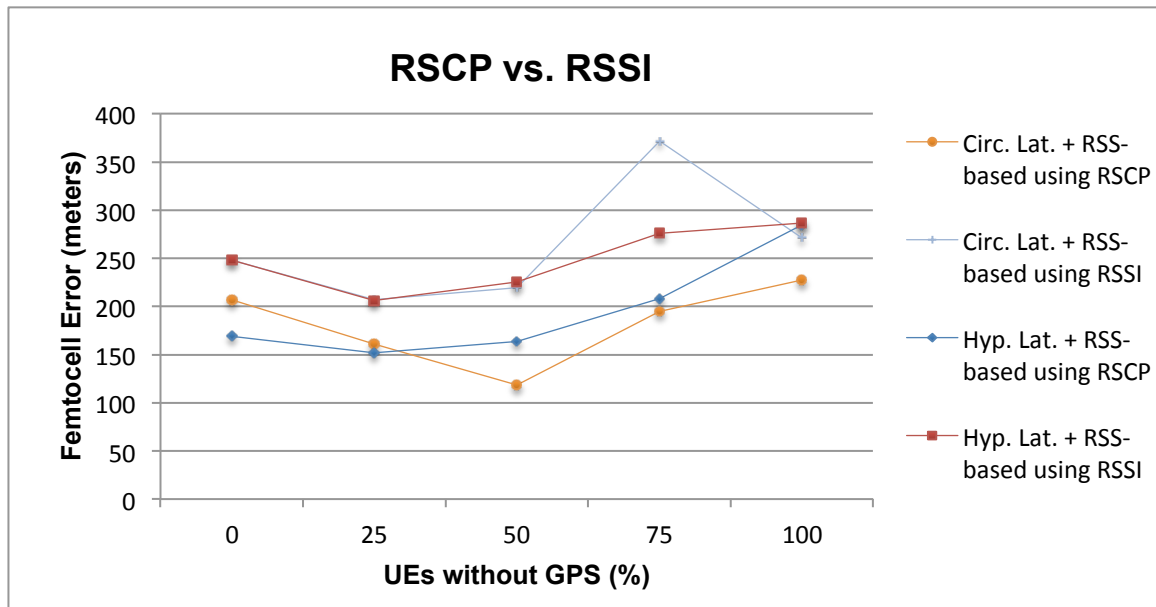


Figure E.6. Comparison between all the methods developed for GPS Dependency (Femtocell 2)

Table E.6. Mean Error and Standard Deviation for GPS Dependency (Femtocell 2)

Proposed Algorithm	Mean Error [Meters]	Standard Deviation [Meters]
Circ. Lat + RSS-based using RSCP	181.76382	38.35893053
Circ. Lat + RSS-based using RSSI	263.385	58.58573131
Hyp. Lat + RSS-based using RSCP	195.54142	48.52972782
Hyp. Lat + RSS-based using RSSI	248.25516	30.10617775

In Figure D.5 and Table D.5 shows that the algorithm using Circular Lateralation with RSCP as the worst performance from all the four, however in Figure D.6 and Table D.6 the same algorithm presents the best performance. As already mentioned the difference between the two Figures is explained with bad values of the RSCP's, which has a great influence on the positioning of the target. Also the same thing happens for the RSSI algorithms, but in an inverse order, however is this case, the influence comes not only by the bad values for the RSSI, but also from a bad selection of the reference cell, as explained in Section 5.3.3.

# References

- [1] I. Cisco Systems, "Cisco Visual Networking Index: Global Mobile Data Traffic Forecast Update, 2011-2016." 2012.
- [2] Alcatel-Lucent, "9360 Small Cells concepts." 2010.
- [3] J. Zhang and G. de la Roche, "Femtocells: Technologies and Deployment." Wiley, Chichester, 2010.
- [4] S. Forum, "Femtocells – Natural Solution for Offload," no. June, 2010.
- [5] S. Forum, "Wireless in the home & office : the need for both 3G femtocells and Wi-Fi access points," no. January, 2010.
- [6] "Small Cell Forum." [Online]. Available: [www.smallcellforum.org](http://www.smallcellforum.org).
- [7] Technical Specification Group Radio Access Network, "UTRAN architecture for 3G Home Node B (HNB) (Release 10)." 3GPP, 2011.
- [8] H.-C. Lee, D.-C. Oh, and Y.-H. Lee, "Mitigation of Inter-Femtocell Interference with Adaptive Fractional Frequency Reuse," in *2010 IEEE International Conference on Communications*, 2010, pp. 1–5.
- [9] J. Andrews, H. Claussen, and M. Dohler, "Femtocells: Past, present, and future," no. Section, pp. 1–12, 2012.
- [10] V. Chandrasekhar and J. Andrews, "Femtocell networks: a survey," *IEEE Communications Magazine*, vol. 46, no. September, pp. 59–67, 2008.
- [11] F. C. Commission, "FCC Wireless 911 Requirements Fact Sheet," Jan-2001. [Online]. Available: [http://transition.fcc.gov/pshs/services/911-services/enhanced911/archives/factsheet\\_requirements\\_012001.pdf](http://transition.fcc.gov/pshs/services/911-services/enhanced911/archives/factsheet_requirements_012001.pdf).
- [12] A. N. de Comunicações, "Regulamento do 112 L," Lisbon, 2002.
- [13] S. Forum, "Femtocell Synchronization and Location," no. May, 2012.
- [14] K. Axel, "Location-Based Services: Fundamentals and Operation," *John Wiley & Sons*. Wiley, Chichester, 2005.
- [15] Technical Specification Group Radio Access Networks, "3G Home NodeB Study Item Technical Report (Release 8)." 3GPP, 2008.

- [16] Technical Specification Group Services and System Aspects, "Architecture aspects of Home NodeB and Home eNodeB (Release 9)." 3GPP, 2009.
- [17] Broadband Forum Technical Report Issue 1 Amendment 2, "CPE WAN Management Protocol," Broadband Forum, 2007.
- [18] M. Sauter, "From GSM to LTE: An introduction to Mobile Networks and Mobile Broadband." Wiley, Chichester, 2010.
- [19] Alcatel-Lucent, "EVOLIUM UMTS Radio Principles," 2004.
- [20] L. M. Correia, "Mobile Communications Systems – Lecture Notes." Instituto Superior Técnico, Lisbon, 2009.
- [21] Alcatel-Lucent, "9300 W-CDMA UA06 HSxPA Radio Principles," no. 1. 2009.
- [22] Alcatel-Lucent, "HSxPA Parameters User Guide." 2011.
- [23] Alcatel-Lucent, "Alcatel-Lucent Whitepaper UMTS In-Building Solutions." 2007.
- [24] Technical Specification Group Radio Access Network, "Improvement of RRM across RNS and RNS/BSS (Release 5)," no. Release 5. 3GPP, 2001.
- [25] Alcatel-Lucent, "Femto Parameter User Guide BCR 2.4." Jun-2011.
- [26] G. de la Roche, A. Valcarce, D. Lopez-Perez, and J. Zhang, "Access control mechanisms for femtocells," *IEEE Communications Magazine*, vol. 48, no. 1, pp. 33–39, Jan. 2010.
- [27] Technical Specification Group Radio Access, "Mobility procedures for Home Node B (HNB), Overall description (Stage 2) (Release 10)." 3GPP, 2011.
- [28] Technical Specification Group Radio Access Network, "Radio Resource Control (RRC), Protocol specification (Release 10)." 3GPP, 2012.
- [29] R. Batista, "Performance Evaluation of UMTS/HSPA+ Data Transmission for Indoor Coverage," Instituto Superior Técnico, 2011.
- [30] E. Damosso and L. M. Correia, "Digital Mobile Radio Towards Future Generation Systems (COST 231 Final Report)," Brussels, 1999.
- [31] M. Hata, "Empirical formula for propagation loss in land mobile radio services," *Vehicular Technology, IEEE Transactions on*, vol. 29, no. 3. pp. 317–325, 1980.
- [32] Y. Okumura, E. Ohmori, T. Kawano, and K. Fukuda, "Field Strength and its Variability in VHF and UHF land mobile radio service," vol. 16, no. 9–10, pp. 825–873, 1968.
- [33] J. Walfisch and H. L. Bertoni, "A theoretical model of UHF propagation in urban environments," *Antennas and Propagation, IEEE Transactions on*, vol. 36, no. 12. pp. 1788–1796, 1988.

- [34] F. Ikegami, S. Yoshida, T. Takeuchi, and M. Umehira, "Propagation factors controlling mean field strength on urban streets," *Antennas and Propagation, IEEE Transactions on*, vol. 32, no. 8. pp. 822–829, 1984.
- [35] A. J. A. Marques, "Modelling of Building Height Interference Dependence in UMTS," Instituto Superior Técnico, 2008.
- [36] ETSI, "Selection Procedures for the Choice of Radio Transmission Technologies of the UMTS," Technical Report 101 112 V3.1.0, 1998.
- [37] A. Schmidt-Dannert and S. SNET, "Positioning Technologies and Mechanisms for mobile Devices," *Master Module SNET2 (TU-Berlin, ed.)*.
- [38] F. C. Commission, "OET Bulletin No. 71 Guidelines for Testing and Verifying the Accuracy of Wireless E911 Location Systems," *Federal Communication Commission*, no. 71, 2000.
- [39] J. Borkowski and J. Lempiäinen, "Pilot correlation positioning method for urban UMTS networks." *Wireless Conference 2005 - Next Generation Wireless and Mobile Communications and Services (European Wireless)*, 11th European, 2005.
- [40] C. Yang, Y. Huang, and X. Zhu, "Hybrid TDOA/AOA method for indoor positioning systems," *The Location Technologies*, 2007.
- [41] F. G. D. Committee, "Geospatial Positioning Accuracy Standards Part 3: National Standard for Spatial Data Accuracy." <http://www.fgdc.gov/>, 1998.
- [42] S. Forum, "Femtocell Market Status," no. December, 2011.
- [43] K. M. Pesyna, K. D. Wesson, R. W. Heath, and T. E. Humphreys, "Extending the reach of GPS-assisted femtocell synchronization and localization through Tightly-Coupled Opportunistic Navigation," in *2011 IEEE GLOBECOM Workshops (GC Wkshps)*, 2011, pp. 242–247.
- [44] Z. Wang, Y. Zhu, and N. Liu, "An improved mobile location approach based on RSCP difference," in *Proceedings of 2011 International Conference on Electronic & Mechanical Engineering and Information Technology*, 2011, pp. 2765–2768.
- [45] H. Laitinen, S. Ahonen, and S. Kyriazakos, "Cellular location technology," *Public deliverable of*, 2001.
- [46] K. S. Division, "65 ° Panel Antenna 65 ° Panel Antenna," vol. 97501, no. 541. 2007.
- [47] Alcatel-Lucent, "Alcatel-Lucent 9362 Enterprise Cell," pp. 1–18, 2010.
- [48] MathWorks, "MATLAB and Simulink for Technical Computing." [Online]. Available: <http://www.mathworks.com/>.
- [49] Ascom, "TEMS Investigation for wireless network testing." [Online]. Available: <http://www.ascom.com/en/index/index/products-solutions/our-solutions/solution/ant-test-and-measurement/product/tems-investigation-3/solutionloader.htm>.
- [50] P. B. Software, "MapInfo Professional 11.5 User Guide." .

- [51] J. Stefanski, "Accuracy analysis of mobile station location in cellular networks," *2nd International Conference on Information Technology (ICIT)*, no. June, pp. 101–102, 2010.
- [52] H. Holma and A. Toskala, "WCDMA For UMTS: Radio Access for Third Generation Mobile Communications." Wiley, Chichester, 2004.
- [53] J. M. C. Lopes, "Performance Analysis of UMTS/HSDPA/HSUPA at Cellular Level," Instituto Superior Técnico, 2008.
- [54] J. A. M. Mestre, "Adaptive flexible spectrum usage algorithms in heterogeneous cell deployment," *IEEE*, 2011.
- [55] J. B. Schodorf and D. B. Williams, "A constrained optimization approach to multiuser detection." IEEE Press, pp. 258–262, 1997.
- [56] J. Holtzman, "DS/CDMA successive Interference Cancellation," *IEEE Transactions on Signal Processing*, vol. 45, no. 1, pp. 161–180, 1997.
- [57] V. Chandrasekhar and J. G. Andrews, "Uplink Capacity and Interference Avoidance for Two-Tier Femtocell Networks," *IEEE Transactions on Wireless Communications*, 2008.
- [58] R. Iovanas, "LuPC Interface Enhancement Feature introduction Strategy & Monitoring," 2013.